How Important Are Inflation Expectations for the Nominal Yield Curve?*

Roberto Gomez-Cram
London Business School

Amir Yaron
University of Pennsylvania
NBER
Bank of Israel

This version: December 2019

Abstract

Macro-finance term structure models too heavily rely on the volatility of expected inflation news as a source for variations in nominal bond yield shocks. We develop and estimate a model featuring inflation nonneutrality and preference shocks. The stochastic volatility of inflation and consumption govern bond risk premia movements, whereas preference shocks generate fluctuations in real rates. The model accounts for key bond market features, without resorting to an overly dominating expected inflation channel. The estimation shows that preference shocks are strongly negatively correlated with market distress factors and that real rate news is the dominant driver of nominal yield shocks.

*Roberto Gomez-Cram: rgomezcram@london.edu
Amir Yaron: yarona@wharton.upenn.edu
The views expressed herein are those of the authors and not necessarily those of Bank of Israel. We thank Mete Kilic, Frank Schorfheide, Dongho Song, and participants at many conferences for helpful comments and discussions. Yaron thanks the Rodney White and Jacobs Levy centers for financial support.

1 Introduction

Macro-finance term structure models are designed to interpret and quantify the economic mechanisms underlying the substantial variation in nominal yields and risk premia in bond markets. To this end, economists have used long-run risk (e.g., Piazzesi and Schneider 2007; Bansal and Shaliastovich 2013; Song 2017), New Keynesian (e.g., Rudebusch and Swanson 2012; Kung 2015), and habit formation (e.g., Wachter 2006) models. However, to match term structure features, these models rely on expected inflation news that are too volatile relative to the data (see Duffee (2018) for extended discussion). At the monthly frequency, the variance of expected inflation news accounts for about 20% of the variance of nominal yield shocks, which is strongly at odds with model-implied ratios, which often exceed 100%.[1]

In this paper, we develop and estimate a nonlinear Bayesian state-space macro-finance endowment model that accounts for key bond market features, without resorting to an expected inflation channel that overly dominates the variation in nominal yield shocks. The model features recursive preferences, inflation nonneutrality, multiple stochastic volatility processes, time preference shocks, and time aggregation of consumption. Specifically, we build on the long-run risks setups of Bansal and Shaliastovich (2013) and Schorfheide, Song, and Yaron (2017); in these setups, time variation in expected consumption and inflation and their respective volatilities are key in accounting for bond risk premia dynamics and matching standard bond market moments. The shocks to time rate of preference, on the other hand, primarily affect real rate fluctuations and thus limit the role of expected inflation shocks in driving nominal yield innovations. To assess the empirical validity of these different channels, we estimate the model using a Bayesian Markov chain Monte Carlo (MCMC) particle filter approach. To the best of our knowledge, this model is the first that does not too heavily rely on the volatility of inflation expectations to fit the nominal yield curve.

The rich model specification accounts for an encompassing set of term structure facts. Specifically, the model matches standard moments, such as the unconditional level, slope, and standard deviation of nominal yields. In addition, the model generates sizable variation in bond risk premia,

[1]For example, in new Keynesian and long-run risks models, these variance ratios can exceed 100%. Although habit formation models fare somewhat better with variance ratios of around 50%, they lack a consistent channel for predictability in bond and currency returns. For example, Wachter (2006) requires countercyclical interest rates to account for bond return predictability, whereas Verdelhan (2010) relies on procyclical interest rates to account for the violations of uncovered interest parity in currency markets.

that is, it generates a time-varying term premium that mimics the estimates based on reduced-form Gaussian affine term structure models (e.g., Adrian, Crump, and Moench 2013; Kim and Wright 2005), and it quantitatively matches the evidence of bond return predictability documented in Cochrane and Piazzesi (2005) and the failure of the expectation hypothesis, as identified in Campbell and Shiller (1991). By shutting down the nominal channel, we find that the model-implied real rates track very closely real yields from the TIPS market. Noteworthy, and consistent with the literature documenting sizeable liquidity premia in TIPS (e.g., Pflueger and Viceira 2011; Abrahams, Adrian, Crump, and Moench 2013; d'Amico, Kim, and Wei 2018), we find that around 75% of the variation in the spreads between TIPS yields and the model-implied real yields can be explained by illiquidity measures in the TIPS market. Finally, an extension of the model accounts for the time-varying cyclical properties of inflation. Importantly, the model accounts for these term structure facts without distorting its macroeconomic fit, requiring a large coefficient of relative risk aversion or giving rise to an unreasonable high maximal Sharpe ratio due to overfitting.

Nominal bond yields substantially vary through time. To understand which components drive this variation, we decompose nominal bond yields as the sum of average ex-ante real rates, expectations of average inflation, and average expected excess returns over the life of the bond. Our model-implied estimates suggest that inflation expectations mainly drive the yield level (accounting for around 60%), given that they are highly persistent. However, because they update little from month to month, variances of news about expected inflation, like in the data, contribute little to the overall variance of bond yield shocks (around 20% at the monthly frequency).[2] So what mainly drives shocks to nominal bond yields? From Duffee (2018), we know that the main driver is not news about inflation expectations. We answer this question more forcefully given the advantage of having a structural model. Specifically, our estimates suggest that nominal yield shocks are primarily news about real rates. At the monthly frequency, variances of news about real rates account for between 77% (short-term bonds) and 57% (long-term bonds) of variances of yield shocks. The importance of term premia shocks increases with maturity and accounts for around 19% of the variance of yield shocks at the 10-year maturity.

[2]In this regard, we extend the *unconditional* inflation variance ratios proposed by Duffee (2018) by modelling the dynamics of *conditional* inflation variance ratios. We find that the inflation variance ratios (for different horizons) are indeed smaller than existing structural models ascribe, yet the point estimates are larger than initially viewed once appropriate econometrics account for stochastic volatility in inflation and bond yields.

The model features two key mechanisms. The first one builds on the long-run risks model of Bansal and Yaron (2004) and follows the formulation in Bansal and Shaliastovich (2013) in assuming that consumption growth and inflation contain a small predictable component with time-varying conditional volatilities. With preferences for early resolution of uncertainty, variations in bond risk premia are entirely driven by these volatilities. Specifically, an increase in real volatility (uncertainty) lowers bond risk premia, whereas nominal volatility raises it, provided that expected inflation negatively predicts one-period-ahead expected consumption growth. In such a setting, nominal shocks are priced, making long-term bonds particularly risky, because innovations that produce a persistent increase in expected inflation generate persistently low real yields and low expected consumption growth. This mechanism is important for generating a positive slope in the nominal yield curve and producing movements in bond risk premia.

The time preference shocks provide the second mechanism. In this model, time preference shocks arise from stochastic changes in agents' discount factor and determine how agents trade off current versus future utilities. Albuquerque, Eichenbaum, Luo, and Rebelo (2016) and Schorfheide et al. (2017) also include time preference shocks in their model specification to better account for the relatively low correlation between the risk-free rate and consumption growth, a feature preserved in this model. Furthermore, with preference for early resolution of uncertainty, exposure to these shocks is an increasing function of the bond's maturity and generates an upward-sloping real yield curve. Hence, time preference shocks complement the first mechanism in producing an upward-sloping nominal yield curve. Importantly, we show empirically that time preference shocks produce realistic real rate dynamics and, at the same time, allow the model to match the empirical volatility of nominal yield shocks without resorting to innovations in inflation expectations that vary too much relative to the data. Moreover, it is important to recognize that parameterizations that are successful in reducing the inflation variance ratios, hamper the model's ability to match other relevant moments of the yield curve, such as movements in real bond yields, slope of the yield curve, level of the term premium, or the regression based evidence on excess bond return predictability. These other moments serve as the overidentifying restrictions that would lead us to reject the variability and persistence of the time preference shocks that allowed the model to succeed. Therefore, it is only through a quantitative model-based approach that we can assess the relative strength of these offsetting effects. This observation points to the necessity of the estimation

procedure we take in this paper since these other moments implicitly enter the likelihood function of our state-space model.

As a by-product of our estimation procedure, we also obtain an estimate of the preference shocks. Time preference shocks determine the attitudes of the representative household toward savings and are, by assumption, one that we subsequently show is supported empirically, orthogonal to the real economy. Interestingly, and in line with this reasoning, the filtered time preference shocks series is highly negatively correlated with market distress factors such as the adjusted National Financial Conditions Index, published by the Federal Reserve of Chicago or the St. Louis Fed's Financial Stress Index. These indices measure risk, liquidity, and leverage in money, debt, and equity markets and the overall degree of financial stress in the U.S. markets, respectively. By contrast, popular liquidity measures in Treasury markets with strong excess bond return predictability power such as the series of Fontaine and Garcia (2012) and Hu, Pan, and Wang (2013) do not have explanatory power for the time-variation in the time preference shocks.

The model contains several other important ingredients that align variations in the levels and volatilities of macroeconomic variables with movements in both the shape of the nominal term structure and fluctuations in bond risk premia. This link has been difficult to establish in the bond-pricing literature, where the current perspective is rather pessimistic (see Duffee (2013) for an overview). We show that monthly measurement errors in the process of consumption that average out at the annual frequency and temporal aggregation aid the identification of the predictable component of consumption growth. Moreover, time-varying volatilities in the *i.i.d.* component of consumption growth and inflation improves the model fit and decreases the posterior uncertainty of the parameter estimates. These ingredients are negligible for the nominal yield curve but are important for tracking the macroeconomic series. Importantly, we show that once we account for them, information in the macro variables drives the level of bond yields. Conversely, we show that yields contain useful information about the beliefs of investors regarding the volatility of expected consumption growth and expected inflation that cannot be extracted by only looking at the second moments of the macro variables. Specifically, we find that the conditional volatilities of the predictable components seem to capture more transient economic movements since they are substantially more variable and persistent relative to the ones obtained by just using macroeconomic variables. Noteworthy, the credible bands are wide enough that, strictly speaking, they are statisti-

cally indistinguishable from each other, and, therefore, this extra variability in the volatilities does not distort the fit of the macroeconomic variables.

This paper contributes to the extensive literature on modeling and estimating term structure models. Important papers on modeling the term structure with recursive preferences are Piazzesi and Schneider (2007), Eraker (2008), Le and Singleton (2010), Van Binsbergen, Fernández-Villaverde, Koijen, and Rubio-Ramírez (2012), Doh (2013), Bansal and Shaliastovich (2013), Kung (2015), Creal and Wu (2016), and Song (2017). Key papers that use time-varying preference shocks, or habit, as a device for generating an upward-sloping real yield curve are Wachter (2006) and Gallmeyer, Hollifield, Palomino, and Zin (2017). Our paper distinguishes itself from this literature by showing that time preference shocks add considerable flexibility to a term structure model. Specifically, time preference shocks break the tight link between macroeconomic variables and bond yields assumed in standard macro-finance models. Moreover, time preference shocks, in conjunction with our rich model specification (including measurement errors, time aggregation, and several volatilities), allow us to reconcile the behavior of the term structure with movements in the macroeconomy.

An important paper by Creal and Wu (2016) (hereafter CW) parallels ours in several ways. CW also combine long-run risks and preference shocks to fit the yield curve. CW ask whether time-varying prices of risk (introduced via their time preference shocks specification) or quantity of risk serve as the key driver of term premia variations. They find that the time-varying quantity of risk cannot produce plausible time variations in term premia. Our paper, however, differs from theirs in overall objective, modeling assumptions, empirical implementation, and findings. Our goal is to address and solve the Duffee (2018) critique, which affects a large strand of existing structural models (CW included), while fitting what we consider to be the most important and extensive set of term structure moments. The term structure literature has sequentially progressed with more stringent and informative data targets and generally richer models. Our paper makes a significantly contribution in this dimension.

This paper is organized as follows. Section 2 introduces the model, casts it into a state-space form, and describes the estimation procedure. Section 3 describes the data set and presents the estimation results. Section 4 discusses the implications of the model estimation for the nominal yield curve. Finally, Section 5 provides concluding remarks.

2 Model Framework

2.1 Preferences

We consider a representative agent that has recursive preferences like in Epstein and Zin (1989). The indirect utility, V_t, takes the form

$$V_t = \underset{C_t}{max} \left[(1-\delta)\lambda_t C_t^{\frac{1-\gamma}{\theta}} + \delta \left(E_t \left[V_{t+1}^{1-\gamma} \right] \right)^{\frac{1}{\theta}} \right]^{\frac{\theta}{1-\gamma}}, \tag{1}$$

where C_t denotes consumption; γ represents the coefficient of relative risk aversion, $\theta = \frac{1-\gamma}{1-\frac{1}{\psi}}$, where ψ is the elasticity of intertemporal substitution; and δ is the time discount factor. Like in Albuquerque et al. (2016) and Schorfheide et al. (2017), we allow for shocks, λ_t, to the time rate of preference. The logarithmic growth of λ_t, denoted by $x_{\lambda,t}$, determines how the agent trades off current versus future utility and follows

$$x_{\lambda,t+1} = \rho_\lambda x_{\lambda,t} + \varphi_\lambda \sigma \eta_{\lambda,t+1} \quad \text{with} \quad \eta_{\lambda,t+1} \sim N(0,1). \tag{2}$$

The agent is subject to the following budget constraint: $W_{t+1} = (W_t - C_t)R_{c,t+1}$, where W_t denotes its wealth at time t and $R_{c,t+1}$ is the return on an asset that pays aggregate consumption as dividends.

2.2 Consumption and Inflation Dynamics

The exogenous dynamics of the logarithm of consumption growth, Δc_{t+1}, and the logarithm of the inflation rate, π_{t+1}, are written as follows:

$$\begin{aligned} \Delta c_{t+1} &= \mu_c + x_{c,t} + \sigma_{c,t}\eta_{c,t+1}, \quad \eta_{c,t+1} \sim N(0,1), \\ \pi_{t+1} &= \mu_\pi + x_{\pi,t} + \sigma_{\pi,t}\eta_{\pi,t+1}, \quad \eta_{\pi,t+1} \sim N(0,1), \end{aligned} \tag{3}$$

where the process of conditional expectations is given by

$$\begin{aligned} x_{c,t+1} &= \rho_{cc}x_{c,t} + \rho_{c\pi}x_{\pi,t} + \sigma_{xc,t}\eta_{xc,t+1}, \quad \eta_{xc,t+1} \sim N(0,1), \\ x_{\pi,t+1} &= \qquad\quad + \rho_{\pi\pi}x_{\pi,t} + \sigma_{x\pi,t}\eta_{x\pi,t+1}, \quad \eta_{x\pi,t+1} \sim N(0,1), \end{aligned} \tag{4}$$

and the volatilities evolve according to log Gaussian processes

$$\sigma_{i,t} = \varphi_i \sigma exp(h_{i,t}), \quad h_{i,t+1} = \rho_{h_i} h_{i,t} + \sigma_{h_i} \omega_{i,t+1}, \quad \omega_{i,t+1} \sim N(0,1) \quad \text{for} \quad i = \{c, \pi, xc, x\pi\} \quad (5)$$

where we normalized $\varphi_c = 1$. Specification (3) is based on Bansal and Yaron (2004), Piazzesi and Schneider (2007), and Bansal and Shaliastovich (2013) and decomposes real consumption growth and inflation into predictable $\{x_{c,t},\ x_{\pi,t}\}$ and transitory $\{\sigma_{c,t}\eta_{c,t+1},\ \sigma_{\pi,t}\eta_{\pi,t+1}\}$ components. The predictable components, that is expected consumption growth, x_c, and expected inflation, x_π, follow a bivariate VAR(1) process, with time-varying volatilities given by $\sigma_{xc,t}$ and $\sigma_{x\pi,t}$, respectively. Moreover, we introduce inflation nonneutrality via the parameter $\rho_{c\pi}$. Finally, in equation (5), we model the conditional volatilities as a stochastic volatility process given that this specification has been successful in capturing the conditional variance of the shocks hitting the economy (see, for instance, Primiceri (2005), Sims and Zha (2006)), and doing so, also ensures that $\sigma_{i,t}$ is nonnegative throughout.[3]

2.3 Bond Pricing

The real price of any asset that does not pay dividends at $t+1$ is given by the asset pricing equation

$$P_t = E_t[M_{t+1} P_{t+1}], \quad (6)$$

where $M_{t+1} = \delta^\theta \left(\frac{\lambda_{t+1}}{\lambda_t}\right)^\theta \left(\frac{C_{t+1}}{C_t}\right)^{-\frac{\theta}{\psi}} R_{c,t+1}^{\theta-1}$ is the real stochastic discount factor (SDF). To price nominal assets, it is useful to specify the nominal discount factor, which is equal to the real one divided by the change in price levels, expressed as dollars per unit of consumption: $M_{t+1}^{\$} = M_{t+1} e^{-\pi_{t+1}}$, where we use the dollar sign superscript, \$, to distinguish nominal from real values.

The solution to (6) depends on the dynamics of consumption growth and inflation specified in (3), (4), and (5). To make the Bayesian estimation in Section 2.4 computationally feasible, we derive analytical model solutions by relying on two different approximations. The first, proposed

[3]The crucial difference of the class of models known as "stochastic volatility models" is that the volatility generated by equation (5) is unobservable. See Shephard (1996) for an overview of the properties of stochastic volatility models.

by Schorfheide et al. (2017), linearly approximates $\sigma^2_{i,t}$ around the unconditional mean of h_i

$$\sigma^2_{i,t+1} = (\varphi_i\sigma)^2(1-\rho_{h_i}) + \rho_{h_i}\sigma^2_{i,t} + 2(\varphi_i\sigma)^2\sigma_{h_i}\omega_{i,t+1} \quad \text{for} \quad i = \{c, \pi, xc, x\pi\} \tag{7}$$

and replaces the variance process in (5) with (7) when solving the asset pricing equation (6). The second approximation utilizes the conventional Campbell and Shiller (1988) log-linearization of returns.

Given these two approximations, the continuously-compounded one-period real interest rate is affine in the state variables

$$r_{f,t} = -E_t(m_{t+1}) - \frac{1}{2}Var_t(m_{t+1}) = B_{0,1} + B_{c,1}x_{c,t} + B_{\lambda,1}x_{\lambda,t} + B_{\sigma_c,1}\sigma^2_{c,t} + B_{\sigma_{xc},1}\sigma^2_{xc,t} + B_{\sigma_{x\pi},1}\sigma^2_{x\pi,t}, \tag{8}$$

where the lowercase m denotes the log of the SDF. Equation (8) links real short rate variations to variations in fundamentals. Because of the agent's motive to smooth consumption intertemporally, the real short rate increases when the one-period-ahead expected consumption growth increases (i.e., $B_{c,1} = \frac{1}{\psi} > 0$). Under this scenario, the agent wants to borrow to increase today's consumption and since assets in the economy are in zero net supply, aggregate borrowing cannot increase. In equilibrium, the real short rate must increase to induce the agent to borrow less. Alternatively, with preference for early resolution of uncertainty (i.e., when $\gamma > \frac{1}{\psi}$), an increase in real volatility increases the agent's uncertainty about future growth and as a result she wants to hedge by buying risk-free assets, and in equilibrium, the real rate falls (i.e., $B_{\sigma_c,1} < 0$ and $B_{\sigma_{xc},1} < 0$). Moreover, when $x_{\lambda,t}$ rises, the agent values tomorrow's consumption more relative to the present. Therefore, she wants to increase savings and the risk-free rate has to fall in order to clear markets (i.e., $B_{\lambda,1} = -\rho_\lambda < 0$). Importantly, if time preference shocks are volatile and persistent, then they will generate similar movements in real short-term rates.

Similarly, the one-period nominal interest rate is

$$r^{\$}_{f,t} = r_{f,t} + E_t\left(\pi_{t+1}\right) + Cov_t\left(m_{t+1}, \pi_{t+1}\right) - \frac{1}{2}Var_t\left(\pi_{t+1}\right). \tag{9}$$

The intuition underlying the movements in the nominal short rate is straightforward. The first two

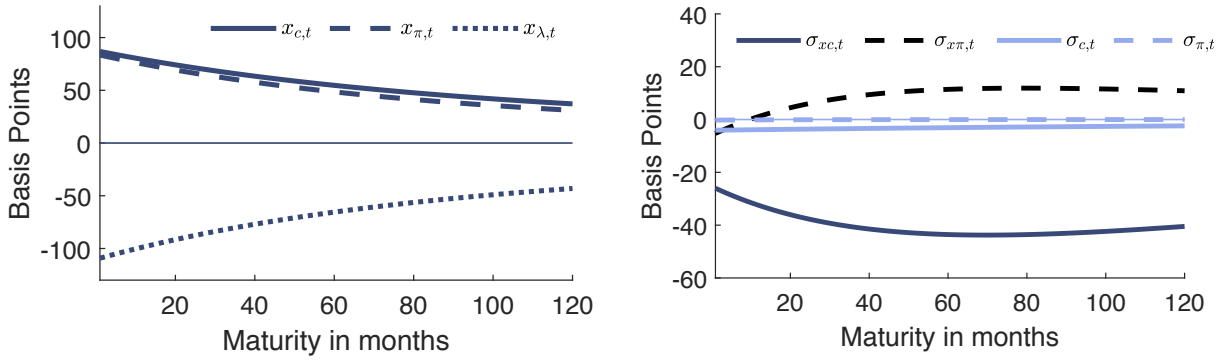

(a) Loadings on levels

(b) Loadings on volatilities

Figure 1. Equilibrium nominal bond yield loadings.
This figure shows model-implied nominal bond yield loadings evaluated at the posterior median values reported in Table 1. The loadings are scaled by the factor's standard deviation. Panel (a) shows the loadings with respect to expected consumption growth, $x_{c,t}$, expected inflation, $x_{\pi,t}$, and time preference shocks, $x_{\lambda,t}$. Panel (b) shows the loadings with respect to long-run real uncertainty, $\sigma^2_{xc,t}$, long-run nominal uncertainty, $\sigma^2_{x\pi,t}$, short-run real uncertainty, $\sigma^2_{c,t}$, and short-run real nominal $\sigma^2_{\pi,t}$, uncertainty. Maturity is in months.

terms on the right-hand side of (9) denote the standard Fisher equation. In turn, the third term recognizes that nominal rates are risky in real terms. If positive shocks to the inflation rate are associated with positive shocks to the SDF, then the covariance term is positive, and the agent requires additional compensation to hold the nominal short rate. Finally, the fourth term is due to Jensen's inequality.

Yields on zero-coupon bonds are also exponential affine functions of the state variables. Using the Euler equation in (6), together with the real and nominal SDF, we can derive the expression of an n-th period real and nominal yield, respectively:

$$\begin{aligned} y_{t,n} &= B_{0,n} + B_{c,n}x_{c,t} + B_{\pi,n}x_{\pi,t} + B_{\lambda,n}x_{\lambda,t} + B_{\sigma_c,n}\sigma^2_{c,t} + B_{\sigma_\pi,n}\sigma^2_{\pi,t} + B_{\sigma_{xc},n}\sigma^2_{xc,t} + B_{\sigma_{x\pi},n}\sigma^2_{x\pi,t}, \\ y^{\$}_{t,n} &= B^{\$}_{0,n} + B^{\$}_{c,n}x_{c,t} + B^{\$}_{\pi,n}x_{\pi,t} + B^{\$}_{\lambda,n}x_{\lambda,t} + B^{\$}_{\sigma_c,n}\sigma^2_{c,t} + B^{\$}_{\sigma_\pi,n}\sigma^2_{\pi,t} + B^{\$}_{\sigma_{xc},n}\sigma^2_{xc,t} + B^{\$}_{\sigma_{x\pi},n}\sigma^2_{x\pi,t}. \end{aligned} \tag{10}$$

Appendix A.4 provides an analytical expression of the B's, which measure the sensitivity of bond yields to the state variables. To develop our economic intuition for the relative size of these loadings across maturities, Figure 1 plots the nominal yield loadings as a function of bond maturity. To ease the figure's interpretation, we also scale the loadings by the factor's standard deviation.

The intuition underlying the sign of the loadings is similar to the real and nominal short rates. However, the size significantly varies across maturities. Under $\psi > 1$ and $\gamma > 1$, $B^{\$}_{\sigma_c,n}$ and

$B^{\$}_{\sigma_{xc},n}$ are negative, so nominal yields decline with a rise in growth uncertainty. Because shocks to expected consumption growth have larger long-term effects, the sensitivity of bond prices to this risk is an order of magnitude larger (in absolute value) than the loading of short-run real volatility risk (see the straight line in panels (b) of Figure 1). Furthermore, the longer the bond maturity, the higher the insurance the bond provides against persistent economic uncertainty and hence the required compensation to hold bonds decreases. This mechanism generates a downward-sloping nominal yield curve.

Empirically, the unconditional mean yield curve slopes up. The model features two key mechanisms that account for this property. The first one builds on the long-run risks model of Bansal and Shaliastovich (2013). If expected inflation reduces expected consumption growth ($\rho_{c\pi} < 0$), times of high long-term inflation rates are times of low consumption growth. Hence, the appropriate covariance term in equation (9), (i.e., $\frac{1}{n}Cov_t(m_{t\to t+n}, \pi_{t\to t+n})$), is positive and increases with maturity. This term captures the inflation premium in the economy. With preference for early resolution of uncertainty, shocks to expected inflation are also priced, which makes long-term bonds particular risky, because shocks that produce a persistent increase in this component generate persistently low real yields and low expected consumption growth. This mechanism is crucial for generating an upward-sloping nominal yield curve (see the upward-sloping dashed lines in panels (b) of Figure 1).

The time preference shocks provide the second mechanism. Panel (a) of Figure 1) shows that the exposure of bond yields to the underlying preference risk increases with maturity. Hence, it complements the first mechanism in producing an upward-sloping nominal yield curve. The main theme in the sections that follow is that time preference shocks add considerable flexibility to a term structure model. Specifically, they break the tight link between conditional expectations of consumption growth, inflation and bond yields assumed in standard macro-finance models.

The relative importance of these different forces jointly affecting the dynamics of short-term interest rates, bond yields, and macroeconomic variables is ultimately a quantitative question. Therefore, to assess the empirical validity of these different channels, we proceed to estimating the model.

2.4 Bayesian Inference

2.4.1 State-Space System. We use Bayesian inference for the parameters of the model and the latent states. To this end, we first need to cast the model into a state-space representation. A state-space system consists of two equations. The first is the measurement equation, which links the observed variables to the model-implied ones. The second is the state transition equation, which describes the law of motion of the state variables.

Measurement Equation. Throughout this paper, we use the superscript o to distinguish observed variables from model-implied ones. Let Y_{t+1}^o be the time: $t+1$ vector of observables. Specifically, Y_{t+1}^o contains consumption growth, Δc_{t+1}^o, inflation, π_{t+1}^o, survey-based expected measures of inflation, the real risk-free rate, $r_{f,t+1}^o$, and nominal bond yields, $y_{t+1,n}^{\$,o}$. Equations (3), (8), and (10) link the observables and the model-implied variables, which, in turn, are functions of the latent states. Given these dynamics, we can write the measurement equation as beginequation

$$Y_{t+1}^o = A_{t+1}(D + Zs_{t+1} + Z^v s_{t+1}^v(h_{t+1}) + \Sigma^u u_{t+1}), \quad \text{with} \quad u_{t+1} \sim N(0, I). \tag{11}$$

The vector $s_{t+1}^v(h_{t+1})$ is a function of the log volatilities $h_{t+1} = [h_{xc,t+1},\ h_{x\pi,t+1},\ h_{c,t+1},\ h_{\pi,t+1}]'$ and stacks the short- and long-run real and nominal uncertainties. The vector s_{t+1} contains the remaining latent states. Broadly, s_{t+1} includes the predictable components of consumption growth, $x_{c,t}$, and inflation, $x_{\pi,t}$, and the time preference shocks, $x_{\lambda,t}$. Moreover, we set up the measurement equation to incorporate the proposed measurement error model for consumption growth of Schorfheide et al. (2017).[4] To this end, we augment s_{t+1} to include leads and lags of $x_{c,t}$, $x_{\pi,t}$ and the corresponding measurement errors. In addition, we sharpen inference about the predictable component of the inflation rate by including survey-based expected inflation measures that are released at a different (quarterly) frequency. We also allow for small deviations between observed yields, $y_n^{\$,o}$, and model-implied yields $y_n^{\$}$. These deviations are captured by $\Sigma^u u_{t+1}$ and can be thought of as cross-sectional errors due to market imperfections, such as measurement errors. Finally, A_{t+1} is a

[4] At the monthly frequency, consumption data have nontrivial measurement errors masking the actual dynamics of consumption (e.g., Wilcox 1992). The measurement error model ensures that monthly measurement errors average out at the annual frequency. Accounting for measurement errors in consumption growth allows one to identify the persistent component of consumption growth and its time-varying short- and long-run volatilities. See the appendix for the precise specification.

selection matrix that accounts for changes in the data availability induced by the specification of the measurement error model of consumption growth, potentially missing observations, and mixed frequency observations.

State-Transition Equation. The state transition equation provides the dynamics of the state variables given by the assumed process of the time preference shocks in (2) and by the processes of the predictable component of consumption growth and inflation in (4). We write the transition equation as

$$s_{t+1} = \Phi s_t + v_{t+1}(h_t), \quad \text{and} \quad h_{t+1} = \Psi h_t + \Sigma_h \omega_{t+1} \quad \text{with} \quad \omega_{t+1} \sim N(0, I) \tag{12}$$

where the variance of $v_{t+1}(h_t)$ depends on the log volatilities at time t. Overall, the combination of equations (11) and (12) leads to a high-dimensional state-space model.

We use a Metropolis-Hastings sampler for posterior inference. Let Θ be the parameter vector that comprises the parameters associated with the preference of the representative agent described in Section 2.1, the assumed process for the macroeconomic dynamics in Section 2.2, and the parameters of the measurement error model of consumption growth. To make a Bayesian inference about Θ and the latent state vectors, we specify a prior distribution $p(\Theta)$ and update our a priori beliefs about the parameter vector Θ, in view of the sample information Y^o. The state of knowledge regarding Θ is summarized by the posterior distribution $p(\Theta|Y)$, and Bayes' theorem provides the formal link:

$$p(\Theta|Y^o) = \frac{p(Y^o|\Theta)p(\Theta)}{p(Y^o)}. \tag{13}$$

Given the presence of nonlinearities induced by the volatility states it is not possible to directly evaluate the likelihood function, $p(Y^o|\Theta)$, via the Kalman filter. Instead, we use a sequential Monte Carlo filter to approximate $p(Y^o|\Theta)$. In essence, we represent the distribution of volatilities using a swarm of particles; conditional on these particles, the model has a linear and Gaussian state-space representation that allows us to apply the Kalman filter to equations (11) and (12). Once we are able to draw from the posterior distribution $p(\Theta|Y^o)$, we use a random-walk Metropolis-Hasting algorithm to draw the parameter vector $\{\Theta^{(s)}\}_{s=1}^{N_{sim}}$, like in Fernández-Villaverde and Rubio-Ramírez (2007) and Andrieu, Doucet, and Holenstein (2010). For further reference regarding the

implementation of the particle filter, see Herbst and Schorfheide (2015).

In Sections 2.3 and 2.4, we rely on analytical approximations to solve the model and to cast the model into a state-space form. As described above, these approximations lead to a conditionally linear state-space model that we can efficiently estimate with reasonable computational burden. The accuracy of these two approximations will depend on the parameterization of the model. Therefore, to assess how accurate these approximations are, we follow Pohl, Schmedders, and Wilms (2018) and compute the global solution of the model via projection methods (see Judd (1992)). For a parameterization equal to the posterior median estimates of the model parameters, we find that the absolute errors in the term structure of interest rates are rather small, with a maximum error of 3.35% for the 1-year bond yield. However, these approximation errors increase somewhat if we use a parametrization closer to the 95% credible set of the posterior distribution. Hence, to be precise, the posterior distribution of the model parameters that we report in the next section should be associated with the approximated model.[5]

The appendix provides precise details of the model's solution, the state-space representation, the estimation procedure, and the errors induced by the analytical approximations.

3 Empirical Results

3.1 Data

The data we use are standard in the macro-finance literature. For the monthly consumption growth data, we use the per capita series of real consumption expenditures on nondurables and services from the National Income and Product Account published by the Bureau of Economic Analysis. The monthly inflation rate corresponds to the CPI series from the Federal Reserve Bank of St. Louis. We constructed growth rates for consumption and inflation by computing the differences of the log series. The survey-based measures of inflation expectations come from the Survey of Professional Forecasters from the Federal Reserve Bank of Philadelphia. We use quarterly mean CPI forecasts for 1 to 4 quarters ahead. Following Beeler and Campbell (2009), the ex-ante monthly real short rate corresponds to the fitted value from regressing the ex post real short rate on current conditioning

[5]See An and Schorfheide (2007) for a similar discussion in the literature on dynamic stochastic general equilibrium (DSGE) models. In this literature, it has been widely accepted to estimate the linearized DSGE model given the computational burden associated with the likelihood evaluation for the nonlinear version of the model.

information. To this end, we use as our measure of the short rate the 3-month yield from CRSP Fama Risk-Free Rates. Finally, we use as our measure of nominal bond yields the monthly U.S. Treasury Zero-Coupon Yield Curve from Gürkaynak, Sack, and Wright (2007). We consider bonds with maturities of 1, 3, 5, 7, and 10 years. The unbalanced panel of mixed frequency observations starts in January of 1962 and ends in December of 2018.[6]

3.2 Model Estimation

3.2.1 Prior Distribution. The first columns of Table 1 show the assumed prior distribution and the 5th and 95th percentiles. In general, we attempted to restrict the parameter space to economically plausible values, while being as uninformative as possible. For example, our prior distribution for the persistence parameter of the predictable component of consumption growth covers values that imply a near *i.i.d.* or a unit root process for consumption growth. Similarly, we do not restrict the preference of the representative household to have early, $\theta < 0$, or late, $\theta > 0$, resolution of uncertainty. The prior for the discount rate, δ, covers steady-state annualized values for the one-period risk-free rate between 0.5% and 5%. Finally, we fixed the standard deviation of the yields measurement error and the real short rate in (12) at 5% of the yields' sample standard deviation, a value consistent with the work of Bekaert, Hodrick, and Marshall (1997).

3.2.2 Posterior Distribution. The last six columns of Table 1 show the 5th, 50th, and 95th percentiles of the posterior distribution of two different models. The first model uses only macroeconomic data to estimate the joint process of consumption growth and inflation. These dynamics are described by equations (3), (4), and (5).[7] The second model uses macroeconomic data, the short real risk-free rate, and the entire yield curve (specifically, five points on the curve) to estimate the macro dynamics and the preference parameters of a representative agent. Theoretically, we can sharpen our inferences about expected future macroeconomic activity and inflation by incorporating the information contained in leading indicators, such as bond yields. Forward-looking investors

[6]The series start at different periods, but all end in December 2018. Specifically, our measures of consumption growth and inflation and the ex-ante risk-free rate start in 1962:M1. The Survey of Professional Forecasters data start in 1981:M3. The bond yields with maturities of 1, 3, 5, and 7 years start in 1962:M1, whereas the 10-year maturity bond starts in 1971:M8.

[7]To estimate the model that only includes macro data in the estimation, we cast equation 3 into a state-space form and use a Metropolis-within-Gibbs sampler for posterior inference, iterating it over the three conditional distributions.

	Prior distribution			Macro data			Macro data and bond prices		
	Distr.	5%	95%	5%	50%	95%	5%	50%	95%
				Household preferences					
δ	B	0.9942	1.0000	-	-	-	0.9975	0.9987	0.9991
ψ	G	0.65	3.80	-	-	-	1.15	1.50	2.05
γ	G	4.50	17.20	-	-	-	7.81	13.01	16.42
				Time preference					
ρ_λ	U	-0.9058	0.9025	-	-	-	0.971	0.981	0.985
φ_λ	U	0.1559	2.8346	-	-	-	0.103	0.120	0.135
				Consumption growth					
μ_c	N	0.0014	0.0018	0.0012	0.0016	0.0020	0.0014	0.0016	0.0019
σ	IG	0.0008	0.0062	0.0011	0.0014	0.0021	0.0013	0.0015	0.0018
ρ_{cc}	U	-0.900	0.900	0.921	0.954	0.987	0.947	0.983	0.993
$\rho_{c\pi}$	U	-0.9000	0.9000	-0.0149	-0.0015	-0.0002	-0.0121	-0.0075	-0.0011
φ_{xc}	U	0.050	0.950	0.128	0.215	0.346	0.052	0.130	0.216
ρ_{h_c}	N^T	0.469	0.999	0.968	0.990	0.999	0.971	0.992	0.998
σ_{h_c}	IG	0.003	0.293	0.050	0.099	0.191	0.065	0.104	0.179
$\rho_{h_{xc}}$	N^T	0.469	0.999	0.659	0.761	0.985	0.977	0.980	0.984
$\sigma_{h_{xc}}$	IG	0.003	0.293	0.039	0.086	0.237	0.076	0.090	0.095
				Inflation					
μ_π	N	0.0019	0.0038	0.0020	0.0027	0.0035	0.0028	0.0034	0.0037
φ_π	U	0.050	2.950	0.874	1.295	1.602	0.937	1.292	1.501
$\rho_{\pi\pi}$	U	-0.900	0.900	0.982	0.984	0.988	0.983	0.985	0.987
$\varphi_{x\pi}$	U	0.050	2.950	0.0577	0.0857	0.1167	0.074	0.080	0.091
ρ_{h_π}	N^T	0.469	0.999	0.829	0.892	0.938	0.862	0.891	0.913
σ_{h_π}	IG	0.003	0.293	0.176	0.231	0.295	0.196	0.241	0.253
$\rho_{h_{x\pi}}$	N^T	0.469	0.999	0.970	0.990	0.999	0.957	0.970	0.981
$\sigma_{h_{x\pi}}$	IG	0.003	0.293	0.058	0.0950	0.162	0.266	0.271	0.275

Table 1. Prior and posterior model estimates.
This table reports the 5th and 95th percentiles of the prior distribution of the model parameter along with the 5th, 50th, and 95th percentiles of their posterior distribution. We present the posterior distribution with (macro data and bond prices) and without (macro data) bond prices included in the estimation. The assumed prior distributions are as follows: B, beta; G, gamma; IG, inverse gamma; N, normal; N^T, truncated normal outside of the $(-1, 1)$ interval; and U, uniform. The sample range is January 1962 through December 2018.

form expectations about future economic growth that are immediately reflected into asset prices. Empirically, however, nominal yields and risk premia in bond markets exhibit substantial variation, yet much of this variation has been difficult to align with plausible similar movements in macroeconomic variables (see Duffee (2013) for an overview). Hence, including bond prices in the estimation could potentially achieve a better fit for bond yields, while sacrificing the fit for consumption growth and inflation. Therefore, this trade-off is at the end of the day an empirical issue.

Conditional Expectations. In the model, conditional expectations of consumption growth and inflation drive a significant fraction of the level of the yield curve. We found that the estimated conditional expectations that incorporate the information in bond prices are in close agreement to those obtained when we only utilize macroeconomic information. Table 1 shows that the posterior median estimates of the persistence parameters ρ_{cc} and $\rho_{\pi\pi}$ are similar with (0.983 and 0.985) or without (0.954 and 0.984) bond prices. For both parameters, the 90% credible intervals of the macro-only estimation contain the posterior median estimates obtained with bond prices. Appendix B.4 shows that this result is mostly driven by incorporating the measurement error structure in consumption growth, accounting for temporal aggregation and the assumed stochastic volatility processes for realized consumption growth and inflation.[8] Furthermore, there is enough information in the macro data to identify $\rho_{c\pi}$, which is negative and significant, as suggested by the 95th percentile in Column 7 of Table 1. Interestingly, when we add bond prices to the estimation, the 90% credible interval shifts toward more negative values. Nevertheless, the credible interval contains the posterior median of $\rho_{c\pi}$ from the macro-only estimation.[9]

Moreover, the estimated time series of conditional expectations (that include and do not include bond yield information) track each other very closely. To see this, panels (a) and (b) of Figure 2 show the posterior medians of expected consumption growth, $x_{c,t}$, and expected inflation, $x_{\pi,t}$, obtained with (blue line) and without (red line) bond prices. We also overlay the 90% credible interval of the macro-only estimation (dotted red lines) and the observed monthly consumption growth and inflation series (gray lines). The panels show that the time series of conditional expectations substantially vary through time and that they indeed capture low-frequency variations in realized consumption growth and inflation. Importantly, the blue and red series move in tandem, suggesting the macro data have enough information to identify the predictable components of consumption growth and inflation.

[8] Accounting for measurement errors in consumption reveals a persistent component in consumption growth: in the absence of measurement errors, ρ_{cc} drops to -0.20. Moreover, adding stochastic volatility to the process of the macro variables considerably improves the model's fit (as measured by the log marginal data density) and decreases the posterior uncertainty of the parameter estimates (as measured by the 90% credible interval). See Table B1 in Appendix B.4.

[9] Recent evidence suggests that for the last two decades the cyclical properties of inflation have changed. This suggests that $\rho_{c\pi}$ potentially switched its sign. In Section 4.5, we extend the benchmark specification by allowing for pro/countercyclical inflation regimes and discuss its economic implications for the yield curve.

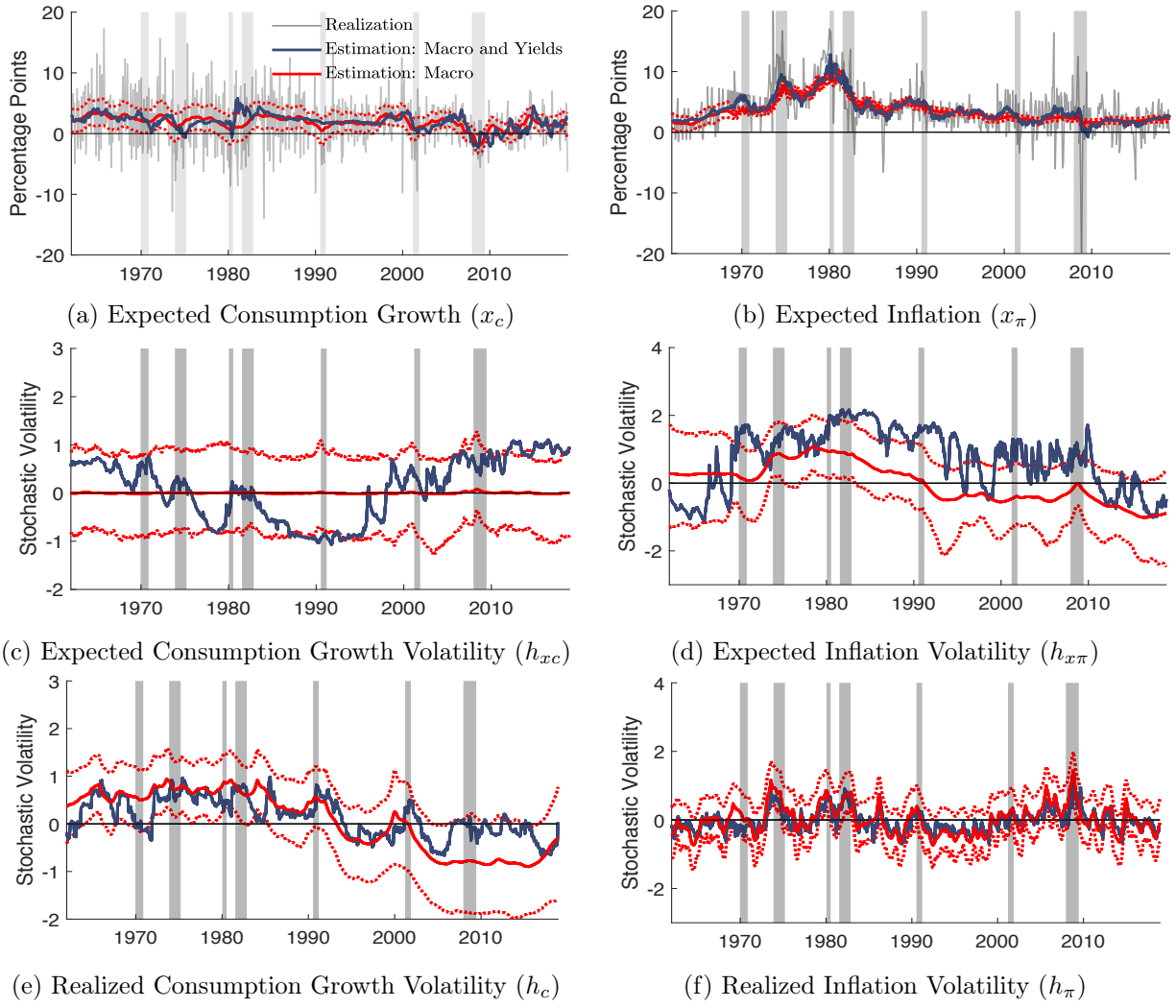

(a) Expected Consumption Growth (x_c)

(b) Expected Inflation (x_π)

(c) Expected Consumption Growth Volatility (h_{xc})

(d) Expected Inflation Volatility ($h_{x\pi}$)

(e) Realized Consumption Growth Volatility (h_c)

(f) Realized Inflation Volatility (h_π)

Figure 2. Macroeconomic state variables.
This figure shows the smoothed mean and volatility states filtered from the macro-finance model. The red lines show these smoothed states from a model that only considers the information contained in the macroeconomic variables. The dotted lines denote the 90th percentile credible intervals. Panels (a) and (b) also include the observed series of consumption growth and inflation, respectively. Light-shaded bars represent recessions, as defined by the National Bureau of Economic Research. Consumption growth and the inflation rate are annualized values. The sample range is January 1962 through December 2018.

Conditional Volatilities. In the model, the conditional volatilities of expected consumption growth and inflation drive variations in bond risk premia. Table 1 shows that bond prices increase the persistence of the stochastic volatility of expected consumption growth, $\rho_{h_{xc}}$, and the standard deviation of its news, $\sigma_{h_{xc}}$, from 0.76 and 0.08 to 0.98 and 0.09, respectively. Similarly, the standard deviation of news to the stochastic volatility of expected inflation, $\sigma_{h_{xc}}$, increases from 0.095 to 0.271. Panels (c) and (d) of Figure 2 confirm this message. The panels depict the smoothed volatility processes obtained from the estimation with (blue line) and without (red line) yield curve

	Macro data			Macro data and bond prices		
	5%	50%	95%	5%	50%	95%
$E[\sigma_{xc,t}] \times 1200\%$	0.20	0.38	0.54	0.09	0.26	0.54
$E[\sigma_{x\pi,t}] \times 1200\%$	0.16	0.19	0.45	0.18	0.27	0.54

Table 2. Unconditional mean volatilities

This table reports the 5th, 50th, and 95th percentiles of the posterior distribution of the unconditional mean of the volatility process implied by the posterior distribution of the model parameters. We present the posterior distribution with (macro data and bond prices) and without (macro data) bond prices included in the estimation. The unconditional mean volatility is computed as follows: $E[\sigma_{i,t}] = \varphi_i \sigma_c exp(0.5 \frac{\sigma_{h_i}^2}{1-\rho_{h_i}^2})$.

information. The addition of yields substantially increases the variability of the volatilities, which seem to exhibit more high-frequency movements relative to estimates based on macro-only information. As shown in the next section, this extra variability is needed to quantitatively account for the sizable variations observed in bond risk premia. Hence, yields contain useful information about the beliefs of investors regarding the volatility of expected consumption growth and expected inflation that cannot be extracted by looking directly at the second moments of the macro variables. Interestingly, the figure shows that, although the volatilities substantially changed when including the information of bond yields, the time-series estimates are contained most of the time inside the 90% credible bands of the volatilities from the macro-only estimation (see the red dotted lines).

How can the model with bond yields accommodate the change in volatilities? The scale variance parameters φ_{xc} and $\varphi_{x\pi}$ decrease enough such that they counteract the increase in the variability of the volatilities. To see this, Table 2 shows the 5th, 50th, and 95th percentiles of the posterior distribution of the unconditional mean of volatility processes $\sigma_{xc,t}$ and $\sigma_{x\pi,t}$, respectively. For both volatilities, the 90% credible interval of the unconditional mean obtained from the macro-only estimation contains the posterior median of $E[\sigma_{xc,t}]$ and $E[\sigma_{x\pi,t}]$ from the bond yield estimation.

Finally, the conditional volatilities of realized consumption growth and inflation are negligible for bond yields but important for tracking the macroeconomic data.[10] Consistent with this view, we do not observe significant changes in the posterior distribution of the model parameters governing these dynamics when we include bond yields in the estimation. Similarly, panels (e) and (f) of Figure

[10]The short-run conditional volatility considerably improves the model's fit of the assumed process of the macro variables. When we do not allow for the short-run volatilities, the log marginal data density drops from 6,054 to 5,870.

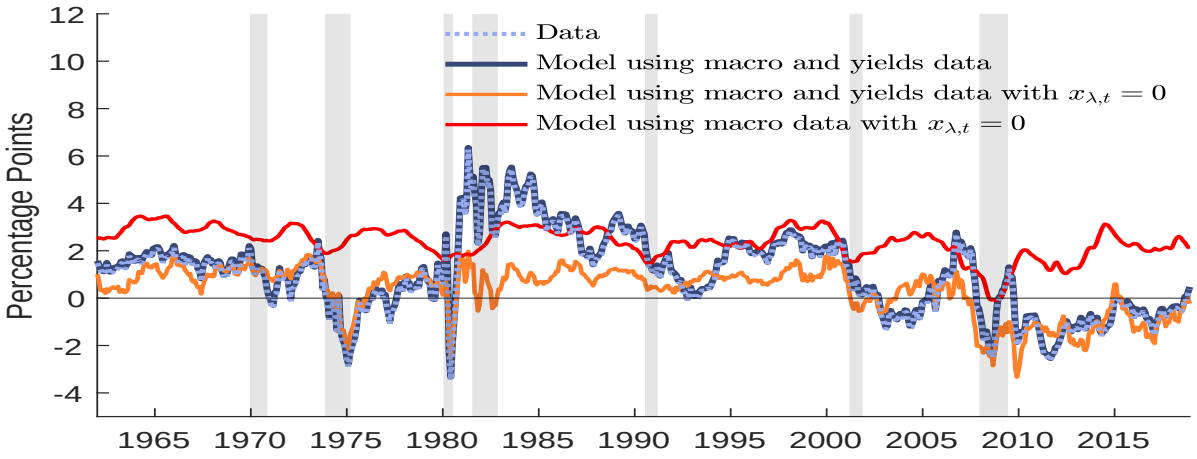

Figure 3. Real risk-free rates.
This figure shows the model-implied risk-free rate. The gray line represents the observed real risk-free rate, and the blue line represents the smoothed posterior median model-implied rate. The orange line represents the risk-free rate estimate by setting $x_{\lambda,t} = 0$. The red line represents the smoothed posterior median model-implied rate obtained by only considering the information contained in the macroeconomic variables. For this case, we set the parameters associated with the household preferences (δ, ψ, γ) to their posterior median estimates reported in Table 1, and we also set $x_{\lambda,t} = 0$. Risk-free rates are annualized. The sample range is January 1962 through December 2018.

2 show that the smoothed stochastic volatilities of realized consumption growth and inflation do not change much when we include asset prices.

Overall, including bond prices in the estimation sharpens inference about the predictable component of expected consumption growth and inflation as well as their conditional volatilities. Specifically, including yield information decreases the posterior uncertainty of the model parameters (as measured by the 90% credible interval) and allows the identification of variable stochastic volatilities that capture more transient economic movements, but, strictly speaking, are statistically indistinguishable from the macro-only estimation.

Preferences and the Real Risk-free Rate. Table 1 also reports estimates of the preference parameters. The coefficient of risk aversion, γ, and the elasticity of substitution, ψ, have a posterior median value of around 13 and 1.5, respectively. These estimates are consistent with the parameter values highlighted in the long-run risk literature and imply preferences for early resolution of uncertainty. Furthermore, the estimated time preference shocks are fairly persistent and volatile. The posterior median estimate of the persistence parameter, ρ_λ, is approximately 0.98, whereas the estimate of φ_λ is 0.12 and implies that shocks to $x_{\lambda,t}$ are roughly as volatile as the volatility of the predictable component of consumption growth.

As shown in equation (8), preference shocks affect the dynamics of the real short rate. To highlight the importance of the preference shock to the real rate, Figure (3) plots the model-implied real risk-free rate. We also overlay the observed real rate (light-blue line) and a counterfactual risk-free rate obtained when we shut down movements in the time preference shocks by setting $x_{\lambda,t} = 0$ (orange line). The main message of Figure (3) is that time preference shocks generate volatile and persistent fluctuations in real rates that are orthogonal to movements in macroeconomic activity.[11] A model that shuts down this channel generates fluctuations in real rates that are too smooth relative to the realized risk-free rate. In addition, the implied rate with macro-only information (red line) fluctuates even less, given the lower variability in the stochastic volatilities of the predictable macro components.

Next, we show that the rich model specification (including the measurement error model, temporal aggregation, several volatility processes, and preference shocks) accounts for an encompassing set of term structure facts. We also discuss the clear trade-offs that the estimation technique faces when fitting different moments of the yield curve.

4 Nominal Yield Curve

4.1 Variation in Yields

The estimated model matches the yields over the entire sample well. Panel (a) of Figure 4 depicts the realized nominal yield on a 5-year bond (dotted light-blue lines) and the smoothed model-implied yield (dark-blue line) for the same bond maturity. We find that the mean absolute pricing errors are small and range from 3.6 to 10.5 basis points for the different bond yields considered. The figure also shows that bond yields substantially vary through time. To understand which components drive this variation, we decompose yields on an nth-period bond as the sum of average ex-ante real rates, future average inflation, and average expected excess returns over the life of the bond:

$$y^{\$}_{t,n} = \frac{1}{n}\sum_{i=1}^{n} E_t r_{f,t+i-1} + \frac{1}{n}\sum_{i=1}^{n} E_t \pi_{t+i} + \frac{1}{n}\sum_{i=1}^{n} E_t rx^{\$}_{t\to t+1,n-i+1}, \tag{14}$$

[11] We do not find strong evidence ex post against the assumption of orthogonal preference shocks. Specifically, we computed the correlation between innovations to the time preference shocks and shocks to consumption growth. The 90% confidence interval of this correlation ranges from -0.08 to 0.10. Similarly, the correlation between innovations to the time preference shocks and shocks to expected consumption growth ranges from 0.01 to 0.15.

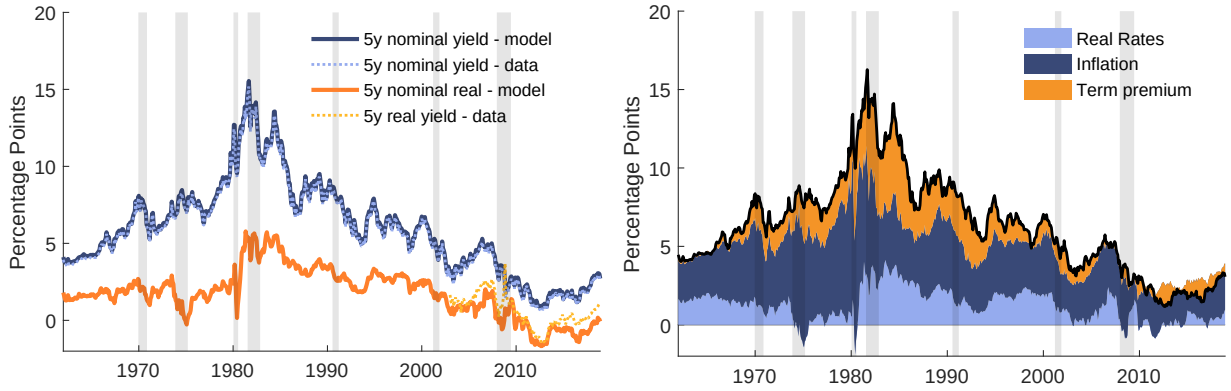

(a) Nominal and Real Bond Yield Estimate

(b) Decomposition of the Nominal Bond Yield

Figure 4. Model-implied 5-year yield.
Panel (a) shows the nominal and real bond yields estimates for a 5-year bond yield. The light-blue line represents the realized 5-year bond yield, and the dark-blue line represents the smoothed model-implied yield. The dark-orange line represents the model-implied real yield obtained by shutting down the inflation channel, whereas the light-orange line shows the observed real yield from TIPS data. Panel (b) shows the posterior median contribution of each state variable to the 5-year bond yield. Light-shaded bars represent recessions, as defined by the National Bureau of Economic Research. Values are annualized. The sample range is January 1962 through December 2018.

where $rx^{\$}_{t\to t+1,n}$ denotes the excess log return on buying an n period bond at time t and selling it at time $t+1$ as an $n-1$ period bond (i.e., $rx^{\$}_{t\to t+1,n} = ny^{\$}_{t,n} - (n-1)y^{\$}_{t+1,n-1} - y^{\$}_{t,1}$). The last term on the right of equation (14) is often described as the bond's nominal term premium. Panel (b) of Figure 4 depicts contributions over time for these three components for a 5-year bond yield. The mean annualized yield during the period that we study is around 5.8%. The major driver is inflation expectations, which account for around 60% of the yield. On the other hand, real rates and the term premium contribute approximately 20% each. These results are for the 5-year bond. Interestingly, and in line with the results of Cieslak and Povala (2015), we find that the contribution of the term premium component increases with maturity.

Real Yields. Real yields are readily available from the model by shutting down the nominal channel. Presenting the model-implied real yields are a useful test on the fit of the real and nominal components. In panel (a) of Figure 4, we plot the model-implied real yield on a 5-year bond (dark orange line) and we find that it closely tracks the 5-year real yield from the TIPS market (dotted light-orange line). Moreover, in panel (a) of Figure 5 we plot the model-implied real yield for maturities of 5, 7, and 10 years. Note that the model-implied real yield curve has a positive slope on average, but the slope became negative for a short period in the early 1980s.

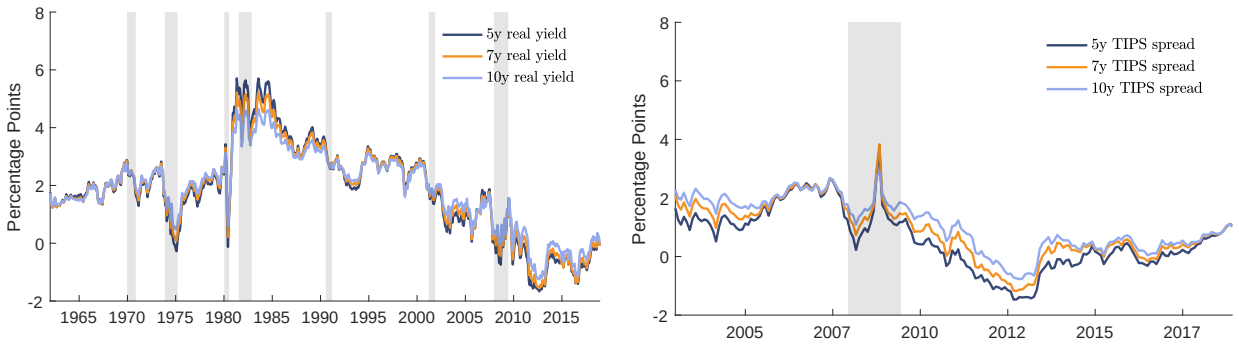

(a) Real Bond Yield Estimates

(b) TIPS spreads

Figure 5. Real yields and TIPS spreads.
Panel (a) shows the model-implied real yield estimatesfor maturities of 5, 7, and 10 years. Panel (b) presents the TIPS spreads defined as the difference between TIPS yields and the model-implied real yield estimates. Light-shaded bars represent recessions, as defined by the National Bureau of Economic Research. Values are annualized. The sample range is January 1962 through December 2018.

A large literature has documented sizeable illiquidities in the TIPS market (e.g., Pflueger and Viceira 2011; Abrahams et al. 2013; d'Amico et al. 2018). However, our model does not formally feature a state variable that captures the liquidity premium TIPS investors demand for holding less liquid securities and we also do not include TIPS data in the estimation. Therefore, we should expected an on average positive spread between TIPS yields and the model-implied real yields. Indeed, panel (a) of Figure 4 shows that this is the case. Next we examine this TIPS spread and find that around 74% of its variations can be explained by proxies of liquidity conditions in the TIPS market.

We start by plotting in panel (b) of Figure 5 the TIPS spread for maturities of 5, 7, and 10 years. For all maturities, the spread exhibit substantial time variations and were particularly high (around 2%) when TIPS for these maturities were reintroduced. The spreads increase to maximum levels (3% - 4% range) during the financial crisis but had been declining ever since. One question that arises is to what extend our TIPS spread captures illiquidities in the TIPS market. To address this question, in Table 3 we report OLS regressions of our 5-year TIPS spread on three widely used proxies of TIPS liquidity.

The first proxy that we consider is the 5-year TIPS bid-ask spread from Tradeweb, since bid-ask spreads are common measures of market liquidity. Another observable measure of TIPS liquidity used in the literature (e.g., Haubrich, Pennacchi, and Ritchken 2012) is the difference between TIPS

	(1)	(2)	(3)	(4)
5y TIPS bid-ask spread	-0.04			-0.14
	[-1.25]			[-1.27]
TIPS - Inflation swap implied real rate		2.37		0.36
		[3.73]		[1.79]
DKW TIPS illiquidity measure			0.97	1.26
			[3.64]	[4.87]
Constant	0.63	-0.56	0.10	-0.07
	[5.06]	[-4.72]	[1.20]	[-0.69]
No. of obs.	170.00	139.00	192.00	139.00
Adj. R^2	0.01	0.30	0.33	0.74

Table 3. TIPS spread and proxies of TIPS liquidity.
This table reports OLS regression coefficients with Newey West t-statistics in squared brackets. In all columns the dependent variable is the 5-year TIPS spread defined as the difference between TIPS yields and the model-implied real yield. The 5-year TIPS bid-ask spread comes from Tradeweb. TIPS - Inflation swap implied real rate is the difference between TIPS yields and real rates computed from inflation swaps and nominal yields of the same maturity. DKW TIPS illiquidity measure comes from d'Amico et al. (2018).

yields and real rates computed from inflation swaps and nominal yields of the same maturity.[12] The third measure that we consider is the TIPS liquidity measure of d'Amico et al. (2018) (hereafter DKW) computed from a Gaussian essentially affine no-arbitrage term structure model. As shown in Column 1 of Table 3, we find no statistical significant relation (t-stats are in brackets) between our TIPS spread and the TIPS bid-ask spread. This result is consistent with results in Fleming and Krishnan (2012) which highlight the limitations of the bid-ask spread as a liquidity measure in the TIPS market. In contrast, the coefficients on the inflation swap based measure and the DKW measure are statistical significant and both carry the expected sign. Together these two variables explain 75% of the variations in our estimates of the 5-year TIPS spread.

Based on this evidence we conclude that the model is able to generate realistic real rate dynamics.

Matching Standard Moments. Although we are targeting the joint distribution of macroeconomic and bond yield variables, it is informative to document how close the model-implied moments are to those observed in the data. Table 4 shows the percentiles of the posterior predictive distri-

[12]Specifically, we use mid-quotes of inflation swap rates for maturities 3, 5, 8, and 10 years from Datastream.

		Macro data			Macro data and bond prices		
	Data	5%	50%	95%	5%	50%	95%
			Macroeconomic moments				
Mean(Δc)	1.93	1.56	1.91	2.37	0.95	1.93	2.92
Std. Dev.(Δc)	1.26	0.92	1.13	1.55	1.09	1.54	2.22
AC1(Δc)	0.52	0.37	0.55	0.71	0.55	0.76	0.88
Mean(π)	3.78	2.52	3.20	4.14	2.80	4.07	5.39
Std. Dev.(π)	2.72	0.95	1.28	2.83	1.22	1.92	3.71
AC1(π)	0.74	0.17	0.46	0.78	0.33	0.64	0.84
Corr(Δc, π)	-0.05	-0.24	-0.01	0.29	-0.51	-0.18	0.16
			Bond yield moments				
Mean							
1y	5.09	3.76	4.55	5.60	3.82	5.01	6.08
5y	5.79	4.89	5.45	6.17	5.11	5.93	7.09
10y	6.44	5.71	6.10	6.59	5.66	6.27	7.22
Std. Dev.							
1y	3.31	1.06	1.39	2.27	1.39	2.01	4.34
5y	2.99	0.67	0.92	1.57	1.12	1.86	4.11
10y	2.92	0.44	0.62	1.09	0.85	1.50	3.65

Table 4. Macroeconomic and bond yield moments
This table reports descriptive statistics for consumption growth, inflation, and nominal yields. We included the sample data moments and the 5th, 50th, and 95th percentiles of the model-implied moments based on 10,000 parameter draws of the posterior distribution with and without bond prices in the estimation. We simulated the series for 684 periods, which equals the number of periods in the sample. To compute the model-implied bond yields based on the macro-only estimation, we set the preference parameters δ, ψ, γ, ρ_λ, and φ_λ equal to the posterior median estimates from Table 1. Values are annualized. The sample range is January 1962 through December 2018.

bution for several sample moments.[13] When bond prices are used in the estimation, the model does a good job of reproducing the macro moments that we considered and matches standard term structure moments, such as the unconditional level, slope, and standard deviation of nominal yields. Note that the model-implied posterior median values are fairly close to their data estimate. It is important to note that when we only consider macro data in the estimation, the model still matches most of these features of the data and generates credible intervals that contain the sample data moments.[14] The only exception is the standard deviation of the nominal yields, which are somewhat lower than the data counterparts.

[13]To this end, we sampled $10,000$ draws of Θ from its posterior distribution and simulated the model for 684 periods, which corresponds to the number of monthly observations in our estimation sample. Doing so gave us $10,000$ simulated trajectories of Y^o. For each trajectory, we computed several statistics.

[14]To simulate yields for the macro-only estimation, we combined the macro-only parameter estimates with the posterior median estimates associated with the preference parameters.

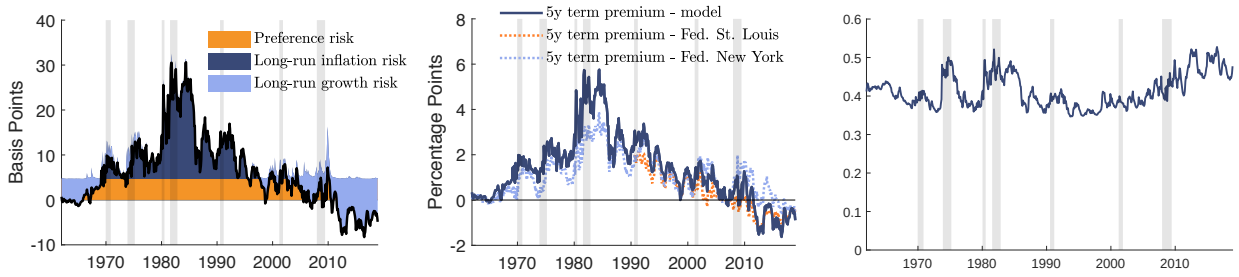

(a) Expected Excess Bond Return (b) Term Premium (c) Maximal Sharpe ratio

Figure 6. Risk premium on a 5-year bond

Panel (a) shows the contribution of long-run growth risk, long-run inflation risk, and preference risk to the 12-month expected excess bond returns for the 5-year bond. Panel (b) shows the posterior median model-implied term premium for the 5-year bond, together with the term premium estimated by Kim and Wright (2005) (orange dotted line, Federal Reserve Bank of St. Louis) and Adrian et al. (2013) (light-blue dotted line, Federal Reserve Bank of New York) for the same bond maturity. Panel (c) shows the maximal Sharpe ratio. The light-shaded bars represent recessions, as defined by the National Bureau of Economic Research. Values are annualized. The sample range is January 1962 through December 2018.

4.2 Risk Premia

With preferences for early resolution of uncertainty, variations in bond risk premia are entirely driven by the conditional volatilities of the predictable components of consumption growth and inflation. Specifically, the one-period nominal expected excess return is determined by the negative covariation between innovations to excess log returns and innovations to the nominal SDF:

$$\begin{aligned} & E_t rx^{\$}_{r\to t+1,n} + \frac{1}{2} Var_t rx^{\$}_{r\to t+1,n} \\ & = -Cov_t(m^{\$}_{t+1}, rx^{\$}_{r\to t+1,n}) \\ & = \sum_{i\in\{\sigma_c,\sigma_\pi,\sigma_{xc},\sigma_{x\pi}\}} \underbrace{-B^{\$}_{i,n-1}\lambda_i \left(2(\varphi_i\sigma)^2\sigma_{h_i}\right)^2}_{\text{Volatility risk}} \underbrace{-B^{\$}_{\lambda,n-1}\lambda_\lambda\sigma^2_\lambda}_{\text{Preference risk}} \underbrace{-B^{\$}_{c,n-1}\lambda_{xc}\sigma^2_{xc,t}}_{\text{long-run growth risk}} \underbrace{-B^{\$}_{\pi,n-1}\lambda_{x\pi}\sigma^2_{x\pi,t}}_{\text{long-run inflation risk}}. \end{aligned} \tag{15}$$

where the $\lambda's$ denote the respective market prices of risk. Hence, the one-period conditional excess return on nominal bonds can be attributed to (1) short- and long-run volatility risks, (2) preference risk, (3) long-run growth risk, and (4) long-run inflation risk. To quantify the magnitude of each source of risk, Figure 6 depicts the posterior median contribution of preference risk, long-run real growth risk, and long-run inflation risk for a one-period expected excess return on a 5-year bond.[15] The mean annualized one-period expected excess return is approximately 0.06%. However, the conditional return substantially varies, ranging from -0.08% to 0.31%. With preference for early

[15] We do not explicitly show the contribution of volatility risk, because its share is too small (less than 0.55%) to distinguish it clearly in the graph.

resolution of uncertainty, long-run growth risk lowers bond risk premia ($\lambda_{xc} > 0$) and accounts for -50% of expected returns. In turn, preference risk and long-run inflation risk ($\lambda_{\lambda} > 0$ and $\lambda_{x\pi} < 0$) generate a positive risk premium of around 76% and 74%, respectively.

In panel (b) of Figure 6, we plot the term premium for a 5-year bond. The figure shows that the model-implied term premium mimics the substantial variations in term premium implied by reduced-form Gaussian affine term structure models (ATSM). To see this, we also depict in panel (b) the term premium estimates of Adrian et al. 2013 (ACM) and Kim and Wright 2005 (KW) that are published by the Federal Reserve Banks of New York and St. Louis, respectively.[16] These reduced-form models produce time variation in term premia via time-varying prices of risk. Note that the three estimates are very similar. In fact, the correlation between the long-run risk model-implied term premium and the estimates of ACM and KW is about 80% and 98%, respectively. The correlation between ACM and KW is 69%.

As described above, time preference shocks add considerable flexibility to a term structure model by breaking the tight link assumed by standard models between variations in yields and fluctuations in the macroeconomy. This extra state variable brings naturally concerns of overfitting. To address these concerns, panel (c) of Figure 6 depicts the model-implied maximal Sharpe ratio given by $\sqrt{Var_t(m^{\$}_{t+1})}$. The maximal Sharpe ratio is quite reasonable. It has a sample average of 0.41 and reaches a peak of around 0.52. At first glance, these values stand in sharp contrast with the evidence of Duffee et al. (2010), who shows that in a yields-only setting the in-sample maximum Sharpe ratios for a 5-factor no-arbitrage model are astronomically large (sometimes exceeding 10^{20}). However, it is important to recall that the 7-factor model proposed in this paper fits not only the nominal yield curve but also the macroeconomic data. In this regard, we show that two of these factors (i.e., the short-run conditional volatilities) improve the fit of the macro aggregates (see Appendix B.4) with marginal effects on bond risk premia (see Appendix B.5).

Matching Return Predictability Evidence. The model is also able to match the bond predictability results documented in Campbell and Shiller (1991) and Cochrane and Piazzesi (2005). Based on simulations of the same length as the data, Table 5 shows that the model-implied distri-

[16]The term premium based on Adrian et al. 2013 can be found here: https://www.newyorkfed.org/research/data_indicators/term_premia.html, whereas the term premium based on Kim and Wright 2005 can be found here: https://fred.stlouisfed.org/series/THREEFYTP5.

		Macro data			Macro data and bond prices		
	Data	5%	50%	95%	5%	50%	95%
Campbell-Shiller regression slope							
3y	-0.66	-0.12	0.33	1.08	-1.21	-0.71	-0.15
5y	-0.90	-0.05	0.40	1.13	-1.83	-1.00	-0.12
10y	-1.39	-0.19	0.23	0.93	-2.92	-1.17	-0.02
Cochrane-Piazzesi regression R^2							
3y	0.29	0.05	0.13	0.31	0.24	0.46	0.78
5y	0.34	0.05	0.13	0.32	0.24	0.41	0.66
10y	0.38	0.06	0.18	0.40	0.17	0.37	0.55
Term premium: Mean							
1y	0.29	0.27	0.27	0.27	0.26	0.40	0.81
5y	1.07	1.13	1.15	1.15	0.82	1.20	2.21
10y	1.63	1.75	1.79	1.80	1.12	1.49	2.38
Term premium: Std. Dev.							
1y	0.40	0.01	0.01	0.01	0.20	0.53	2.20
5y	0.95	0.01	0.01	0.03	0.53	1.34	5.42
10y	1.26	0.01	0.02	0.08	0.52	1.23	4.83

Table 5. Bond return predictability evidence

This table reports descriptive statistics for consumption growth, inflation, and nominal yields. We included the sample data moments and the 5th, 50th, and 95th percentiles of the model-implied moments based on 10,000 parameter draws of the posterior distribution with and without bond prices in the estimation. We simulated the series for 684 periods, which equals the number of periods in the sample. For the Campbell-Shiller regression, we report the slope, β_n, from the following regression: $y_{t+12,n-12} - y_{t,n} = \alpha_n + \beta_n \frac{12}{n-12}(y_{t,n} - y_{t,12}) + \epsilon_{t+12} \quad \text{for} \quad n \in \{36, 60, 120\}$.
For the Cochrane-Piazzesi regression, we report the R^2 from the following regression: $rx^{\$}_{r\to t+12,n} = a_n + b_n \hat{rx}_t + \epsilon_{t+1,n}$, where $\hat{rx}_t$ is the fitted value from $\frac{1}{4}\sum_{n=2y}^{10y} rx^{\$}_{r\to t+1,n} = \gamma_0 + \gamma_1 f^{\$}_{t,1y} + \gamma_2 f^{\$}_{t,3y} + \gamma_3 f^{\$}_{t,5y} + \gamma_4 f^{\$}_{t,7y} + \gamma_5 f^{\$}_{t,10y} + \epsilon_{t+1}$. $rx^{\$}_{r\to t+1,n}$ denotes the excess log return on buying an n period bond at time t and selling it at time $t+1$ as an $n-1$ period bond defined by $rx^{\$}_{r\to t+1,n} = ny^{\$}_{t,n} - (n-1)y^{\$}_{t+1,n-1} - y^{\$}_{t,1} \quad \text{for} \quad n \in \{36, 60, 84, 120\}$. $f^{\$}$ denotes the corresponding forward rates. To compute the model-implied bond yields based on macro data only, we set the preference parameters δ, ψ, γ, ρ_λ, and φ_λ to the posterior median estimates from Table 1. The data estimates for the term premium come from Adrian et al. 2013. Values are annualized. The sample range is January 1962 through December 2018.

bution of the slope coefficients in the term spread regression of Campbell and Shiller (1991) are in line with the estimates based on observed data. The posterior median estimates are negative, decline with maturity, and are considerably close to the point estimates obtained from observed bond yields. Furthermore, we ran the same regressions as in Cochrane and Piazzesi (2005) and conclude that the model-simulated yields also exhibit excess bond return predictability. The model-implied R^2 from the predictive regressions are close to the data estimates and are covered by the 90% confidence interval. Finally, the last rows of Table 5 confirm the message of panel (b) of Figure 6. The model-implied term premium mimics the level and variability of the term-premium, computed from reduced-form models like in Adrian et al. 2013.

Section 3 documents that the addition of yields in the estimation substantially increases the variability of the conditional volatilities. To assess the asset pricing implications of this change in volatilities, Table 5 replicates the same set of regressions using the macro-only parameter estimates. The macro-only model still generates some excess return predictability, as evidenced by the R^2, and matches the level of the term premium. However, the R^2 is considerably smaller; variations in the term premium are close to zero; and the model fails to account for the Campbell-Shiller return predictability evidence.

4.3 Determinants of Bond Yield News

In Section 4.1 we decomposed the level of bond yields as the sum of expected future short-term real rates, expected inflation, and expected future excess returns. We further documented that inflation expectations drive a dominant fraction of yield variations. In this section, we ask what are the main drivers of shocks to bond yields. To preview the results, we conclude that the real rate channel is the most important driver of shocks to yields.

From equation (14), we have that a yield shock can be written as the sum of shocks to the individual components:

$$\epsilon_{y^\$,t,n} = \epsilon_{r,t,n} + \epsilon_{\pi,t,n} + \epsilon_{tp^\$,t,n}, \tag{16}$$

where the shocks are given by

$$\begin{aligned} \epsilon_{y^\$,t,n} &= E_t y^\$_{t,n} - E_{t-1} y^\$_{t,n}, & \epsilon_{r,t,n} &= \tfrac{1}{n}\textstyle\sum_{i=1}^n E_t r_{f,t+i-1} - \tfrac{1}{n}\sum_{i=1}^n E_{t-1} r_{f,t+i-1}, \\ \epsilon_{tp^\$,t,n} &= E_t tp^\$_{t,n} - E_{t-1} tp^\$_{t,n}, & \epsilon_{\pi,t,n} &= \tfrac{1}{n}\textstyle\sum_{i=1}^n E_t \pi_{t+i} - \tfrac{1}{n}\sum_{i=1}^n E_{t-1} \pi_{t+i}. \end{aligned}$$

The variance of yield news is then given by the sum of the variance of the individual component news and twice their respective covariances:

$$\begin{aligned} Var(\epsilon_{y^\$,t,n}) = {} & Var(\epsilon_{r,t,n}) + Var(\epsilon_{\pi,t,n}) + Var(\epsilon_{tp^\$,t,n}) \\ & + 2Cov(\epsilon_{r,t,n}, \epsilon_{\pi,t,n}) + 2Cov(\epsilon_{r,t,n}, \epsilon_{tp^\$,t,n}) + 2Cov(\epsilon_{\pi,t,n}, \epsilon_{tp^\$,t,n}) \end{aligned} \tag{17}$$

Inflation Variance Ratios. Duffee (2018) defines the unconditional inflation variance ratio of an

	Std. Dev. inflation news						Std. Dev. yield news						Inflation variance ratios					
	Data			Model			Data			Model			Data			Model		
	5%	50%	95%	5%	50%	95%	5%	50%	95%	5%	50%	95%	5%	50%	95%	5%	50%	95%
1y	0.12	0.14	0.16	0.07	0.13	0.24	0.25	0.27	0.42	0.26	0.30	0.37	0.12	0.28	0.39	0.08	0.22	0.48
5y	0.09	0.10	0.11	0.05	0.10	0.17	0.18	0.19	0.21	0.19	0.22	0.26	0.17	0.28	0.37	0.08	0.22	0.50
10y	0.06	0.07	0.08	0.04	0.07	0.12	0.16	0.17	0.27	0.14	0.16	0.18	0.07	0.17	0.23	0.07	0.21	0.50

Table 6. Inflation variance ratios.
This table reports the posterior distribution of the standard deviation of shocks to average expected inflation over the life of the bond (Std. Dev. inflation news), standard deviation of yield shocks (Std. Dev. yield news), and the inflation variance ratios. We include the 5th, 50th, and 95th percentiles based on 10,000 parameter draws of the posterior distribution from the macro-finance model. We also report the 5th, 50th, and 95th percentiles from the statistical model. For the statistical model we assume than nominal yields follow a random walk. Standard deviations are expressed as an annualized percentage. The sample range is January 1962 through December 2018.

nth-period nominal bond as the ratio of variance of inflation news to the variance of yield shocks:

$$\text{inflation variance ratio} \equiv \frac{Var(\epsilon_{\pi,t,n})}{Var(\epsilon_{y^{\$},t,n})}. \tag{18}$$

The model-implied ratio for various maturities is readily available from the posterior predictive distribution of the model. However, to compute the data-implied ratio for long horizons, we need to rely on a statistical model for expected inflation and bond yields. In this regard, we first extend the unconditional inflation variance ratios by modeling the dynamics of conditional inflation variance ratios. Accounting for conditional information (stochastic volatility) improves the statistical model's fit and better aligns the data- and model-implied ratios.

To compute the data-implied shocks to the nth-period yield, $\epsilon_{y^{\$},t,n}$, we follow Duffee (2018) and assume that bond yields follow martingales

$$y^{\$}_{t+1,n} = y^{\$}_{t,n} + \sigma_{y_n,t}\ \eta_{y_n,t+1} \qquad \text{and} \qquad \eta_{y_n,t+1} \sim i.i.d.N(0,1) \qquad \text{where} \tag{19}$$

$$\sigma_{y_n,t} = \sigma_{y_n} exp(h_{y,t}), \quad h_{y,t+1} = \rho_{h_y} h_{y,t} + \sigma_{h_y}\omega_{y,t+1}, \quad \text{and} \quad \omega_{y,t+1} \sim i.i.d.N(0,1),$$

where shocks to yields are $\epsilon_{y^{\$},t,n} = \sigma_{y_n,t}\ \eta_{y_n,t+1}$. For bond yields, the martingale assumption generates lower forecast errors than both survey-based (e.g., Cieslak 2016) and parametrized models (e.g., Duffee 2002). For consistency, we extract inflation forecast innovations, $\epsilon_{\pi,t,n}$, from the process of inflation specified in equations (3), (4) , and (5) using only macro data.

Table 6 reports the result. We report percentiles of the posterior predictive distribution for 1-, 5-, and 10-year bonds based on simulations of the same length as the data. The last columns show the inflation variance ratios along with the 90% credible interval. In the previous section we found that inflation expectations mainly drive the yield level, given that they are highly persistent. However, because they update little from month to month, they only contribute a small part of the variance of bond yield shocks. Note that the data-implied conditional inflation variance ratios are small, in the neighborhood of 17% to 28%, and are less than 40% for all the bond maturities that we considered (as shown by the 95% credible set). These results are, by and large, consistent with the unconditional estimates at the quarterly frequency of Duffee (2018) and can be viewed as corroborating his findings. Importantly, the model-implied inflation variance ratios are in close agreement with the data-implied estimates, and the 90% credible interval contains the corresponding posterior medians. This is a novel moment that our model is able to match. Based on the evidence, we conclude that the model does not resort to an expected inflation channel that counterfactually dominates the variation in nominal yield shocks.

A successful model should match not only the sample inflation variance ratio but also the sample volatilities of yield shocks (or inflation shocks). With this in mind, Table 6 also reports the percentiles of the posterior distribution of the standard deviation of shocks to average expected inflation (SD Inflation News) and the standard deviation of yield shocks (SD Yield News). Many aspects of this table are noteworthy. Here, we just mention three. First, the model also generates plausible values of the numerator and denominator of the inflation variance ratios in equation (18). All the data-implied moments are well within the 90% credible interval of the corresponding posterior predictive distribution. Second, in the model and in the data, the standard deviation of inflation and yield shocks decline as maturity increases. Third, shocks to nominal yields are highly variable. Across bond maturities, the standard deviation of yield news accounts for approximately 13% of the overall yield standard deviation.

Robustness. The results in Table 6 are based on estimates at the monthly frequency and account for stochastic volatility, while Duffee (2018) presents results based on a quarterly frequency without stochastic volatility. As these magnitudes are not directable comparable we present several robustness checks in the Appendix. Specifically, we repeated the same exercise for a quarterly version

		Contributions to total yield news variance					
Maturity	Std. Dev. yield news	[1] Average expected real rate	[2] Average expected inflation	[3] Average expected excess returns	2Cov([1], [2])	2Cov([1],[3]	2Cov([2],[3]
1y	0.30	0.77	0.22	0.01	-0.02	0.02	0.00
	[0.26,0.37]	[0.54,0.91]	[0.08,0.48]	[0.00,0.03]	[-0.03,-0.00]	[0.01,0.02]	[0.00,0.00]
5y	0.22	0.68	0.22	0.08	-0.05	0.07	0.00
	[0.19,0.26]	[0.51,0.77]	[0.08,0.50]	[0.06,0.10]	[-0.12,-0.02]	[0.05,0.09]	[0.00,0.00]
10y	0.15	0.57	0.21	0.19	-0.08	0.11	0.00
	[0.14,0.18]	[0.47,0.64]	[0.07,0.50]	[0.15,0.22]	[-0.20, -0.03]	[0.08,0.13]	[0.00,0.00]

Table 7. Yield news variance decomposition
The table reports model-implied variance decompositions of nominal yield news. Yield news can be decomposed as the sum of news about ex-ante real rates, expected average inflation, and excess returns. The unconditional variance of yield news is then given by the sum of the individual component variances and twice their respective covariances. We report the contribution of these components to total yield news variance. The contributions sum to 1. Yields are expressed as a percentage per year. Brackets display [5%, 95%] confidence bounds. The sample range is January 1962 through December 2018.

of the statistical model with and without stochastic volatility. In Appendix B.6, we report the estimates in detail, while briefly describing the results here. For all bond maturities considered, expected inflation news does not contribute much to the variation of bond yield innovations. The posterior medians are around 12 percent. Allowing for stochastic volatility almost doubles the inflation variance ratios relative to the homoskedastic case and improves the model fit as measured by the log marginal data density.

Other Determinants of Yield News. We know from Duffee (2018) and the conditional estimates of this paper that news about expected inflation contribute little to the overall variation on yield shocks. However, current empirical literature does not agree on the answer to the question "what is the main driver of shocks to bond yields?" For instance, estimates in Hanson and Stein (2015) imply that term premia shocks are the dominant source at the long end of the yield curve, while results in Nakamura and Steinsson (2018) suggest that news to expected future short-term interest rates are more important. Next, we answer this question more forcefully given the advantage of having a structural model.

Table 7 reports the fraction of total yield news variance explained by the individual components on the right-hand side of equation (17). The contributions sum to 1. We report percentiles of the posterior predictive distribution for different bond maturities based on simulations of the same

length as the data. Table 7 documents three new results. First, according to the model estimates, nominal yield shocks are primarily news about real rates. The contribution of real rate news to the total variance of shocks to nominal yields ranges from about 77% at the short end to around 57% at the long end. Second, the importance of term premia shocks increases with maturity, but they do not become the dominant source of yield news variation. For instance, at the 10-year maturity, 19% of the variance of yield shocks is attributable to term premia shocks, which is significantly lower than the contribution of real rates news. Third, the contributions of the covariance terms are small and practically cancel each other out. The covariance between news about expected real rates and expected inflation is negative because of the nonneutral effect of inflation on growth. Intuitively, bad news for expected inflation translates into bad news for expected consumption growth, which, in turn, lowers expected future real rates (the appendix shows the math). This negative covariance is offset by the positive covariance between news about expected real rates and expected excess returns. Notably, the 90% credible intervals are reasonably tight, allowing us to reliably disentangle the contribution of each individual component from the total variance of yield shocks.

In Appendix B.7, we present two sets of results that indicate that our variance decomposition does not necessarily contradict the implied estimates in the reduced-form literature. In essence, in the appendix we show that due to lack of economic structure, these models cannot pin down the relative contributions of news about average expected real rates and news to the term premium. First, we computed the fraction of total yield news variance explained by term premia shocks for various leading term structure models (e.g., Duffee (2018), Cieslak and Povala (2015), Kim and Wright (2005), and Adrian et al. (2013)). The point estimates indicate that at the 10-year maturity between 20% and 39% of the variance of yield shocks is attributable to term premia shocks. These point estimates are fairly close to our 19% posterior median estimate and their confidence bounds nest the right tail of the posterior distribution from our model-implied term premia variance ratio. Second, full yield decompositions in Duffee (2018) and Cieslak and Povala (2015) show that these models cannot distinguish statistically between the role played by the real short rate channel and the term premia channel.[17] The point estimates imply that real rate shocks play a dominant contribution at the 1-year maturity, while term premia news is more important at the 10-year maturity. However,

[17]For the models in Kim and Wright (2005) and Adrian et al. (2013) we cannot distinguish shocks to real rates from shocks to inflation since these two papers do not model the process of inflation and expected inflation.

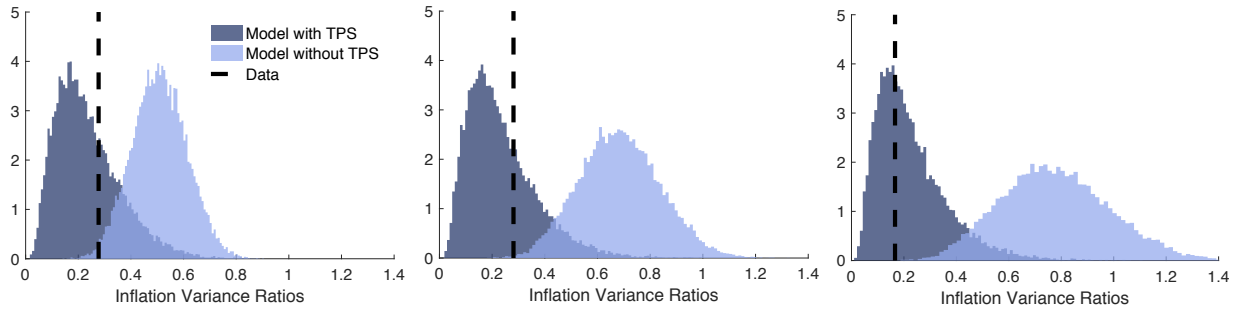

(a) 1y (b)5y (c) 10y

Figure 7. Inflation variance ratios and preference shocks
This figure shows the probability density function of the inflation variance ratios obtained from two different versions of the macro-finance model and for different bond maturities. The dark-shaded density is based on the macro-finance model that includes time preference shocks, whereas the light-shaded density does not include them. The dashed black line represents the posterior median inflation variance ratios from the statistical model. The sample range is January 1962 through December 2018.

for both models the confidence bounds are big and do not preclude the possibility that real rate shocks are the dominant source of yield news at the long end of the yield curve.

In principle, it is possible that we are overestimating the role of the real short channel and underestimating the role of risk premia at long maturities. In the model, the conditional volatilities of expected consumption growth and inflation drive variations in the term premia. Empirically, however, as shown in Table 1 and Figure 2 , these conditional volatilities become substantially more variable relative to estimates based on macro-only information in order to match risk premia dynamics. The tension might arise because these volatilities can only increase so much before distorting the fit on the macroeconomic variables. Overall, we do not find evidence that suggests that this tension is quantitative important for the empirical relevant parameter values. The estimated model is able to account for many asset pricing moments including variations in risk premia without distorting the fit of the macroeconomic variables.

4.4 Importance of Preference Shocks

As shown in Section 3, empirically, time preference shocks allow the model to generate realistic real rate dynamics. Next we show that this state variable also leads to plausible inflation variance ratios.

In panels (a) through (c) of Figure 7, we plot the probability density distribution of the model-implied inflation variance ratios for 1-, 5-, and 10-year bonds, respectively. The dark-blue shaded densities are based on the model that includes time preference shocks (model with TPS) and the

dashed black lines denote the data-implied posterior median inflation variance ratios (Data). We previously showed these values in the last columns of Table 6. To highlight the importance of the preference shocks, we computed the inflation variance ratios implied by a model that does not allow them.[18] We depict these values via the light-blue shaded densities (model without TPS). Note that the implied densities shift to the right to values approximately centered on 80%. Moreover, the 90% credible intervals do not contain the data-implied posterior median estimates. Hence, in the absence of the preference shocks, the model seems to rely too heavily on the volatility of inflation expectations to fit the yield curve.

Trade-off. Appendix B.8 further shows that parameterizations that are successful in reducing the inflation variance ratios, hamper the model's ability to match other relevant moments of the yield curve. For instance, enlarging the variability and persistence of the time preference shocks reduces the inflation variance ratios. However, more persistent and variable time preference shocks also produces similar movements in real rates, generates an increasingly steep term structure, increases the level of the term premium, and mutes the excess bond return predictability evidence. Given this trade-off, time preference shocks might even increase the onus on the inflation process to match these other moments of the data. Ultimately, the relative strength of these offsetting effects is a quantitative issue that implicitly enters the likelihood function of our state-space model.

What Drives Preference Shocks? A key advantage of our estimation procedure is that as a by-product, we also obtain a time-series estimate of the time preference shocks. Therefore, we can then examine the relation between these preference shocks and other financial variables.

Time preference shocks determine the attitudes of the representative household toward savings. With this in mind, an interesting candidate to relate the smoothed demand shocks estimates is the adjusted National Financial Conditions Index (ANFC index), published by the Federal Reserve of Chicago. This index measures risk, liquidity, and leverage in money, debt, and equity markets

[18] To this end, we solved the model without time preference shocks, casted it into a state-space representation, and utilized the same estimation procedure. We ensured that the model estimation matched the same data moments and predictability results as the model that assumes time preference shocks. Alternatively, we could have computed the inflation variance ratios by setting $\rho_\lambda = 0$ and $\varphi_\lambda = 0$ and keeping the rest of the parameter estimates unchanged. When we did this, we arrived at a similar conclusion. The implied ratios are too high relative to the data, and they misss other moments of the yield curve, such as the slope.

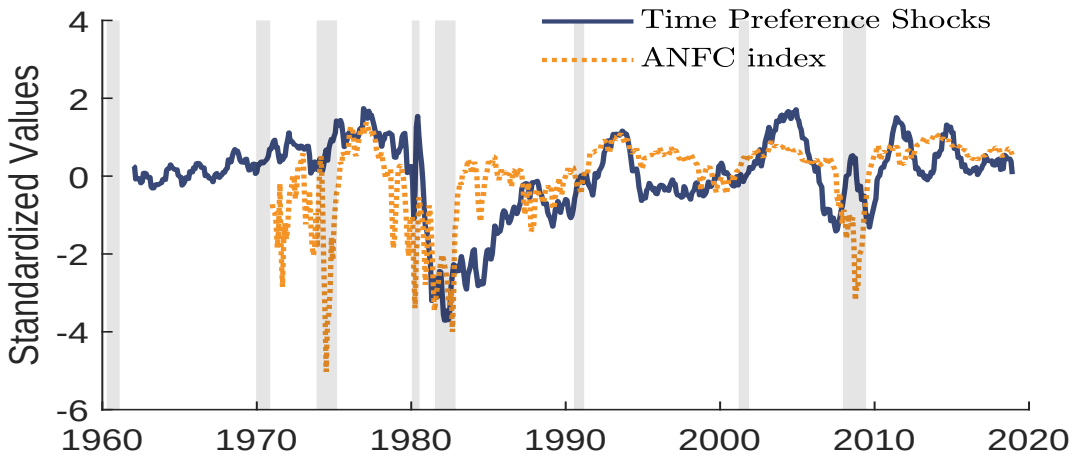

Figure 8. Time preference shocks and the financial conditions index
This figure shows the latent time preference shocks state variable filtered from the macro-finance model along with the adjusted National Financial Conditions Index, published by the Federal Reserve Bank of Chicago. Light-shaded bars represent recessions, as defined by the National Bureau of Economic Research. The adjusted National Financial Conditions Index started in 1973 and is published at https://alfred.stlouisfed.org/series?seid=ANFCI. To ease an interpretation of the figure, we standardized both series and show the negative value of the National Financial Conditions Index. The sample range is January 1962 through December 2018.

and isolates a component of financial conditions uncorrelated with economic conditions.[19] Figure 8 depicts the smoothed estimate of preference shocks (blue line) and the ANFC index (dashed orange line). To ease the figure's interpretation, we standardized both series and show the negative value of the ANFC index. Given these adjustments, a positive value of the ANFC index suggests loose financial markets relative to the historical average. The correlation between these series is remarkably high, with a value of around 53%, suggesting that tighter financial conditions today are associated with a lower willingness of agents to save for future periods and therefore higher bond yields.

To further investigate the connection between the time preference shocks variable and other measures of market liquidity, in Table 8 we report results of OLS regressions of the time preference shocks on various popular market measures. Column (2) shows that there is a negative and statistically significant relation between the time preference shocks variable and default spreads, as measured by the spread in yields between Baa- and Aaa- rated bonds. Similarly, Column (3) shows a negative and significant relation between the CBOE VIX index and the time preference shocks series. Noteworthy, as shown in Column (8), the statistical significance of these two variables dis-

[19]The Adjusted National Financial Conditions Index is provided by the Federal Reserve Bank of Chicago; the series starts in 1973 and can be downloaded at https://alfred.stlouisfed.org/series?seid=ANFCI.

	(1)	(2)	(3)	(4)	(5)	(6)	(7)	(8)
ANFC index	-0.46							-0.32
	[-7.42]							[-2.85]
Baa-Aaa		-1.03						0.20
		[-8.94]						[0.94]
VIX			-0.02					0.02
			[-3.59]					[1.59]
Fin. Stress Index				-0.36				-0.55
				[-7.49]				[-2.40]
CFNA index					0.08			0.17
					[1.36]			[1.33]
HPW measure						-0.14		0.15
						[-6.46]		[1.45]
FG measure							-0.25	-0.08
							[-5.32]	[-1.39]
No. of obs.	576	684	348	300	622	384	376	279
Adj. R^2	0.27	0.10	0.04	0.16	0.00	0.10	0.07	0.34

Table 8. Time preference shocks and proxies of market distress.
This table reports OLS regression coefficients with Newey West t-statistics in squared brackets. In all columns the dependent variable is the filtered time preference shocks variable. In all columns the dependent variable is the filtered time preference shocks variable. ANFC index denotes the the adjusted National Financial Conditions Index. Baa-Aaa is the spread in yields between Baa- and Aaa- rated bonds and the VIX index denotes the CBOE VIX index. Fin. Stress Index and CFNA index are the St. Louis Fed's Financial Stress Index and the Chicago Fed National Activity Index. The HPW and FG measures are the liquidity measures computed by Hu et al. (2013) and Fontaine and Garcia (2012), respectively.

appears once we include the ANFC index in the regressions. This is not surprising since the ANFC index measures the joint evolution of 105 indicators of financial activity including the information contain in the Baa-Aaa yield spread and the VIX index.

Columns (4) and (5) of Table 8 examine the connection between the time preference shocks variable and other broad based measures of financial conditions and economic activity. The first is the St. Louis Fed's Financial Stress Index that measures the degree of financial stress in the U.S. markets. This measure tracks 18 data series including various interest rates, yield spreads, and other financial variables such as the VIX index. As show in Column (4), this financial stress measure has a negative statistically significant relation with the time preference shocks variable. Noteworthy, in a bivariate OLS regression that includes both the ANFC index and the Financial Stress Index we find that the slope coefficients are negative for both variables and highly statistically significant.

The second broad measure that we consider is the Chicago Fed National Activity Index (CFNA index). The CFNA index is a weighted average of 85 indicators and measures the overall U.S. economic activity and related inflationary pressure. Since in the model the time preference shocks are orthogonal to economic growth and inflation, it is important to make sure that movements in time preference shocks are not related to broad measures of macroeconomic activity. Column (5) shows that this is indeed the case. We find no statistical relation between the CFNA index and the time preference shocks variable.

Two important series measuring liquidity and financial conditions in the fixed income literature are proposed by Fontaine and Garcia (2012) and Hu et al. (2013) (hereafter FG and HPW, respectively). Fontaine and Garcia (2012) identify and measure the value of funding liquidity from the cross-section of treasury securities, while Hu et al. (2013) propose a market-wide liquidity measure computed as pricing errors in yields. These measures have been shown to be priced risk factors with strong excess bond return predicability power. It is therefore interesting to see how these liquidity measures relate to the filtered time preference shocks. As shown in Columns (6) and (7), regressing time preference shocks on these two measures, we find a negative and statistically significant relation. However, as shown in Column (8), these negative relations disappear once we include the ANFC index and the Financial Stress Index in the regression. In other words, time-preference shocks are highly correlated with market distress measures in a way that are uncorrelated with popular liquidity premium measures in the Treasury market.

Conditional Volatility in Preference Shocks. We assume that time preference shocks are homoscedastic, and, therefore, they do not drive variations in risk premia. We assess the homoskedastic assumption as follows. First, in the data, the liquidity measures that are correlated with the extracted preference shocks (i.e., the ANFC index and the Fin. Stress Index) don't seem to predict, like in the model, excess bond returns. Second, we solve and simulate a model that allows for stochastic volatility in the time preference shocks. These simulations suggest that adding stochastic volatility to $x_{\lambda,t}$ does not help one match the inflation variance ratios and significantly distorts other moments of the term structure. Third, we estimate this extended model and find that the MCMC chain sends the persistence and scale variance parameters governing the stochastic volatility process of $x_{\lambda,t}$ toward zero. Based on these results, we conclude that there is no strong

evidence that contradicts the homoskedastic assumption of shocks to $x_{\lambda,t}$.

4.5 Cyclical Properties of Inflation and Bond Pricing

We introduced inflation nonneutrality via the parameter $\rho_{c\pi}$. As shown in Table 1, $\rho_{c\pi}$ is estimated to be negative, which is consistent with countercyclical inflation. However, recent evidence suggests that for the last two decades the cyclical properties of inflation have changed, as inflation has become predominantly procyclical (see e.g., Campbell, Pflueger, and Viceira 2014; Campbell, Sunderam, and Viceira 2017; Song 2017). This suggests that the parameter $\rho_{c\pi}$ potentially switched signs over time, ultimately affecting bond pricing. This section addresses the time-varying cyclical properties of inflation.

We extend the benchmark model by introducing pro/counter-cyclical inflation via the following state-transition equation:

$$\begin{aligned} \Delta c_{t+1} &= \mu_c + x_{c,t} + \sigma_{c,t}\eta_{c,t+1}, \quad \eta_{c,t+1} \sim N(0,1), \\ x_{c,t+1} &= \rho_{cc}x_{c,t} + \rho_{c\pi}(S_t)x_{\pi,t} + \sigma_{xc,t}\eta_{xc,t+1}, \quad \eta_{xc,t+1} \sim N(0,1), \end{aligned} \tag{20}$$

where the rest of the specification for inflation and the volatility processes is the same as that in Section 2.2. $S_t \in \{0,1\}$ denotes the regime indicator variable. The regime-switching parameter, $\rho_{c\pi}(S_t)$, attempts to capture transitions from counter-cyclical to pro-cyclical inflation periods. Transitions between regimes are governed by a standard Markov process. With regime changes, agents consider three sources of uncertainty. Specifically, when agents form expectations, they face uncertainty about the regime that will prevail in the next period, uncertainty about the current regime, and uncertainty about the Gaussian shocks to the state variables. Appendix D provides details about the model's solution and estimation procedure, while we briefly discuss the results here.

The extended model delivers three main results. First, consistent with the previous literature, the cyclical properties of inflation are subject to regime switches. Figure 9 shows the smoothed probabilities assigned to the procyclical inflation regime (top panel). The countercyclical inflation regime prevails over the early years, during the first half of the 1990s and for a couple of years in the early 2000s. Procyclical inflation was dominant for the last part of the sample. Based on

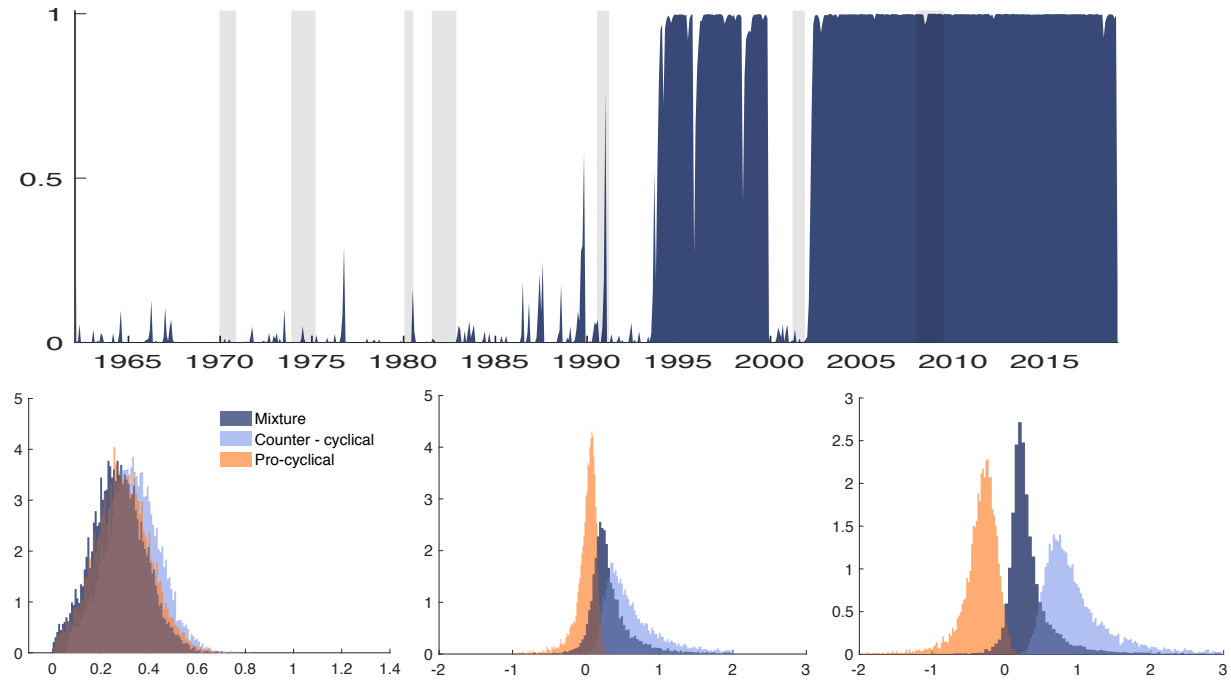

(a) Inflation Variance Ratios: 10Y (b) Slope: 10Y - 5Y (c) Term Premium: 10Y

Figure 9. Cyclical properties of inflation

The top panel shows the posterior median probability for the procyclical inflation regime. Light-shaded bars represent recessions, as defined by the National Bureau of Economic Research. The bottom panels show the model-implied distribution for several moments. The dark-blue area takes into account the possibility of regime changes. The light-blue and light-orange areas assume that a particular regime is in place over the entire sample. The slope of the yield curve and the average term premium are annualized. The sample range is January 1962 through December 2018.

the posterior median estimates, the unconditional regime probabilities for the counter/procyclical inflation regimes are 0.6 and 0.4, respectively. The timing of the regime changes roughly coincides with the estimates of Song (2017), who models regime switching via a conditional covariance matrix of shocks.

Second, the regime in place has important implications for the slope and the term premium moments. In the countercyclical inflation regime, the implications for bond pricing are very similar to those for the benchmark model. That is, the nominal yield curve slopes upward (panel (b)), and the term premium is positive (panel (c)). In contrast, during the procyclical regime, nominal bonds hedge against bad economic states. In this regime, periods of low inflation tend to be periods of low consumption growth and hence high marginal utility. Thus, nominal bonds provide insurance against bad economic states. Therefore, the term premium is negative (panel (c)) and produces a downward-sloping curve that counteracts the upward-sloping curve from the time preference shocks channel. We obtained these results by assuming that the counter/procyclical inflation regimes

prevail over the entire sample. However, when we allow for regime changes, the bond prices take into account both the regime in place and the probability of moving across regimes through the law of iterated expectations. Notably, in this "mixture" of regimes, the unconditional moments are qualitatively similar to those in the predominant countercyclical regime and hence to those in the benchmark specification.

Third, the regime in place does not significantly affect the inflation variance ratios. In principle, the model generates variations in real rates, in part, by the nonneutrality of inflation. During the countercyclical regime, positive shocks to expected inflation are bad news for expected consumption growth, translating into negative real rate news. Hence, real rate news and inflation news are negatively correlated, potentially increasing the model-implied inflation variance ratios. In contrast, during the procyclical regime, these two shocks are positively correlated which could reduce the implied ratios. In practice, however, panel (a) of Figure 9 shows that this channel is quantitatively small for the empirically relevant parameter values. The inflation variance ratios are quite similar in both regimes and in the mixture. Thus, in the absence of time preference shocks, the regime-switching model would excessively rely on the inflation expectations news channel.

Based on these results, we conclude that accounting for the time-varying cyclical properties of inflation does not reduce the onus on the inflation process to fit the yield curve. Moreover, once we allow for regime changes, the unconditional model's simulated moments are similar to the moments that we obtained under the benchmark specification. Although, within each regime, bond yields exhibit interesting properties from which the benchmark specification model abstracts.

5 Conclusion

We develop and estimate a nonlinear Bayesian state-space macro-finance endowment model that accounts for key bond market features, without resorting to an expected inflation channel that overly dominates the variation in nominal yield shocks and without sacrificing the fit of the macroeconomic aggregates. The key ingredients of the model include time preference shocks, time variation in the predictable component of consumption growth and inflation, non-neutral effects of inflation on growth, multiple stochastic volatility processes, and measurement errors and time-aggregation of consumption. With preference for early resolution of uncertainty, variations in bond risk premia are

driven entirely by fluctuations in expected growth and expected inflation uncertainty. The shocks to time rate of preference, on the other hand, generate volatile and persistent fluctuations in expected short-term real rates. This, in turn, allows the model to match the empirical volatility of nominal yield shocks without relying too much on the volatility of expected inflation news. Finally, we show that the time-varying volatilities in the *i.i.d.* component of consumption growth and inflation, the measurement error structure, and time aggregation of consumption are negligible features for the nominal yield curve but are important for the tracking the macroeconomic series.

To assess the empirical validity of these different channels, we estimate the model using a Bayesian MCMC particle filter approach, which, among other things, addresses one crucial trade-off of the model: although time preference shocks help generate news about real rates, they significantly deteriorate the model's implications for bond return predictability. Importantly, the model delivers smoothed estimates of the state variables, allowing us to decompose the yield curve in real time. We find that, inflation expectations drive the level yields, whereas news about real rates is the dominant driver of shocks to nominal bond yields.

The estimation shows that preference shocks are strongly negatively correlated with liquidity measures and stresses in financial markets. This result provides new interesting insights about the type of features that are worth pursuing in macro-finance models. Such information can be used, for instance, to help model a liquidity provider intermediary-sector to New Keynesian asset-pricing models (e.g., Kung 2015; Rudebusch and Swanson 2012). Doing so might enlarge the real-rate channel without distorting the model's implications along other dimensions. Thus, the estimation output is helpful for not only economic interpretation but also guiding future research by shedding light on the type of features that are worth pursuing in macro-finance models.

Appendix

A Economic Model

Appendix A provides de model solution and it is organized as follows. In Section A.1, we introduce the model set-up. In Section A.2, we present the solution to the price-consumption ratio. In Section A.3, we write the equilibrium real and nominal stochastic discount factor (SDF). In Section A.4, we solve the equilibrium nominal bond yield loadings. In sections A.5 and A.6, we derive the equilibrium expected excess bond returns and the term premium dynamics. Finally, in Section A.7, we solve the model-implied inflation variance ratios.

A.1 Model Set-Up

In this section, we provide a solution for the economic model. The assumed stochastic process for the logarithm of consumption growth, Δc_{t+1}, and the logarithm of the inflation rate, π_{t+1} are:

$$\begin{aligned} \Delta c_{t+1} &= \mu_c + x_{c,t} + \sigma_{c,t}\eta_{c,t+1} \\ \pi_{t+1} &= \mu_\pi + x_{\pi,t} + \sigma_{\pi,t}\eta_{\pi,t+1} \end{aligned} \tag{A.1}$$

where the process for the predictable components and the stochastic volatilities are given by:

$$\begin{aligned} x_{c,t+1} &= \rho_{cc}x_{c,t} + \rho_{c\pi}x_{\pi,t} + \sigma_{xc,t}\eta_{xc,t+1} \\ x_{\pi,t+1} &= \quad\quad + \rho_{\pi\pi}x_{\pi,t} + \sigma_{x\pi,t}\eta_{x\pi,t+1} \end{aligned} \tag{A.2}$$

and

$$\sigma_{i,t} = \varphi_i \sigma exp(h_{i,t}), \quad \text{with} \quad h_{i,t+1} = \rho_{h_i} h_{i,t} + \sigma_{h_i}\omega_{i,t+1}$$

All innovations are distributed according to

$$\eta_{i,t+1}, \quad \omega_{i,t+1}, \quad \epsilon_{i,t+1} \quad \sim i.i.d.N(0,1) \quad \text{for} \quad i = \{c, \pi, xc, x\pi\}$$

Given the assumed preference for the representative agent, the logarithm of the real stochastic discount factor (SDF) is given by

$$m_{t+1} = \theta log\delta + \theta x_{\lambda,t+1} - \frac{\theta}{\psi}\Delta c_{t+1} + (\theta - 1) r_{c,t+1} \tag{A.3}$$

with $\theta = \dfrac{1-\gamma}{1-\frac{1}{\psi}}$. The time preference shocks evolve as:

$$x_{\lambda,t+1} = \rho_\lambda x_{\lambda,t} + \sigma_\lambda \eta_{\lambda,t+1} \quad \text{with} \quad \eta_{\lambda,t+1} \sim i.i.d.N(0,1) \tag{A.4}$$

To entertain an analytical model solution we rely on two different approximations. The first, proposed by Campbell and Shiller (1988), involves a log-linear Taylor expansion to $r_{c,t+1}$:

$$r_{c,t+1} = \kappa_0 + \kappa_1 pc_{t+1} - pc_t + \Delta c_{t+1} \tag{A.5}$$

where pc_{t+1} is the log price-to-consumption ratio, and κ_0 and κ_1 are constants determined endogenously by the unconditional mean of the price-consumption ratio, $\bar{pc}$, in the economy and are given by

$$\kappa_1 = \frac{exp(\bar{pc})}{1 + exp(\bar{pc})} \quad \text{and} \quad \kappa_0 = log(1 + exp(\bar{pc})) - \kappa_1 \bar{pc}$$

The second approximation, considers a linear approximation of the volatility process around the unconditional mean of h as in Schorfheide et al. (2017):

$$\begin{aligned}
\sigma^2_{i,t+1} &\approx (\varphi_i \sigma)^2 + 2(\varphi_i \sigma)^2 h_{i,t+1} \\
&= (\varphi_i \sigma)^2 + 2(\varphi_i \sigma)^2 \rho_{h_i} h_{i,t} + 2(\varphi_i \sigma)^2 \sigma_{h_i} \omega_{i,t+1} \\
&\approx (\varphi_i \sigma)^2 + \rho_{h_i}(\sigma^2_{i,t} - (\varphi_i \sigma)^2) + 2(\varphi_i \sigma)^2 \sigma_{h_i} \omega_{i,t+1} \\
&= \sigma^2_{i,0} + \nu_i(\sigma^2_{i,t} - \sigma^2_{i,0}) + \sigma_{\omega_i} \omega_{i,t+1} \quad \text{for} \quad i = \{c, \pi, xc, x\pi\}
\end{aligned} \tag{A.6}$$

where to simplify notation we defined

$$\nu_i = \rho_{h_i}, \quad \sigma^2_{i,0} = (\varphi_i \sigma)^2, \quad \text{and} \quad \sigma_{\omega_i} = 2(\varphi_i \sigma)^2 \sigma_{h_i}.$$

The Euler equation is

$$E_t[exp(m_{t+1} + r_{t+1})] = 1 \tag{A.7}$$

which can be used to price any asset return r_{t+1} in the economy.

A.2 Solution for the Price-Consumption Ratio

In equilibrium, the price-consumption ratio is linear in the state variables:

$$pc_t = A_0 + A_c x_{c,t} + A_\pi x_{\pi,t} + A_\lambda x_{\lambda,t} + A_{\sigma_c}\sigma^2_{c,t} + A_{\sigma_\pi}\sigma^2_{\pi,t} + A_{\sigma_{xc}}\sigma^2_{xc,t} + A_{\sigma_{x\pi}}\sigma^2_{x\pi,t} \tag{A.8}$$

To solve for the coefficients As we use the log-linear approximation for $r_{c,t+1}$ in (A.5) and substitute it along with the SDF in (A.3) in the Euler equation in (A.7). Using the method of undetermined coefficient it follows that:

$$A_c = \frac{1-\frac{1}{\psi}}{1-\kappa_1\rho_{cc}}, \quad A_\pi = \kappa_1\rho_{c\pi}\frac{1-\frac{1}{\psi}}{(1-\kappa_1\rho_{cc})(1-\kappa_1\rho_{\pi\pi})}, \quad A_\lambda = \frac{\rho_\lambda}{1-\kappa_1\rho_\lambda} \tag{A.9}$$

$$A_{\sigma_c} = \frac{(1-\gamma)(1-\frac{1}{\psi})}{2(1-\kappa_1\nu_c)}, \quad A_{\sigma_\pi} = 0, \quad A_{\sigma_{xc}} = \theta\frac{(\kappa_1 A_c)^2}{2(1-\nu_{xc})}, \quad A_{\sigma_{x\pi}} = \theta\frac{(\kappa_1 A_\pi)^2}{2(1-\nu_{x\pi})}$$

and the constant is given by

$$A_0 = (1-\kappa_1)^{-1}\{log\delta + (1-\frac{1}{\psi})\mu_c + \kappa_0 + \frac{1}{2}\theta(1+\kappa_1 A_\lambda)^2\sigma^2_\lambda + \kappa_1[\sum_{i\in\{\sigma_c,\sigma_\pi,\sigma_{xc},\sigma_{x\pi}\}}(1-\nu_i)A_i\sigma^2_{0,i} + \frac{1}{2}\kappa_1\theta A_i^2\sigma^2_{\omega_i}]\} \tag{A.10}$$

To complete the derivation of the equilibrium price-consumption ratio we need to solve for steady state value of pc_t. To this end, we need to solve the following system of equations:

$$\begin{aligned}
\bar{pc} &= A_0(\kappa_1,\kappa_0) + \sum_{i\in\{\sigma_c,\sigma_\pi,\sigma_{xc},\sigma_{x\pi}\}} A_i(\kappa_1)\sigma^2_{i,0} \\
\kappa_1 &= \frac{exp(\bar{pc})}{1+exp(\bar{pc})} \\
\kappa_0 &= log(1+exp(\bar{pc})) - \kappa_1\bar{pc}
\end{aligned}$$

which can be done numerically. Having solved these constants, we now proceed to derive an expression for the SDF which we will use to price the term structure of interest rates.

A.3 Expression for the Real and Nominal SDF

Evaluating $r_{c,t+1}$ with the solution that we just derived for pc_t in (A.9) and (A.10) and using the assumed process for consumption growth we can rewrite the real SDF in terms of the state variables

and the underlying shocks (risk). In particular, we have:

$$\begin{aligned} m_{t+1} = m_0 + m_c x_{c,t} + m_\pi x_{\pi,t} + m_\lambda x_{\lambda,t} + m_{\sigma_c}\sigma^2_{x,t} + m_{\sigma_\pi}\sigma^2_{\pi,t} + m_{\sigma_{xc}}\sigma^2_{xc,t} + m_{\sigma_{x\pi}}\sigma^2_{x\pi,t} \\ - \lambda_c\sigma_{c,t}\eta_{c,t+1} - \lambda_\pi\sigma_{\pi,t}\eta_{\pi,t+1} - \lambda_\lambda\sigma_\lambda\eta_{\lambda,t+1} - \lambda_{xc}\sigma_{xc,t}\eta_{xc,t+1} - \lambda_{x\pi}\sigma_{x\pi,t}\eta_{x\pi,t+1} \\ - \sum_{i\in\{\sigma_c,\sigma_\pi,\sigma_{xc},\sigma_{x\pi}\}} \lambda_i\sigma_{\omega_i}\omega_{i,t+1} \end{aligned} \tag{A.11}$$

Where the λ's represent the market price of each source of risk. The discount factor parameters and market price of risks are equal to:

$$m_c = -\tfrac{1}{\psi}, \quad m_\pi = 0, \quad m_\lambda = \rho_\lambda, \quad m_{\sigma_c} = (1-\theta)(1-\kappa_1\nu_c)A_{\sigma_c}, \quad m_{\sigma_\pi} = 0 \tag{A.12}$$

$$m_{\sigma_{xc}} = (1-\theta)(1-\kappa_1\nu_{xc})A_{\sigma_{xc}}, \quad m_{\sigma_{x\pi}} = (1-\theta)(1-\kappa_1\nu_{x\pi})A_{\sigma_{x\pi}}$$

the constant is given by

$$m_0 = log\delta - \frac{1}{\psi}\mu_c + \frac{1}{2}(1-\theta)\theta(1+\kappa_1 A_\lambda)^2\sigma^2_\lambda + \frac{1}{2}(1-\theta)\theta\kappa_1^2[\sum_{i\in\{\sigma_c,\sigma_\pi,\sigma_{xc},\sigma_{x\pi}\}} A_i^2\sigma^2_{\omega_i}] \tag{A.13}$$

and the market prices of risk are

$$\lambda_c = \gamma, \quad \lambda_\pi = 0, \quad \lambda_\lambda = \frac{\kappa_1\rho_\lambda - \theta}{1-\kappa_1\rho_\lambda}, \quad \lambda_{xc} = (1-\theta)\kappa_1 A_c, \quad \lambda_{x\pi} = (1-\theta)\kappa_1 A_\pi \tag{A.14}$$

$$\lambda_{\sigma_c} = (1-\theta)\kappa_1 A_{\sigma_c}, \quad \lambda_{\sigma_\pi} = 0, \quad \lambda_{\sigma_{xc}} = (1-\theta)\kappa_1 A_{\sigma_{xc}}, \quad \lambda_{\sigma_{x\pi}} = (1-\theta)\kappa_1 A_{\sigma_{x\pi}}$$

To price nominal payoffs is useful to specify the nominal discount factor which is equal to the real one minus the inflation rate:

$$m^{\$}_{t+1} = m_{t+1} - \pi_{t+1} \tag{A.15}$$

We can derive a similar expression for $m^{\$}_{t+1}$ as in equation (A.11), where the nominal discount factor parameters and the nominal market price of risks are equal to the real counterparts with the exception of $m^{\$}_0$, $m^{\$}_\pi$ and $\lambda^{\$}_\pi$, which are equal to:

$$m^{\$}_0 = m_0 - \mu_\pi, \quad m^{\$}_\pi = m_\pi - 1 \quad \text{and} \quad \lambda^{\$}_\pi = \lambda_\pi + 1$$

For convenience, it is useful to express the nominal version of equation (A.11) in terms of a time t expected component and innovations to the nominal SDF:

$$\begin{aligned} m^{\$}_{t+1} - E_t m^{\$}_{t+1} = & \underbrace{-\lambda^{\$}_{c}\sigma_{c,t}\eta_{c,t+1}}_{\text{short-run consumption risk}<0} \quad \underbrace{-\lambda^{\$}_{\pi}\sigma_{\pi,t}\eta_{\pi,t+1}}_{\text{short-run inflation risk}>0} \quad \underbrace{-\lambda^{\$}_{\lambda}\sigma_{\lambda}\eta_{\lambda,t+1}}_{\text{preference risk }<0} \\ & \underbrace{-\lambda^{\$}_{xc}\sigma_{xc,t}\eta_{xc,t+1}}_{\text{long-run consumption risk}<0} \quad \underbrace{-\lambda^{\$}_{x\pi}\sigma_{x\pi,t}\eta_{x\pi,t+1}}_{\text{long-run inflation risk}>0} \\ & \underbrace{- \sum_{i\in\{\sigma_c,\sigma_\pi,\sigma_{xc},\sigma_{x\pi}\}} \lambda^{\$}_{i}\sigma_{\omega_i}\omega_{i,t+1}}_{\text{Volatility risk}>0} \end{aligned} \tag{A.16}$$

Using the nominal discount factor in equation (A.15), we can solve the equilibrium nominal yields in the economy.

A.4 Solution for Equilibrium Nominal Bond Yields

In this section we solve the yields of nominal zero-coupon bonds of different maturities. Let $P^{\$}_{t,n}$ be the time-t price of an n-period zero-coupon nominal bond that pays one unit of numeraire in n periods. Using the Euler equation we can write the price in logs recursively as

$$p^{\$}_{t,n} = logE_t exp(m^{\$}_{t+1} + p^{\$}_{t+1,n-1}) \tag{A.17}$$

where we define $p^{\$}_{t,n} = logP^{\$}_{t,n}$. Conjecture that $p^{\$}_{t,n}$ is a linear function of the state variables

$$p^{\$}_{t,n} = -(B^{\$}_{0,n} + B^{\$}_{c,n}x_{c,t} + B^{\$}_{\pi,n}x_{\pi,t} + B^{\$}_{\lambda,n}x_{\lambda,t} + B^{\$}_{\sigma_c,n}\sigma^2_{c,t} + B^{\$}_{\sigma_\pi,n}\sigma^2_{\pi,t} + B^{\$}_{\sigma_{xc},n}\sigma^2_{xc,t} + B^{\$}_{\sigma_{x\pi},n}\sigma^2_{x\pi,t}) \tag{A.18}$$

To solve the Bs we again use the method of undetermined coefficients and it follows that:

$$\begin{aligned} B^{\$}_{c,n} &= B^{\$}_{c,n-1}\rho_{cc} - m^{\$}_{c} \\ B^{\$}_{\pi,n} &= B^{\$}_{c,n-1}\rho_{c\pi} + B^{\$}_{\pi,n-1}\rho_{\pi\pi} - m^{\$}_{\pi} \\ B^{\$}_{\lambda,n} &= B^{\$}_{\lambda,n-1}\rho_{\lambda} - m^{\$}_{\lambda} \\ B^{\$}_{\sigma_c,n} &= B^{\$}_{\sigma_c,n-1}\nu_{c} - \frac{1}{2}(\lambda^{\$}_{c})^2 - m^{\$}_{\sigma_c} \\ B^{\$}_{\sigma_\pi,n} &= B^{\$}_{\sigma_\pi,n-1}\nu_{\pi} - \frac{1}{2}(\lambda^{\$}_{\pi})^2 - m^{\$}_{\sigma_\pi} \\ B^{\$}_{\sigma_{xc},n} &= B^{\$}_{\sigma_{xc},n-1}\nu_{xc} - \frac{1}{2}(\lambda^{\$}_{xc} + B^{\$}_{c,n-1})^2 - m^{\$}_{\sigma_{xc}} \\ B^{\$}_{\sigma_{x\pi},n} &= B^{\$}_{\sigma_{x\pi},n-1}\nu_{x\pi} - \frac{1}{2}(\lambda^{\$}_{x\pi} + B^{\$}_{\pi,n-1})^2 - m^{\$}_{\sigma_{x\pi}} \\ B^{\$}_{0,n} &= B^{\$}_{0,n-1} - \frac{1}{2}(\lambda_\lambda + B^{\$}_{\lambda,n-1})^2\sigma^2_\lambda - \sum_{i\in\{\sigma_c,\sigma_\pi,\sigma_{xc},\sigma_{x\pi}\}} [(B^{\$}_{i,n-1})\sigma^2_{i,0}(1-\nu_i) + \frac{1}{2}(\lambda_i + B^{\$}_{i,n-1}))^2\sigma^2_{\omega_i}] - m^{\$}_{0} \end{aligned} \tag{A.19}$$

with initial conditions $B^{\$}_{c,n} = B^{\$}_{\pi,n} = B^{\$}_{\lambda,n} = B^{\$}_{\sigma_c,n} = B^{\$}_{\sigma_\pi,n} = B^{\$}_{\sigma_{xc},n} = B^{\$}_{\sigma_{x\pi},n} = B^{\$}_{0,n} = 0$. Given the price of a zero-coupon bond, bond yields are defined $y^{\$}_{t,n} = -\frac{1}{n} ln P^{\$}_{t,n}$. Hence,

$$y^{\$}_{t,n} = \frac{1}{n}(B^{\$}_{0,n} + \underbrace{B^{\$}_{c,n}}_{>0} x_{c,t} + \underbrace{B^{\$}_{\pi,n}}_{>0} x_{\pi,t} + \underbrace{B^{\$}_{\lambda,n}}_{<0} x_{\lambda,t} + \underbrace{B^{\$}_{\sigma_c,n}}_{<0} \sigma^2_{c,t} + \underbrace{B^{\$}_{\sigma_\pi,n}}_{<0} \sigma^2_{\pi,t} + \underbrace{B^{\$}_{\sigma_{xc},n}}_{<0} \sigma^2_{xc,t} + \underbrace{B^{\$}_{\sigma_{x\pi},n}}_{>0 \text{ for high } n} \sigma^2_{x\pi,t})$$

A.5 Expected Excess Bond Returns

Define the excess log return on buying an n period bond at time t and selling it at time $t+1$ as an $n-1$ period bond:

$$rx^{\$}_{t\to t+1,n} = n y^{\$}_{t,n} - (n-1) y^{\$}_{t+1,n-1} - y^{\$}_{t,1}$$

As we did for the nominal SDF, the excess log return can be expressed in terms of a time t expected component and return innovations:

$$rx^{\$}_{r\to t+1,n} - E_t rx^{\$}_{r\to t+1,n} = -B^{\$}_{c,n-1}\sigma_{xc,t}\eta_{xc,t+1} - B^{\$}_{\pi,n-1}\sigma_{x\pi,t}\eta_{x\pi,t+1} - B^{\$}_{\lambda,n-1}\sigma_\lambda \eta_{\lambda,t+1} - \sum_{i\in\{\sigma_c,\sigma_\pi,\sigma_{xc},\sigma_{x\pi}\}} B^{\$}_{i,n-1}\sigma_{\omega_i}\omega_{i,t+1}$$

In the model, one-period expected excess return on nominal bonds is determined by the negative covariation between the innovations to excess log returns and the innovations to the nominal SDF in equation (A.16):

$$\begin{aligned} E_t rx^{\$}_{r\to t+1,n} + \frac{1}{2} Var_t rx^{\$}_{r\to t+1,n} &= -cov_t(m^{\$}_{t+1}, rx^{\$}_{r\to t+1,n}) \\ &= \underbrace{-\sum_{i\in\{\sigma_c,\sigma_\pi,\sigma_{xc},\sigma_{x\pi}\}} B^{\$}_{i,n-1}\lambda_i\sigma^2_{\omega_i}}_{\text{Volatility risk}} \underbrace{-B^{\$}_{\lambda,n-1}\lambda_\lambda\sigma^2_\lambda}_{\text{Preference risk}} \underbrace{-B^{\$}_{c,n-1}\lambda_{xc}\sigma^2_{xc,t}}_{\text{long-run growth risk}} \underbrace{-B^{\$}_{\pi,n-1}\lambda_{x\pi}\sigma^2_{x\pi,t}}_{\text{long-run inflation risk}} \end{aligned} \tag{A.20}$$

A.6 Term Premium

We can decompose the n-period yield into expectations of average expected future short rates and average excess returns over the life of the bond:

$$y^{\$}_{t,n} = \frac{1}{n}\sum_{i=1}^{n} E_t y^{\$}_{t+i-1,1} + \frac{1}{n}\sum_{i=1}^{n} E_t rx^{\$}_{t\to t+1,n-i+1} \tag{A.21}$$

The last term on the right is often described as the bond's nominal term premium, and we will denote it as $tp^{\$}_{t,n}$. In this model, the term premia is time-varying due to variations in bond risk

premia driven by short and long-run real and inflation volatilities. Specifically,

$$\begin{aligned} tp^{\$}_{t,n} &= y^{\$}_{t,n} - \frac{1}{n}\sum_{i=1}^{n} E_t y^{\$}_{t+i-1,1} \\ &= \frac{1}{n}B^{\$}_{0,n} - B^{\$}_{0,1} - \frac{1}{n}\sum_{i\in\{c,\pi,xc,x\pi\}} B^{\$}_{\sigma_i,1}(n-\nu_i\frac{1-\nu_i^n}{1-\nu_i})\sigma^2_{i,0} + \frac{1}{n}\sum_{i\in\{xc,x\pi\}}(B^{\$}_{\sigma_i,n} - B^{\$}_{\sigma_i,1}\frac{1-\nu_i^n}{1-\nu_i})\sigma^2_{i,t} \end{aligned} \tag{A.22}$$

A.7 Inflation Variance Ratios: Model-Implied

Equation (A.21) decomposes an n-period yield into expectations of average expected future short rates and a term premium component. If we define the ex-ante real rate as the yield of a one-period nominal bond minus expected inflation,

$$r_t = y^{\$}_{t,1} - E_t\pi_{t+1}$$

We can further decompose the bond yield as

$$y^{\$}_{t,n} = \frac{1}{n}\sum_{i=1}^{n} E_t r_{f,t+i-1} + \frac{1}{n}\sum_{i=1}^{n} E_t\pi_{t+i} + tp^{\$}_{t,n} \tag{A.23}$$

From this last equation it is clear that innovations in the n- maturity yield from $t-1$ to t are equal to the sum of news about ex-ante real rates, expected average inflation and term premium shocks:

$$\epsilon^{(n)}_{y^{\$},t} = \epsilon^{(n)}_{r,t} + \eta^{(n)}_{\pi,t} + \epsilon^{(n)}_{tp^{\$},t} \tag{A.24}$$

with

$$\epsilon^{(n)}_{y^{\$},t} = E_t y^{\$}_{t,n} - E_{t-1}y^{\$}_{t,n}, \qquad \epsilon^{(n)}_{r,t} = \tfrac{1}{n}\textstyle\sum_{i=1}^{n} E_t r_{f,t+i-1} - \tfrac{1}{n}\sum_{i=1}^{n} E_{t-1} r_{f,t+i-1}.$$
$$\epsilon^{(n)}_{tp^{\$},t} = E_t tp^{\$}_{t,n} - E_{t-1}tp^{\$}_{t,n}, \qquad \epsilon^{(n)}_{\pi,t} = \tfrac{1}{n}\textstyle\sum_{i=1}^{n} E_t \pi_{t+i} - \tfrac{1}{n}\sum_{i=1}^{n} E_{t-1} \pi_{t+i}.$$

Given the equilibrium solution of bond yields and the assumed process for the inflation rate we are able to derive analytical expressions for each one of this shocks. In particular, ex-ante real rates are given by

$$\begin{aligned} \frac{1}{n}\sum_{i=1}^{n} E_t r_{f,t+i-1} = \frac{1}{n}(B^{\$}_{0,1} - \mu_\pi + \sum_{i\in\{c,\pi,xc,x\pi\}} B^{\$}_{\sigma_i,1}(n-\nu_i\frac{1-\nu_i^n}{1-\nu_i})\sigma^2_{i,0}) + \frac{1}{n}B^{\$}_{c,1}\frac{1-\rho_{cc}^n}{1-\rho_{cc}}x_{c,t} + \frac{1}{n}B^{\$}_{\lambda,1}\frac{1-\rho_\lambda^n}{1-\rho_\lambda}x_{\lambda,t} \\ + \frac{1}{n}\frac{\rho_{c\pi}}{1-\rho_{cc}}B^{\$}_{c,1}[(1-\rho_{cc}^{n-1}) + \rho_{\pi\pi}(1-\rho_{cc}^{n-2}) + \rho^2_{\pi\pi}(1-\rho_{cc}^{n-3}) + \cdots + \rho^{n-2}_{\pi\pi}(1-\rho_{cc})]x_{\pi,t} \\ + \frac{1}{n}\sum_{i\in\{c,\pi,xc,x\pi\}} B^{\$}_{\sigma_i,1}\frac{1-\nu_i^n}{1-\nu_i}\sigma^2_{i,t} \end{aligned}$$

Thus, we can write the innovations to this component as

$$\begin{aligned}\epsilon_{r,t}^{(n)} &= \frac{1}{n}B_{c,1}^{\$}\frac{1-\rho_{cc}^{n}}{1-\rho_{cc}}\sigma_{xc,t-1}\eta_{xc,t} + \frac{1}{n}B_{\lambda,1}^{\$}\frac{1-\rho_{\lambda}^{n}}{1-\rho_{\lambda}}\sigma_{\lambda}\eta_{\lambda,t} \\ &+ \frac{1}{n}\frac{\rho_{c\pi}}{1-\rho_{cc}}B_{c,1}^{\$}[(1-\rho_{cc}^{n-1}) + \rho_{\pi\pi}(1-\rho_{cc}^{n-2}) + \rho_{\pi\pi}^{2}(1-\rho_{cc}^{n-3}) + \cdots + \rho_{\pi\pi}^{n-2}(1-\rho_{cc})]\sigma_{x\pi,t-1}\eta_{x\pi,t} \\ &+ \frac{1}{n}\sum_{i\in\{c,\pi,xc,x\pi\}} B_{\sigma_i,1}^{\$}\frac{1-\nu_i^{n}}{1-\nu_i}\sigma_{\omega_i}\omega_{i,t+1}\end{aligned} \tag{A.25}$$

Similarly, expected average inflation is equal to

$$\frac{1}{n}\sum_{i=1}^{n} E_t\pi_{t+i} = \mu_{\pi} + \frac{1}{n}B_{\pi,1}^{\$}\frac{1-\rho_{\pi\pi}^{n}}{1-\rho_{\pi\pi}}x_{\pi,t}$$

with shocks given by

$$\epsilon_{\pi,t}^{(n)} = \frac{1}{n}B_{\pi,1}^{\$}\frac{1-\rho_{\pi\pi}^{n}}{1-\rho_{\pi\pi}}\sigma_{x\pi,t-1}\eta_{x\pi,t} \tag{A.26}$$

Furthermore, equation (A.22) provides an expression for the term premia. It follows that shocks to this component are

$$\epsilon_{tp^{\$},t}^{(n)} = \frac{1}{n}\sum_{i\in\{xc,x\pi\}}(B_{\sigma_i,n}^{\$} - B_{\sigma_i,1}^{\$}\frac{1-\nu_i^{n}}{1-\nu_i})\sigma_{\omega_i}\omega_{i,t+1} \tag{A.27}$$

It is straightforward to show that the sum of $\epsilon_{r,t}^{(n)}$, $\epsilon_{\pi,t}^{(n)}$ and $\epsilon_{tp^{\$},t}^{(n)}$ (given by equations (A.25), (A.26) and (A.27)) is equal to innovations in the n- maturity yield:

$$\epsilon_{y^{\$},t}^{(n)} = B_{c,n}^{\$}\sigma_{xc,t-1}\eta_{xc,t} + B_{\pi,n}^{\$}\sigma_{x\pi,t-1}\eta_{x\pi,t} + B_{\lambda,n}^{\$}\sigma_{\lambda}\eta_{\lambda,t} + \sum_{i\in\{c,\pi,xc,x\pi\}} B_{\sigma_i,n}^{\$}\sigma_{\omega_i}\omega_{i,t+1} \tag{A.28}$$

Finally, the model-implied inflation variance ratios are equal to the variance of (A.26) divided by the variance of (A.28).

B State-Space Representation of the Macro-Finance Model

In this section we describe a state-space representation of the model and its estimation procedure. In Section B.1, we derive the measurement equation, while in Section B.2, we show the state transition equation. In Section B.3, we describe the algorithm for posterior inference. Section B.4 highlights the importance of the measurement error model of consumption and stochastic volatility.

B.1 Measurement Equation

The goal of this section is to derive the coefficients of the measurement equation described in Section 2.4 given by:

$$Y^o_{t+1} = A_{t+1}(D + Zs_{t+1} + Z^v s^v_{t+1}(h_{t+1}) + \Sigma^u u_{t+1}), \quad \text{with} \quad u_{t+1} \sim N(0, I) \tag{B.1}$$

The aggregate measurement equation in (B.1) stacks the following individual measurement equations:

1.- Measurement equation for consumption growth. Following Schorfheide et al. (2017), we include monthly measurement errors in the process of consumption that average out under temporal aggregation. In the main estimation we assumed that the measurement errors average out at the annual frequency. Here, to simplify the exposition, we assume that the errors average out at the quarterly frequency.

Let the subscript t represent the monthly time as $t = 3(j-1) + m$, where m indexes the month within quarter j and $m = 1, 2, 3$. Specifically, we assume that:

$$\begin{aligned}\Delta c^o_{3(j-1)+1} &= \Delta c_{3(j-1)+1} + \sigma_\epsilon(\epsilon_{3(j-1)+1} - \epsilon_{3(j-2)+3}) \\ &\quad - \frac{1}{3}\sum_{m=1}^{3} \sigma_\epsilon(\epsilon_{3(j-1)+m} - \epsilon_{3(j-2)+m}) + \sigma^q_\epsilon(\epsilon^q_{(j)} - \epsilon^q_{(j-1)}) \end{aligned} \tag{B.2}$$

$$\Delta c^o_{3(j-1)+m} = \Delta c_{3(j-1)+m} + \sigma_\epsilon(\epsilon_{3(j-1)+m} - \epsilon_{3(j-2)+m-1}) \text{ for } m = 2, 3 \text{ and } \epsilon, \epsilon^q \sim N(0, 1).$$

σ_ϵ and σ^q_ϵ denote the standard deviation of monthly and quarterly consumption measurement errors. Note that under this specification, aggregating the monthly consumption series to the quarterly frequency according to

$$\Delta c^{q,o}_j = c^{q,o}_j - c^{q,o}_{j-1} = \sum_{\tau=1}^{5} \frac{3 - |\tau - 3|}{3} \Delta c^o_{3j-\tau+1}$$

averages out the monthly measurement errors; $\Delta c^{q,o}_j = \Delta c^q_j + \sigma^q_\epsilon(\epsilon^q_{(j)} - \epsilon^q_{(j-1)})$. Under this specification, the levels of monthly consumption are constructed by distributing quarterly consumption over the three months of a quarter; this distribution is based on a noisy monthly proxy series. Furthermore, monthly consumption growth rates are proportional to the growth rates of the proxy series

and monthly consumption adds up to quarterly consumption. At quarterly frequency, consumption growth is strongly positively autocorrelated, while, at the monthly frequency, it exhibits a significant negative autocorrelation, which provides evidence for a negative moving average component. The assumed measurement error model for consumption is able to reconcile these features.

2.- Measurement Equation for Inflation. We assume that inflation is measured without any measurement errors and define

$$\pi^{o}_{t+1} = \pi_{t+1} \tag{B.3}$$

Following Duffee (2016), to sharpen inference about the predictable component of the inflation rate we also include information from surveys of market practitioners that are released in a different (quarterly) frequency. Specifically,, we consider the forecasts from the Survey of Professional Forecasters of one to four quarters ahead. To this end, we assume that the forecasts are published at the second month of the quarter, which is consistent with the release date of the Federal Reserve Bank of Philadelphia. To gain some insight into how to include this information, let t be the second month of the quarter. Then the market practitioners make an inflation forecast for say, one quarter ahead, starting from period $t+1$, which we label as $\tilde{\pi}^{o,1}_{t+1}$. Using the process for inflation in equation A.1 the following relation follows:

$$\tilde{\pi}^{o,1}_{t+1} = E_t[\pi_{t+2} + \pi_{t+3} + \pi_{t+4}] = 3\mu_p + \tilde{\rho}_1 x_t$$

where to simplify the notation we defined $\tilde{\rho}_1 = \rho_{\pi\pi} + \rho^2_{\pi\pi} + \rho^3_{\pi\pi}$. The same applies for the inflation forecasts of two $\tilde{\pi}^{o,2}_{t+1}$, three $\tilde{\pi}^{o,3}_{t+1}$ and four $\tilde{\pi}^{o,4}_{t+1}$ quarters ahead. Hence, the measurement equation for the quarterly survey-based data is:

$$\tilde{\pi}^{o,i}_{t+1} = 3\mu_\pi + \tilde{\rho}_i x_{\pi,t} + \sigma^i_{spf,\epsilon}\epsilon^i_{t+1} \quad \text{for} \quad i \in \{1,2,3,4\} \tag{B.4}$$

The standard deviation of the measurement errors are free parameters given by $\sigma^i_{spf,\epsilon}$.

3.-Measurement equation for bond yields and the real risk-free rate. We assume that nominal bond yields are given by

$$y^{\$,o}_{t+1,n} = y^{\$}_{t+1,n} + \sigma_{y_n}\epsilon_{y_n,t+1}, \quad \text{with} \quad \epsilon_{y_n,t+1} \sim N(0,1) \tag{B.5}$$

where $\sigma_{y_n}\epsilon_{y_n,t+1}$ captures deviations from the exact factor model and can be thought of as cross-sectional errors due to market imperfections such as measurement errors. We impose a similar structure to (B.5) for the risk-free rate.

Joining the individual measurement equations and assuming that $t+1$ is the last month of quarter m we have:

$$
\begin{aligned}
\Delta c^o_{t+1} &= \mu_c + x_{c,t} + \sigma_{c,t}\eta_{c,t+1} + \sigma_\epsilon(\epsilon_{t+1} - \epsilon_t) \\
\Delta c^o_{t} &= \mu_c + x_{c,t-1} + \sigma_{c,t-1}\eta_{c,t} + \sigma_\epsilon(\epsilon_{t} - \epsilon_{t-1}) \\
\Delta c^o_{t-1} &= \mu_c + x_{c,t-2} + \sigma_{c,t-2}\eta_{c,t-1} - \frac{1}{3}\sigma_\epsilon(\epsilon_{t+1} + \epsilon_t) + \frac{2}{3}\sigma_\epsilon\epsilon_{t-1} - \frac{2}{3}\sigma_\epsilon\epsilon_{t-2} \\
&\quad + \frac{1}{3}\sigma_\epsilon(\epsilon_{t-3} + \epsilon_{t-4}) + \sigma^q_\epsilon(\epsilon^q_{t+1} + \epsilon^q_{t-2}) \\
\pi^o_{t+1} &= \mu_\pi + x_{\pi,t} + \sigma_{\pi,t}\eta_{\pi,t+1} \\
\tilde{\pi}^{o,i}_{t+1} &= 3\mu_\pi + \tilde{\rho}_i x_{\pi,t} + \sigma^i_{spf,\epsilon}\epsilon^i_{t+1} \quad \text{for} \quad i \in \{1,2,3,4\} \\
r^o_{f,t} &= B_0 + B_c x_{c,t} + B_\lambda x_{\lambda,t} + B_{\sigma_c}\sigma^2_{c,t} + B_{\sigma_{xc}}\sigma^2_{xc,t} + B_{\sigma_{x\pi}}\sigma^2_{x\pi,t} + \sigma_{r_f}\epsilon_{r_f,t+1}, \\
y^{\$,o}_{t+1,n} &= B^\$_{0,n} + B^\$_{c,n}x_{c,t+1} + B^\$_{\pi,n}x_{\pi,t+1} + B^\$_{\lambda,n}x_{\lambda,t+1} \\
&\quad + B^\$_{\sigma_c,n}\sigma^2_{c,t+1} + B^\$_{\sigma_\pi,n}\sigma^2_{\pi,t+1} + B^\$_{\sigma_{xc},n}\sigma^2_{xc,t+1} + B^\$_{\sigma_{x\pi},n}\sigma^2_{x\pi,t+1} + \sigma_{y_n}\epsilon_{y_n,t+1}
\end{aligned}
$$

Given these expressions, it is just a matter of ordering all the pieces adequately. The state vector s_{t+1} and s^v_{t+1} are given by:

$$
\begin{aligned}
s_{t+1} = [&x_{c,t+1},\ x_{c,t},\ x_{c,t-1},\ x_{c,t-2}\ \sigma_{c,t}\eta_{c,t+1},\ \sigma_{c,t-1}\eta_{c,t},\ \sigma_{c,t-2}\eta_{c,t-1}, \\
&\sigma_\epsilon\epsilon_{t+1},\ \sigma_\epsilon\epsilon_t,\ \sigma_\epsilon\epsilon_{t-1},\ \sigma_\epsilon\epsilon_{t-2},\ \sigma_\epsilon\epsilon_{t-3},\ \sigma_\epsilon\epsilon_{t-4},\ \sigma^q_\epsilon\epsilon^q_{t+1},\ \sigma^q_\epsilon\epsilon^q_t,\ \sigma^q_\epsilon\epsilon^q_{t-1},\ \sigma^q_\epsilon\epsilon^q_{t-2}, \\
&x_{\pi,t+1},\ x_{\pi,t},\ \sigma_{\pi,t}\eta_{\pi,t+1},\ x_{\lambda,t+1},\ x_{\lambda,t},\ \sigma^i_{spf,\epsilon}\epsilon^i_{t+1}]', \\
s^v_{t+1} = [&\sigma^2_{xc,t+1},\ \sigma^2_{x\pi,t+1},\ \sigma^2_{c,t+1},\ \sigma^2_{\pi,t+1}]'.
\end{aligned}
$$

Given these state vectors, we write the matrices D, Z, Z^v and Σ^u as follows:

$$
Z = \begin{bmatrix}
0 & 1 & 0 & 0 & 1 & 0 & 0 & 1 & -1 & 0 & 0 & 0 & 0 & 0 & 0 & 0 & 0 & 0 & 0 & 0 & 0 & 0 \\
0 & 0 & 1 & 0 & 0 & 1 & 0 & 0 & 1 & -1 & 0 & 0 & 0 & 0 & 0 & 0 & 0 & 0 & 0 & 0 & 0 & 0 \\
0 & 0 & 0 & 1 & 0 & 0 & 1 & 0 & -\frac{1}{3} & -\frac{1}{3} & \frac{2}{3} & -\frac{2}{3} & \frac{1}{3} & \frac{1}{3} & 1 & 0 & 0 & -1 & 0 & 0 & 0 & 0 & 0 \\
0 & 0 & 0 & 0 & 0 & 0 & 0 & 0 & 0 & 0 & 0 & 0 & 0 & 0 & 0 & 0 & 0 & 0 & 1 & 1 & 0 & 0 & 0 \\
0 & 0 & 0 & 0 & 0 & 0 & 0 & 0 & 0 & 0 & 0 & 0 & 0 & 0 & 0 & 0 & 0 & 0 & \tilde{\rho}_i & 0 & 0 & 0 & 1 \\
B_c & 0 & 0 & 0 & 0 & 0 & 0 & 0 & 0 & 0 & 0 & 0 & 0 & 0 & 0 & 0 & 0 & 0 & 0 & 0 & B_\lambda & 0 & 0 \\
B^\$_{c,n} & 0 & 0 & 0 & 0 & 0 & 0 & 0 & 0 & 0 & 0 & 0 & 0 & 0 & 0 & 0 & 0 & 0 & B^\$_{\pi,n} & 0 & B^\$_{\lambda,n} & 0 & 0
\end{bmatrix}
$$

$$D = \begin{bmatrix} \mu_c \\ \mu_c \\ \mu_c \\ \mu_\pi \\ 3\mu_\pi \\ B_0 \\ \frac{1}{n}B^{\$}_{0,n} \end{bmatrix}, \quad Z^v = \begin{bmatrix} 0 & 0 & 0 & 0 \\ 0 & 0 & 0 & 0 \\ 0 & 0 & 0 & 0 \\ 0 & 0 & 0 & 0 \\ 0 & 0 & 0 & 0 \\ B_{\sigma_{xc}} & B_{\sigma_{x\pi}} & B_{\sigma_c} & 0 \\ B^{\$}_{\sigma_{xc},n} & B^{\$}_{\sigma_{x\pi},n} & B^{\$}_{\sigma_c,n} & B^{\$}_{\sigma_\pi,n} \end{bmatrix}, \quad \Sigma^u = \begin{bmatrix} 0 & 0 & 0 & 0 & 0 & 0 & 0 \\ 0 & 0 & 0 & 0 & 0 & 0 & 0 \\ 0 & 0 & 0 & 0 & 0 & 0 & 0 \\ 0 & 0 & 0 & 0 & 0 & 0 & 0 \\ 0 & 0 & 0 & 0 & \sigma^i_{spf,\epsilon} & 0 & 0 \\ 0 & 0 & 0 & 0 & 0 & \sigma_{r_f} & 0 \\ 0 & 0 & 0 & 0 & 0 & 0 & \sigma_{y_n} \end{bmatrix}$$

Finally, the vector of observables Y^o_{t+1} and the selection matrix A_{t+1} can be written as:

- If t+1 is the last month of the quarter:

$$Y^o_{t+1} = \begin{bmatrix} \Delta c^o_{t+1} \\ \Delta c^o_t \\ \Delta c^o_{t-1} \\ \pi^o_{t+1} \\ \tilde{\pi}^{o,i}_{t+1} \\ r^o_{f,t} \\ y^{\$}_{t+1,n} \end{bmatrix}, \qquad A_{t+1} = \begin{bmatrix} 1 & 0 & 0 & 0 & 0 & 0 & 0 \\ 0 & 1 & 0 & 0 & 0 & 0 & 0 \\ 0 & 0 & 1 & 0 & 0 & 0 & 0 \\ 0 & 0 & 0 & 1 & 0 & 0 & 0 \\ 0 & 0 & 0 & 0 & 1 & 0 & 0 \\ 0 & 0 & 0 & 0 & 0 & 1 & 0 \\ 0 & 0 & 0 & 0 & 0 & 0 & 1 \end{bmatrix}$$

- If t+1 is not the last month of the quarter:

$$Y^o_{t+1} = \begin{bmatrix} \pi^o_{t+1} \\ r^o_{f,t} \\ y^{\$}_{t+1,n} \end{bmatrix}, \qquad A_{t+1} = \begin{bmatrix} 0 & 0 & 0 & 1 & 0 & 0 & 0 \\ 0 & 0 & 0 & 0 & 0 & 1 & 0 \\ 0 & 0 & 0 & 0 & 0 & 0 & 1 \end{bmatrix}.$$

B.2 State Transition Equation

The goal of this section is to derive the coefficients of the state-transition equation:

$$\begin{aligned} &s_{t+1} = \Phi s_t + v_{t+1}(h_t) \\ &h_{t+1} = \Psi h_t + \Sigma_h \omega_{t+1}, \quad h_{t+1} = [h_{xc,t+1},\ h_{x\pi,t+1},\ h_{c,t+1},\ h_{\pi,t+1}]' \quad \text{with} \quad \omega_{t+1} \sim N(0, I). \end{aligned} \tag{B.6}$$

The state variables evolve according to

$$\begin{aligned} x_{c,t+1} &= \rho_{cc} x_{c,t} + \rho_{c\pi} x_{\pi,t} + \sigma_{xc,t} \eta_{xc,t+1} \\ x_{\pi,t+1} &= \qquad\quad + \rho_{\pi\pi} x_{\pi,t} + \sigma_{x\pi,t} \eta_{x\pi,t+1} \\ x_{\lambda,t+1} &= \rho_\lambda x_{\lambda,t} + \sigma_\lambda \eta_{\lambda,t+1} \end{aligned}$$

Hence, Φ and $v_{t+1}(h_t)$ just make sure that these dynamics are preserved with zeros and ones in the adequate places:

$$\Phi = \left[\begin{array}{c|c|c|c|c|c|c}
\begin{matrix}\rho_{cc} & 0 & 0 \\ & & \\ I_{3\times 3} & & \end{matrix} \; O_{4\times 1} & O_{4\times 3} & O_{4\times 6} & O_{4\times 4} & \begin{matrix}\rho_{c\pi} & \\ & \\ O_{3\times 1} & \end{matrix} \; O_{4\times 2} & O_{4\times 2} & O_{4\times 1} \\ \hline
O_{3\times 4} & \begin{matrix}0 & 0 \\ I_{2\times 2} & \end{matrix} \; O_{3\times 1} & O_{3\times 6} & O_{3\times 4} & O_{3\times 3} & O_{3\times 2} & O_{3\times 1} \\ \hline
O_{6\times 4} & O_{6\times 3} & \begin{matrix}O_{1\times 5} \\ I_{5\times 5}\end{matrix} \; O_{6\times 1} & O_{6\times 4} & O_{6\times 3} & O_{6\times 2} & O_{6\times 1} \\ \hline
O_{4\times 4} & O_{4\times 3} & O_{4\times 6} & \begin{matrix}O_{1\times 3} \\ I_{3\times 3}\end{matrix} \; O_{4\times 1} & O_{4\times 3} & O_{4\times 2} & O_{4\times 1} \\ \hline
O_{3\times 4} & O_{3\times 3} & O_{3\times 6} & O_{3\times 4} & \begin{matrix}\rho_{\pi\pi} & 0 & 0 \\ 1 & 0 & 0 \\ 0 & 0 & 0\end{matrix} & O_{3\times 2} & O_{3\times 1} \\ \hline
O_{2\times 4} & O_{2\times 3} & O_{2\times 6} & O_{2\times 4} & O_{2\times 3} & \begin{matrix}\rho_{\lambda} & 0 \\ 1 & 0\end{matrix} & O_{4\times 1} \\ \hline
O_{1\times 4} & O_{1\times 3} & O_{1\times 6} & O_{1\times 4} & O_{1\times 3} & O_{1\times 2} & O_{1\times 1}
\end{array}\right]_{23\times 23}$$

$$v_{t+1}(h_t) = [\sigma_{xc,t}\eta_{xc,t+1},\ O_{1\times 3},\ \sigma_{c,t}\eta_{c,t+1},\ O_{1\times 2},\ \sigma_{\epsilon}\epsilon_{t+1},\ O_{1\times 5},\ \sigma_{\epsilon}^{q}\epsilon_{t+1}^{q},\ O_{1\times 3},$$

$$\sigma_{x\pi,t}\eta_{x\pi,t+1},\ 0,\ \sigma_{\pi,t}\eta_{\pi,t+1},\ \sigma_{\lambda}\eta_{\lambda,t+1},\ 0,\ \sigma_{spf,\epsilon}^{i}\epsilon_{t+1}^{i}]'_{23\times 1}$$

Finally, Ψ, Σ_h and ω_{t+1} can be written as

$$\Psi = \begin{bmatrix} \rho_{h_{xc}} & 0 & 0 & 0 \\ 0 & \rho_{h_{x\pi}} & 0 & 0 \\ 0 & 0 & \rho_{h_c} & 0 \\ 0 & 0 & 0 & \rho_{h_\pi} \end{bmatrix}, \qquad \Psi = \begin{bmatrix} \sigma_{h_{xc}} & 0 & 0 & 0 \\ 0 & \sigma_{h_{x\pi}} & 0 & 0 \\ 0 & 0 & \sigma_{h_c} & 0 \\ 0 & 0 & 0 & \sigma_{h_\pi} \end{bmatrix}, \qquad \omega_{t+1} = \begin{bmatrix} \omega_{xc,t+1} \\ \omega_{x\pi,t+1} \\ \omega_{c,t+1} \\ \omega_{\pi,t+1} \end{bmatrix}$$

with $\sigma_{i,t} = \varphi_i \sigma exp(h_{i,t})$ for $i = \{c, \pi, xc, x\pi\}$.

B.3 Posterior Inference

For posterior inference we use a Bayesian MCMC particle filter to the state-space representation described by equations B.1 ,and D.14, which is linear conditional on the log volatilities h_t. We briefly summarize the main steps below; for further details, refer to Algorithm 13 in Herbst and Schorfheide (2015).

1. We initialize the Markov Chain at some parameter values Θ^0.
2. Given Θ^k
   (a) **Initialization.** At time $t = 0$, we draw M particles $\{h_0^j\}_{j=1}^M$ from the unconditional distribution of equation D.14. Conditional on each particle h_0^j, we generate s_0^j from the unconditional distribution of equation D.14. We set each particle weight to $\pi_0^j = \frac{1}{M}$, $j = 1, \ldots, M$.
   (b) **Recursion.** For $t = 1, \ldots, T$:
      i. **Forecasting s_t.** We propagate each particle h_{t-1}^j using the law of motion in equation D.14 to get h_t^j. Given s_{t-1}^j and (h_{t-1}^j, h_t^j) we run one iteration of the Kalman filter using the state-space system given by equations B.1 and D.14, which is conditionally linear. This step delivers the distribution of s_t^j, denoted by $p(s_t|y_t^o, s_{t-1}^j, h_{t-1}^j, h_t^j)$, which is normal with mean $s_{t|t}^j$ and variance $P_{t|t}^j$. Hence,

$$s_t^j \sim N(s_{t|t}^j, P_{t|t}^j).$$

      ii. **Forecasting y_t.** We compute the incremental weights $\tilde{\omega}_t^j$ according to

$$\tilde{\pi}_t^j = \pi_{t-1}^j \times p(y_t^o|\tilde{y}_{t|t-1}^j, F_{t|t-1}^j)$$

      where the Kalman filter step in i delivers $\tilde{y}_{t|t-1}^j$ and $F_{t|t-1}^j$. The likelihood $p(y_t^o|\tilde{y}_{t|t-1}^j, F_{t|t-1}^j)$ is conditionally Gaussian and follows from the measurement equation B.1.
      iii. **Updating.** We define the normalized weights by

$$\pi_t^j = \frac{\tilde{\pi}_t^j}{\sum_{i=1}^M \tilde{\pi}_t^i}$$

      and resample the particles h_t^j and states s_t^j using multinomial resampling with weights π_t^j.
   (c) **Likelihood Approximation.** The approximation of the log-likelihood function is given by

$$ln\hat{p}(y_t^o|Y_{1:t-1}^o) = ln\hat{p}(y_{t-1}^o|Y_{1:t-2}^o) + ln(\sum_{i=1}^M \tilde{\pi}_t^j)$$

   (d) **Metropolis-Hastings algorithm** Once we are able to approximate the likelihood function, we use a standard random walk Metropolis-Hastings algorithm to obtain a new parameter draw Θ^{k+1}. See Algorithm 18 in Herbst and Schorfheide (2015) for further details regarding this step.
   (e) We repeat steps (a) to (b) N_{sim} times.

In the implementation, we used 10,000 particles ($M = 10,000$), generated $50,000$ draws ($N_{sim} = 50,000$) and set the burn in period at $25,000$. We targeted an acceptance rate of approximately 30 percent. In addition, we checked that the results do not changed if we increase the number of particles.

Macro data	Posterior Distribution												$lnp(Y^o)$
	ρ_{cc}				$\rho_{c\pi}$				$\rho_{\pi\pi}$				
	5%	50%	95%	Width	5%	50%	95%	Width	5%	50%	95%	Width	
(a) No Me.	-0.28	-0.20	-0.13	0.15	-0.22	-0.13	-0.04	0.18	0.85	0.91	0.96	0.11	5855
(b) Me.	0.82	0.89	0.94	0.12	-0.01	-0.001	-0.00	0.01	0.87	0.93	0.97	0.09	5870
(c) Me. Sv.	0.91	0.95	0.98	0.07	-0.01	-0.001	-0.00	0.01	0.96	0.98	0.99	0.03	6055

Table B1. Posterior estimates of the persistence parameters.
This table reports the 5, 50, and 95 percentiles of the posterior distribution for the persistent parameters ρ_{cc}, $\rho_{c\pi}$ and $\rho_{\pi\pi}$ for the monthly version of the model. We also include the 90% confidence width and the log marginal data density. We consider three different specifications of the process of consumption growth and inflation. No Me., consumption growth is measured without any errors, (i.e., $c_t^o = c_t$), and homoskedastic innovations; Me. assumes the measurement error model of consumption; Me. Sv., assumes the measurement error model of consumption and short- and long-run stochastic volatility.

B.4 Role of Measurement Error Model of Consumption and Stochastic Volatility

In Section 3.2 of the main text, we documented that the posterior median estimates of $\{\rho_{cc}, \rho_{c\pi}, \rho_{\pi\pi}\}$ are remarkably similar with or without including bond prices in the estimation. The result is mostly driven by the assumed measurement error model for consumption. To see this, in Table B1, we show the 5, 50, 95 percentiles of the posterior distribution of the persistent parameters under three different specifications of the consumption growth and the inflation process. In (a) we assume homoskedastic innovations and that consumption growth is measured without any errors, (i.e., $c_t^o = c_t$). In (b) we add the measurement error model of consumption, while in (c), we assume the measurement error model of consumption and consider short- and long-run stochastic volatility. Furthermore, in the last column of the table, we report the log marginal data densities to provide formal support in terms of model fit for each specification. In all cases we only consider macro data in the estimation.

Without the measurement error model, the posterior median ρ_{cc} is equal to -0.20 in order to match the monthly negative autocorrelation observed in the data of -0.17. Nevertheless, this version of the model cannot reconcile the monthly negative autocorrelation with a positive autocorrelation observed at a quarterly or annual frequency. Accounting for measurement errors in consumption that average out every year alleviates this problem. Under this specification, the posterior median of ρ_{cc} jumps to 0.90, and the fit of the model measured by the log marginal data density improves significantly from 5855 to 5870. At the same time, the persistence parameter associated with

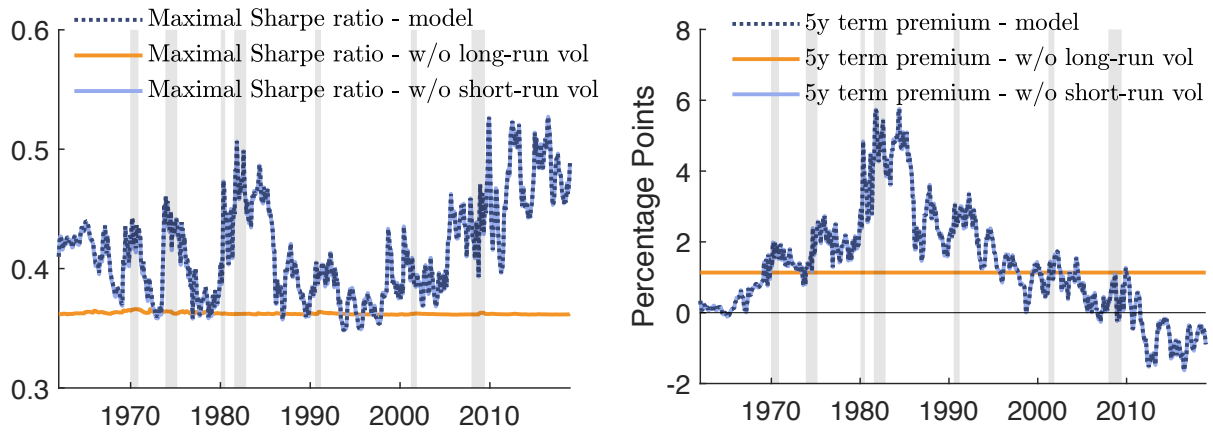

(a) Maximal Sharpe ratio

(b) TIPS spreads

Figure B1. 5-year term premium.
Panel (a) shows the model-implied maximal Sharpe ratio, while (b) presents the term premium on a 5-year bond. We present counterfactual estimates obtained by shutting down the estimated long-run (i.e., $\sigma^2_{xc,t}$, and $\sigma^2_{x\pi,t}$) and short-run (i.e., $\sigma^2_{c,t}$, and $\sigma^2_{\pi,t}$) volatilities, respectively. Light-shaded bars represent recessions, as defined by the National Bureau of Economic Research.

expected inflation, $\rho_{\pi\pi}$, remains largely unchanged at a value of 0.91, while the parameter that measures the effect of expected inflation on expected growth, $\rho_{c\pi}$, increases from -0.13 to -0.001. Adding stochastic volatility to the process of the macro variables improves the model fit considerably, the posterior uncertainty decreases (tighter credible intervals) and the persistence parameters ρ_{cc} and $\rho_{\pi\pi}$ jump to 0.95 and 0.98, respectively.[20] In terms of model fit, adding stochastic volatility increases the log marginal data density from 5870 to 6055.

B.5 Role of Stochastic Volatility for Maximal Sharpe Ratio and Term Premium.

The maximal Sharpe ratio provides a useful diagnosis regarding the validity of the stochastic discount factor and is given by

$$\sqrt{Var_t(m^{\$}_{t+1})} = (\lambda^{\$}_c)^2\sigma^2_{c,t} + (\lambda^{\$}_\pi)^2\sigma^2_{\pi,t} + (\lambda^{\$}_\lambda)^2\sigma^2_\lambda + (\lambda^{\$}_{xc})^2\sigma_{xc,t} + (\lambda^{\$}_{x\pi})^2\sigma^2_{x\pi,t} + \sum_{i\in\{\sigma_c,\sigma_\pi,\sigma_{xc},\sigma_{x\pi}\}} (\lambda^{\$}_i)^2\sigma^2_{\omega_i} \quad \text{(B.7)}$$

As equation (B.7) shows, the maximal Sharpe ratio depends on the inner product of the market prices of risk and the quantity of risk. To assess the relative importance of the stochastic volatilities in driving movements in equation (B.7), we generate counterfactual maximal Sharpe ratios by shutting down the estimated long-run (i.e., $\sigma^2_{xc,t}$, and $\sigma^2_{x\pi,t}$) and short-run (i.e., $\sigma^2_{c,t}$, and $\sigma^2_{\pi,t}$)

[20]The intuition for why the ρ_{cc} and $\rho_{\pi\pi}$ increases goes as follows. The presence of stochastic volatility allows for sharp fluctuations in Δc^o_{t+1} and π^o_{t+1} by incurring in similar movements in their conditional variance without the need of large temporary shocks by increasing σ and φ_π and reducing the estimates of the persistent parameters.

	Homoskedastic			Heteroskedastic		
	5%	50%	95%	5%	50%	95%
1y	0.075	0.103	0.142	0.164	0.236	0.327
5y	0.084	0.120	0.167	0.136	0.193	0.274
10y	0.11	0.132	0.183	0.134	0.205	0.281
$\ln p(Y^o)$		7088			7422	

Table B2. Inflation variance ratios at the quarterly frequency.
This table reports the population values of inflation variance ratios measured at the quarterly frequency. The inflation variance ratio is computed as the ratio of the variance of shocks to expected inflation to the variance of yield shocks. We include the 5, 50, and 95 percentiles of the moments based on 10,000 parameter draws of the posterior distribution. The table reports inflation variance ratio under the assumption of homoskedastic and heteroskedastic innovations.

volatilities, respectively. Figure B1 presents the results. Panel (a) shows that almost all of the variability of the maximal Sharpe ratio is due to the variation in $\sigma^2_{xc,t}$, and $\sigma^2_{x\pi,t}$. The short-run volatilities, $\sigma^2_{c,t}$, and $\sigma^2_{\pi,t}$, have negligible effects (less than 0.5% on average) on the variability of $\sqrt{Var_t(m^{\$}_{t+1})}$. As shown in panel (b), we arrive to the same conclusion if we focus instead on movements in the term premium. All of the movements in the term premium are driven by the long-run stochastic volatilities.

B.6 Inflation Variance Ratios at the Quarterly Frequency.

In the main text, we present estimates of the inflation variance ratios computed at the monthly frequency considering stochastic volatility. As a robustness check, here we repeated the same exercise for a quarterly version of the model.

The last three columns of Table B2 show the inflation variance ratios along with the 90 percent confidence interval for maturities of 1, 5, and 10 years. Following Duffee (2016), we also report the estimates based on the homoskedastic version of the model. In the case of homoskedastic innovations, the posterior medians of the unconditional inflation variance ratios for all bond maturities are around 12 percent whereas the 95 percentiles are below 20 percent. These estimates are similar to the estimates in Duffee (2016). Nevertheless, a careful inspection of the innovations suggests that these vary through time and exhibit heteroskedasticity. Therefore, instead of doing subperiod analysis, in the last three columns of Table B2 we report the estimates of the model that allows for stochastic volatility. Allowing for heteroskedasticity in inflation shocks and innovations to bond yields improves the model fit significantly, as evidenced by the log marginal data density reported at the end of Table B2 . It also shifts the distribution of the unconditional inflation variance ratios

towards higher values: the posterior medians were around 22 percent.[21] However, the 95 percentiles are all below 40 percent. These ratios are still at odds with corresponding values from standard macro-finance term structure models and are by and large similar to the estimates based on the monthly frequency.

B.7 Variance Decomposition in Reduced-Form Term Structure Models.

Table B3 reports the fraction of total yield news variance explained by term premia shocks for various leading models. Specifically, we consider the yield decomposition in Duffee (2018), Cieslak and Povala (2015), Kim and Wright (2005), and Adrian et al. (2013).[22] Depending on the model, the point estimates indicate that at the 10-year maturity between 20% and 39% of the variance of yield shocks is attributable to term premia shocks. These point estimates are fairly close to our 19% posterior median estimate and their confidence bounds nest the right tail of the posterior distribution from our implied term premia variance ratio. Hence, we conclude that the variation in term premia shocks in our model does not necessarily contradict the implied estimates in the literature.

Table B4 presents the full yield decomposition for the models in Duffee (2018) and Cieslak and Povala (2015).[23] This decomposition documents a second result. The confidence bounds on the contribution of real short rate news and term premia news to yield news is huge. For instance, at the 10-year maturity we cannot distinguish statistically between the role played by the real short

[21] The inflation variance ratios are expected to increase under the stochastic volatility case due to a Jensen's term, provided that the correlation between $Var_t(\epsilon^{(n)}_{\pi,t})$ and $Var_t(\epsilon^{(n)}_{y^{\$},t})$ is not too high. To see this, note that

$$E\left[\frac{Var_{t-1}(\epsilon^{(n)}_{\pi,t})}{Var_{t-1}(\epsilon^{(n)}_{y^{\$},t})}\right] \approx \frac{E[Var_{t-1}(\epsilon^{(n)}_{\pi,t})]}{E[Var_{t-1}(\epsilon^{(n)}_{y^{\$},t})]} + \frac{E[Var_{t-1}(\epsilon^{(n)}_{\pi,t})]}{E[Var_{t-1}(\epsilon^{(n)}_{y^{\$},t})]^3} Var(Var_{t-1}(\epsilon^{(n)}_{y^{\$},t})) \left[1 - \rho_{\epsilon^{(n)}_{\pi,t},\epsilon^{(n)}_{y^{\$},t}} \sqrt{\frac{Var(Var_{t-1}(\epsilon^{(n)}_{\pi,t}))}{Var(Var_{t-1}(\epsilon^{(n)}_{y^{\$},t}))}} \frac{E[Var_{t-1}(\epsilon^{(n)}_{y^{\$},t})]}{E[Var_{t-1}(\epsilon^{(n)}_{\pi,t})]}\right]$$

where $\rho_{\epsilon^{(n)}_{\pi,t},\epsilon^{(n)}_{y^{\$},t}}$ denotes the correlation between the corresponding variance terms. The first term on the right hand side corresponds to the inflation variance ratios under homoskedastic shocks.

[22] For the yield decomposition in Duffee (2018) we use directly the estimates reported in his paper (see Table VI). For Cieslak and Povala (2015) we decompose the yield shocks using the affine model that the authors present in Section 1 together with the calibrated parameters shown in Table 7. We obtained confidence intervals by simulating yield shocks of the same length as their data (470 months). For the models in Kim and Wright (2005) and Adrian et al. (2013), we took the time series of term premia from `https://www.federalreserve.gov/pubs/feds/2005/200533/200533abs.html` and `https://www.newyorkfed.org/research/data_indicators/term_premia.html`, respectively. We estimate term premia news and yield innovatons from an ARMA(1,1) model and obtained confidence intervals via bootstrap. We selected the ARMA model based on the Bayesian information criterion but we also checked that the results were similar under different specifications of the econometric model.

[23] For the models in Kim and Wright (2005) and Adrian et al. (2013) we cannot distinguish shocks to real rates from shocks to inflation since these two papers do not model the process of inflation and expected inflation.

	Duffee (2018)	Cieslak and Povala (2015)	Kim and Wright (2005)	Adrian et al. (2013)
1y	0.03	0.03	0.03	0.05
	[0.01,0.10]	[0.01,0.06]	[0.01,0.04]	[0.04,0.06]
5y	0.22	0.19	0.18	0.19
5y	[0.09,0.66]	[0.09,0.42]	[0.14,0.20]	[0.18,0.23]
10y	0.29	0.39	0.20	0.23
10y	[0.13,1.28]	[0.20,0.74]	[0.18,0.23]	[0.20,0.25]

Table B3. Term premia variance ratios across models.
This table reports term premia variance ratio implied by various models. The term premia variance ratio is defined as the variance of term premia news relative to the variance of the yield shock. Brackets display [2.5%, 97.5%] confidence bounds.

	Contributions to total yield news variance					
Maturity	[1] Average expected real rate	[2] Average expected inflation	[3] Average expected excess returns	2Cov([1], [2])	2Cov([1],[3]	2Cov([2],[3]
Duffee (2018)						
1y	0.72	0.14	0.03	-0.02	0.16	-0.03
	[0.53,0.97]	[0.05,0.18]	[0.01,0.10]	[-0.27,0.10]	[-0.02,0.38]	[-0.09,0.03]
5y	0.32	0.16	0.22	0.14	0.30	-0.14
	[0.13,1.06]	[0.03,0.20]	[0.09,0.66]	[-0.22,0.28]	[-0.50,0.55]	[-0.38,0.01]
10y	0.24	0.22	0.29	0.31	0.15	-0.21
	[0.07,1.28]	[0.03,0.29]	[0.13,1.28]	[-0.18,0.56]	[-1.39,0.53]	[-0.73,0.08]
Cieslak and Povala (2015)						
1y	0.74	0.12	0.03	0.11	-0.00	-0.00
	[0.53,1.03]	[0.06,0.25]	[0.01,0.06]	[-0.20,0.28]	[-0.14,0.11]	[-0.06,0.05]
5y	0.51	0.16	0.19	0.14	0.00	0.00
	[0.31,0.84]	[0.08,0.32]	[0.09,0.41]	[-0.14,0.32]	[-0.35,0.20]	[-0.20,0.13]
10y	0.26	0.18	0.39	0.16	0.00	0.00
	[0.14,0.51]	[0.09,0.35]	[0.20,0.75]	[-0.02,0.34]	[-0.41,0.21]	[-0.32,0.18]

Table B4. Yield News Variance Decomposition Across Models
The table reports model-implied variance decompositions of nominal yield news for the models in Duffee (2018) and Cieslak and Povala (2015). Yield news can be decomposed as the sum of news about ex-ante real rates, expected average inflation, and excess returns. The unconditional variance of yield news is then given by the sum of the individual component variances and twice their respective covariances. We report the contribution of these components to total yield news variance. The contributions sum to 1. Brackets display [2.5%, 97.5%] confidence bounds.

rate channel and the term premia channel. The point estimates imply that real rate shocks play a dominant contribution at the 1-year maturity, while term premia news is more important at the 10-year maturity. However, for both models the confidence bounds do not preclude the possibility that real rate shocks are the dominant source of yield news at the long end of the yield curve.

B.8 Time Prefence Shocks and Moments of the Yield Curve

The estimation approach implicitly jointly targets the macro and term structure moments, including the inflation variance ratios recently put forth by Duffee (2018). An immediate consequence is that the estimation approach faces a clear trade-off between enlarging the role of the time preference shocks to match the inflation variance ratios and simultaneously accounts for other important as-

		Posterior Median	$\rho_\lambda = 0.98$ and grid for φ_λ			
	Data	($\rho_\lambda = 0.98$ & $\varphi_\lambda = 0.12$)	0.05	0.20	0.30	0.60
Inflation variance ratios						
1y	0.28	0.21	0.35	0.12	0.06	0.02
5y	0.28	0.20	0.31	0.12	0.07	0.02
10y	0.17	0.19	0.27	0.13	0.07	0.02
Yield slope						
10y - 1y	1.34	1.26	-0.19	4.65	11.06	45.94
Term premium						
1y	0.29	0.40	0.09	1.04	2.30	9.11
5y	1.07	1.20	0.03	3.80	8.94	36.54
10y	1.63	1.49	0.35	5.42	13.15	54.78
Campbell-Shiller regression slope						
3y	-0.66	-0.71	-0.87	-0.41	-0.31	0.01
5y	-0.90	-1.00	-1.14	-0.56	-0.43	0.03
10y	-1.39	-1.17	-1.16	-0.51	-0.34	0.04

Table B5. Importance of the time preference shocks.
This table shows data and model-implied inflation variance ratios, the slope of the term structure, the Campbell-Shiller regression slope, and the term premium. We report estimates based on the posterior median estimates and for alternative parameterizations. The table reports the 50th percentile of the finite sample distribution.

pects of bond yields. These other moments serve as the overidentifying restrictions that would lead us to reject the time preference shocks that allowed the model to succeed. In this section we discuss this trade-off.

In principle, it is easy to fit the inflation variance ratios across maturities. For instance, we can produce highly volatile short-term real rates by gradually increasing the variability of the preference shocks. Table B5 shows that by making the shocks big enough (i.e., increasing φ_λ), the model-implied inflation variance ratios decrease monotonically. For instance, a scale variance parameter of $\varphi_\lambda = 0.3$ produces ratios well below 10%. Unfortunately, such a parameterization significantly distorts the model's fit along three important dimensions.

First, enlarging the variability of the time preference shocks produces an increasingly steep term structure. Given mean reversion, the higher volatility of the time preference shocks raises the hedging demand for short-term bonds relative to long-term bonds. Therefore, as shown in Table B5, the slope of the yield curve significantly increases. For example, if we increase φ_λ from its posterior median value of 0.12 to 0.30, the annualized slope increases from 1.26% to 11.06%. This value is clearly at odds with the value observed in the data. Second, bonds are so risky that their term premium is too large to be consistent with the data. Table B5 shows that increasing φ_λ to 0.3 generates a mean term premium 8 times as large as the one obtained from reduced-form models.

Third, there is so much real rate news that model-implied Campbell-Shiller regression coef-

ficients don't look like observed Campbell-Shiller regression coefficients. This mechanism is more subtle. Campbell and Shiller (1991) test the expectation hypothesis by running the following regression:

$$y^{\$}_{t+12,n-12} - y_{t,n} = \alpha_n + \beta_n \frac{12}{n-12}(y^{\$}_{t,n} - y^{\$}_{t,12}) + \epsilon_{t+12}.$$

Under the expectations hypothesis $\beta_n = 1$, which relates the slope of the term structure to expected changes in the bond yield, $y^{\$}_{t,n}$, from time period t to $t+12$. Table B5 shows that in the data β_n is not only different from 1 but is also negative. This result implies that a positively sloped term structure predicts a decrease in future bond yields. It follows that, on average, the bond term premium has to be positively related to the slope of the nominal yield curve. To see this, note that that the following equation holds:

$$E_t[y^{\$}_{t+12,n-12} - y^{\$}_{t,n}] + tp^{\$}_{t,n} = \frac{12}{n-12}(y^{\$}_{t,n} - y^{\$}_{t,12}).$$

Because variations in time preference shocks affect the slope of the yield curve, $y^{\$}_{t,n} - y^{\$}_{t,12}$, but do not affect variations in the bond term premium, $tp^{\$}_{t,n}$,[24] an increase in the slope via this channel (say by increasing φ_λ to match the inflation variance ratios) must also increase the expected change in the bond yield, $E_t[y^{\$}_{t+12,n-12} - y^{\$}_{t,n}]$, which, in turn, will move the estimated slope, β_n, toward one. Table B5, shows these movements in the slope of a Campbell-Shiller regression. For example, if we increase φ_λ from 0.12 to 0.30, the slope β_n for the 10-year bond increases from -1.17 to -0.34. Hence, enlarging the time preference shocks channel mutes the model-implied predictability of bond returns.

Overall, parameterization that are successful in reproducing the inflation variance ratio distort other model-implied moments. Specifically, time preference shocks not only affect the slope of the term structure or the level of the term premium, but they also reduce the bond return predictability evidence. Given these trade-offs, time-preference shocks might even increase the onus on the inflation process to match these other moments of the data. It is not obvious a priori that adding time preference shocks can address Duffee's critique without distorting other bond yield features. This

[24] In the model, variations in the bond term premium are entirely driven by time-varying conditional volatilities of the predictable components of consumption growth and inflation and are not affected by the time preference shock channel.

is a quantitative question, and the estimation of the model fundamentally provides a quantitative answer.

C Global solution and approximation errors

We rely on analytical approximations to solve the model and to cast it into a state-space form. The advantage of this approach is that allows us to cast the model into a conditionally linear state-space representation for which we can evaluate the likelihood function using a standard particle filter with reasonable computational burden. Here, we provide the magnitude of the error induced by the analytical approximations. For the empirically relevant parameter values, we conclude that the approximation errors are rather small.

Table C1 reports the annualized model-implied moments using analytical approximations and global solutions. To solve for a global solution of the model we use projection methods, along the lines of Pohl et al. (2018).[25] We also report the relative errors induced by the analytical approximations. For a parameterization equal to the posterior median estimates of the model parameters, we find that the differences between the yield curves obtained under these two different solution methods are negligible with small errors in absolute value. For example, the maximum error is 3.35% for the one-year bond yield. The errors for the other bond maturities are even smaller, with an average absolute error of 0.31%.

However, these approximation errors increase if we use a parametrization closer to the 95% credible set of the posterior distribution. Table C1 presents the corresponding results when we use one of the 95% credible value of the persistence parameter ρ_{cc}, $\rho_{\pi\pi}$, ρ_{λ}, $\rho_{h_{xc}}$, and $\rho_{h_{x\pi}}$. We find that if we increase ρ_{cc} from 0.983 to 0.993, the maximum error increases to 55.45%. For the persistence parmaeters of the expected inflation component, $\rho_{\pi\pi}$, time preference shocks, ρ_{λ}, and the volatility of expected consumption consumption and expected inflation, $\rho_{h_{xc}}$ and $\rho_{h_{x\pi}}$, the errors are significantly smaller. Hence, to be precise, the parameter estimates that we obtained should be associated with the approximated model.[26]

[25] See Pohl et al. (2018) for a detailed description of projection solution methods applied to long-run risk models.

[26] See An and Schorfheide (2007) for a similar discussion in the literature on dynamic stochastic general equilibrium models. In this literature it has been widely accepted to estimate the linearized DSGE model given the computational burden associated with the likelihood evaluation for the non-linear version of the model.

		Mean nominal bond yields for various maturities				
	$log(\frac{W}{C})$	1y	3y	5y	7y	10y
Posterior median estimates						
Lin-Approx	6.05	5.15	5.77	6.15	6.39	6.62
Global	6.11	5.33	5.80	6.13	6.38	6.64
Error	0.95%	3.35%	0.56%	0.21%	0.18%	0.30%
Posterior median estimates with $\rho_{cc} = 0.993$						
Lin-Approx	5.69	3.30	3.54	3.38	3.01	2.27
Global	5.91	4.61	4.93	5.07	5.13	5.10
Error	3.76%	28.37%	28.09%	33.38%	41.36%	55.45%
Posterior median estimates with $\rho_{\pi\pi} = 0.987$						
Lin-Approx	6.05	5.14	5.80	6.21	6.47	6.71
Global	6.11	5.33	5.81	6.15	6.40	6.67
Error	0.97%	3.55%	0.09%	0.98%	1.07%	0.59%
Posterior median estimates with $\rho_{\lambda} = 0.985$						
Lin-Approx	5.85	4.59	5.37	5.90	6.29	6.72
Global	5.91	4.80	5.43	5.92	6.31	6.75
Error	1.05%	4.23%	1.20%	0.31%	0.22%	0.49%
Posterior median estimates with $\rho_{h_{xc}} = 0.984$						
Lin-Approx	6.04	5.07	5.64	5.97	6.18	6.37
Global	6.11	5.32	5.80	6.13	6.38	6.64
Error	1.14%	4.84%	2.76%	2.57%	3.07%	4.11%
Posterior median estimates with $\rho_{h_{x\pi}} = 0.981$						
Lin-Approx	6.04	5.24	6.34	6.97	7.31	7.55
Global	6.12	5.38	5.86	6.19	6.43	6.69
Error	1.19%	2.45%	8.29%	12.55%	13.66%	12.87%

Table C1. Annualized Moments and Approximation Errors.
This table shows the mean model-implied log wealth-consumption ratio ($log(\frac{W}{C})$) and annualized bond yields for various maturities. The results are obtained using the log-linearized solution and the global solution. The relative error is the percentage difference between these two solutions. The posterior median parameters are shown in Table 1.

D Cyclical Properties of Inflation and Bond Pricing

This appendix presents the model solution for the model that accounts for the time-varying cyclical properties of inflation, presents its state-space representation, and describes it's estimation procedure.

D.1 Asset Pricing Solution

D.1.1 Endowment process. The endowment process is given by

$$\begin{aligned} \Delta c_{t+1} &= \mu_c + x_{c,t} + \sigma_{c,t}\eta_{c,t+1} \\ \pi_{t+1} &= \mu_\pi + x_{\pi,t} + \sigma_{\pi,t}\eta_{\pi,t+1} \end{aligned} \tag{D.1}$$

where the assumed evolution of the state variables is:

$$\begin{aligned} x_{c,t+1} &= \rho_{cc}(S_t)x_{c,t} + \rho_{c\pi}(S_t)x_{\pi,t} + \sigma_{xc,t}\eta_{xc,t+1} \\ x_{\pi,t+1} &= \qquad\quad +\rho_{\pi\pi}(S_t)x_{\pi,t} + \sigma_{x\pi,t}\eta_{x\pi,t+1} \end{aligned} \tag{D.2}$$

$$\sigma_{i,t} = \varphi_i \sigma exp(h_{i,t}), \quad \text{with} \quad h_{i,t+1} = \rho_{h_i} h_{i,t} + \sigma_{h_i}\omega_{i,t+1}$$

All innovations are distributed according to

$$\eta_{i,t+1}, \quad \omega_{i,t+1}, \quad \epsilon_{i,t+1} \quad \sim i.i.d.N(0,1) \quad \text{for} \quad i = \{c, \pi, xc, x\pi\}$$

where the unobservable Markov process $S_t \in \{0,1\}$ specifies the regime in place at time t, and evolves according to the transition matrix:

$$\Pi = \begin{bmatrix} p_{00}, & p_{01} \\ p_{10}, & p_{11} \end{bmatrix}$$

where $p_{ij} = Pr[S_t = 0 | S_{t-1} = 0]$ and $\sum_j p_{ij} = 1$. Furthermore, we assume that Π is ergodic and independent from the Gaussian shocks assumed in the model.

D.1.2 Euler equation. The Euler equation is given by

$$E_t \left[exp(m_{t+1} + r_{t+1}) \right] = 1, \tag{D.3}$$

To obtain an analytical solution, we rely on the same two approximation methods as in the benchmark model specification.

D.1.3 Solution for the price-consumption ratio. To derive the derive the dynamics of the price-consumption ratio, we conjecture that

$$pc_t = A_0(S_t) + A_c(S_t)x_{c,t} + A_\pi(S_t)x_{\pi,t} + A_\lambda x_{\lambda,t} + A_{\sigma_c}\sigma^2_{c,t} + A_{\sigma_\pi}\sigma^2_{\pi,t} + A_{\sigma_{xc}}\sigma^2_{xc,t} + A_{\sigma_{x\pi}}\sigma^2_{x\pi,t}$$

Solving for the *pc*-ratio loading coefficients via

$$\begin{aligned} 1 &= E_t\left[exp(m_{t+1}+r_{c,t+1})1_{S_t=i}\right], \\ &= \sum_{j=1}^{2} E\left[exp(m_{t+1}+r_{c,t+1})|S_{t+1}=j, S_{t+1}=i\right] Pr[S_{t+1}=j|S_t=i]Pr[S_t=i] \\ &= \sum_{j=1}^{2} E\left[exp(m_{t+1}+r_{c,t+1})|S_{t+1}=j\right] p_{i,j}\pi_{i,t} \end{aligned} \tag{D.4}$$

where $1_{S_t=i}$ is an indicator variable for the regime in place at time t and $\pi_{i,t} = Pr[S_t = i]$ denotes the probability of being in regime i. Note that equation (D.4) has to hold in each state i. Therefore, the solution of the A's loadings have to solve the following system of equations:

$$1 = \sum_{j=1}^{2} \left(E\left[exp(m_{t+1}+r_{m,t+1})|S_{t+1}=j\right] + \frac{1}{2} Var\left[exp(m_{t+1}+r_{m,t+1})|S_{t+1}=j\right] \right) p_{i,j}\pi_{i,t} \quad \text{for} \quad i = 1, 2. \tag{D.5}$$

and are given by

$$A_c = (I - \kappa_1\phi_{cc}\Pi)^{-1}(1 - \frac{1}{\psi})e_1, \quad A_\pi = (I - \kappa_1\phi_{\pi\pi}\Pi)^{-1}(\kappa_1\phi_{c\pi}\Pi A_c), \qquad A_\lambda = \frac{\rho_\lambda}{1-\kappa_1\rho_\lambda} \tag{D.6}$$

$$A_{\sigma_c} = \frac{(1-\gamma)(1-\frac{1}{\psi})}{2(1-\kappa_1\nu_c)}, \quad A_{\sigma_\pi} = 0, \quad A_{\sigma_{xc}} = (I - \kappa_1\nu_{xc}\Pi)^{-1}\tfrac{1}{2}\theta\kappa_1^2\Pi A_c^2 \quad A_{\sigma_{x\pi}} = (I - \kappa_1\nu_{x\pi}\Pi)^{-1}\tfrac{1}{2}\theta\kappa_1^2\Pi A_\pi^2$$

and the constant is given by

$$\begin{aligned} A_0 &= (I - \kappa_1\Pi)^{-1}\Pi\left(A_{0,1} + A_{0,2}\right) \\ A_{0,1} &= \left(log\delta + (1-\frac{1}{\psi})\mu_c + \kappa_0 + \frac{1}{2}\theta(1+\kappa_1 A_\lambda)^2\sigma_\lambda^2 \right) e_1 \\ A_{0,1} &= \kappa_1 \begin{bmatrix} \sum_{i\in\{\sigma_c,\sigma_\pi,\sigma_{xc},\sigma_{x\pi}\}}(1-\nu_i)A_i(S_t=1)\sigma_{0,i}^2 + \frac{1}{2}\kappa_1\theta A_i^2(S_t=1)\sigma_{\omega_i}^2 \\ \sum_{i\in\{\sigma_c,\sigma_\pi,\sigma_{xc},\sigma_{x\pi}\}}(1-\nu_i)A_i(S_t=2)\sigma_{0,i}^2 + \frac{1}{2}\kappa_1\theta A_i^2(S_t=2)\sigma_{\omega_i}^2 \end{bmatrix} \end{aligned}$$

where we introduced the following notation: $\phi_{cc} = diag(\rho_{cc}, \rho_{cc})$, $\phi_{c\pi} = diag(\rho_{c\pi}, \rho_{c\pi})$, $\phi_{\pi\pi} = diag(\rho_{\pi\pi}, \rho_{\pi\pi})$ and e_1 is a column vector of ones. *diag* is a scalar operator that takes a sequence of scalars and use them to construct a diagonal matrix with zeros on the non-diagonals.

D.1.4 Linearization Parameters. The linearization parameters κ_0 and κ_1 solve the following system of equations

$$\begin{aligned}
\hat{pc} &= \sum_{j=1}^{2} \hat{\pi}_j \left(A_{0,j}(\kappa_0, \kappa_1) + \sum_{i \in \{\sigma_c, \sigma_\pi, \sigma_{xc}, \sigma_{x\pi}\}} A_{i,j}(\kappa_1) \sigma_{i,0}^2 \right) \\
\kappa_1 &= \frac{exp(\bar{pc})}{1 + exp(\bar{pc})} \\
\kappa_0 &= log(1 + exp(\bar{pc})) - \kappa_1 \bar{pc}
\end{aligned}$$

which can be done numerically. Finally, $\hat{\pi}$ is a 2×1 vector of steady-state probabilities of S_t:

$$\hat{\pi} = \begin{bmatrix} Pr[S_t = 0] \\ Pr[S_t = 1] \end{bmatrix} = \begin{bmatrix} \dfrac{1 - p_{11}}{2 - p_{00} - p_{11}} \\ \dfrac{1 - p_{00}}{2 - p_{00} - p_{11}} \end{bmatrix}$$

D.2 Expression for the real and nominal SDF

Similar to Section A.3 we can rewrite the real SDF in terms of the state variables and shocks:

$$\begin{aligned}
m_{t+1} = {} & m_0(S_t, S_{t+1}) + m_c(S_t, S_{t+1}) x_{c,t} + m_\pi(S_t, S_{t+1}) x_{\pi,t} + m_\lambda(S_t, S_{t+1}) x_{\lambda,t} \\
& + m_{\sigma_c}(S_t, S_{t+1}) \sigma_{x,t}^2 + m_{\sigma_\pi}(S_t, S_{t+1}) \sigma_{\pi,t}^2 + m_{\sigma_{xc}}(S_t, S_{t+1}) \sigma_{xc,t}^2 + m_{\sigma_{x\pi}}(S_t, S_{t+1}) \sigma_{x\pi,t}^2 \\
& - \lambda_c(S_{t+1}) \sigma_{c,t} \eta_{c,t+1} - \lambda_\pi(S_{t+1}) \sigma_{\pi,t} \eta_{\pi,t+1} - \lambda_\lambda(S_{t+1}) \sigma_{\lambda,t} \eta_{\lambda,t+1} - \lambda_{xc}(S_{t+1}) \sigma_{xc,t} \eta_{xc,t+1} \\
& - \lambda_{x\pi}(S_{t+1}) \sigma_{x\pi,t} \eta_{x\pi,t+1} - \sum_{i \in \{\sigma_c, \sigma_\pi, \sigma_{xc}, \sigma_{x\pi}\}} \lambda_i(S_{t+1}) \sigma_{\omega_i} \omega_{i,t+1}
\end{aligned} \tag{D.7}$$

The discount factor parameters and market price of risks are equal to:

$$\begin{aligned}
m_c(S_t, S_{t+1}) &= \left(\theta - 1 + \frac{\theta}{\psi} + \theta \left[\kappa_1 A_c(S_{t+1}) \rho_{cc}(S_t) - A_c(S_t) \right] \right) \\
m_\pi(S_t, S_{t+1}) &= (\theta - 1) \left(\kappa_1 A_c(S_{t+1}) \rho_{c\pi}(S_t) + \kappa_1 A_\pi(S_{t+1}) \rho_{\pi\pi}(S_t) - A_\pi(S_t) \right) \\
m_\lambda(S_t, S_{t+1}) &= \left(\theta \rho_\lambda + (\theta - 1) \left[\kappa_1 A_\lambda(S_{t+1}) \rho_\lambda - A_\lambda \right] \right) \\
m_i(S_t, S_{t+1}) &= (\kappa_1 A_i(S_{t+1}) \nu_i - A_i(S_t)) \quad \text{for} \quad i \in \{\sigma_c, \sigma_\pi, \sigma_{xc}, \sigma_{x\pi}\}
\end{aligned} \tag{D.8}$$

the constant is given by

$$\begin{aligned}
m_0(S_t, S_{t+1}) = {} & log\delta + (\theta - 1)\kappa_0 - \frac{1}{\psi} \mu_c + \\
& + (\theta - 1) \left[\kappa_1 A_0(S_{t+1}) - A_0(S_t) + \kappa_1 \sum_{i \in \{\sigma_c, \sigma_\pi, \sigma_{xc}, \sigma_{x\pi}\}} A_i \sigma_{i,0}^2 (1 - \nu_i) \right]
\end{aligned} \tag{D.9}$$

and the market prices are

$$\begin{aligned}\lambda_c(S_{t+1}) = \gamma, \qquad \lambda_\pi(S_{t+1}) = 0, \qquad \lambda_\lambda(S_{t+1}) = \frac{\kappa_1\rho_\lambda - \theta}{1-\kappa_1\rho_\lambda},\\ \lambda_{xc}(S_{t+1}) = (1-\theta)\kappa_1 A_c(S_{t+1}), \quad \lambda_{x\pi}(S_{t+1}) = (1-\theta)\kappa_1 A_\pi\end{aligned} \tag{D.10}$$

Similarly, the nominal SDF is equal to the real one minus inflation.

D.3 Nominal Bond Prices

Conjecture that $p^{\$}_{t,n}$ is a linear function of the state variables

$$p^{\$}_{t,n} = (B^{\$}_{0,n} + B^{\$}_{c,n}x_{c,t} + B^{\$}_{\pi,n}x_{\pi,t} + B^{\$}_{\lambda,n}x_{\lambda,t} + B^{\$}_{\sigma_c,n}\sigma^2_{c,t} + B^{\$}_{\sigma_\pi,n}\sigma^2_{\pi,t} + B^{\$}_{\sigma_{xc},n}\sigma^2_{xc,t} + B^{\$}_{\sigma_{x\pi},n}\sigma^2_{x\pi,t}) \tag{D.11}$$

Then we can show that the bond price loadings for a given state i are

$$\begin{aligned}
B^{\$}_{c,n}(i) &= \sum_{j=1}^{2} p_{i,j}\left(B^{\$}_{c,n-1}(j)\rho_{cc}(i) + m^{\$}_{c}(i,j)\right)\\
B^{\$}_{\pi,n}(i) &= \sum_{j=1}^{2} p_{i,j}\left(B^{\$}_{\pi,n-1}(j)\rho_{\pi\pi}(i) + B^{\$}_{c,n-1}(j)\rho_{c\pi}(i) + m^{\$}_{\pi}(i,j)\right)\\
B^{\$}_{\lambda,n} &= B^{\$}_{\lambda,n-1}\rho_\lambda + m^{\$}_{\lambda}\\
B^{\$}_{\sigma_c,n}(i) &= \sum_{j=1}^{2} p_{i,j}\left(B^{\$}_{\sigma_c,n-1}(j)\nu_c + m^{\$}_{\sigma_c}(i,j) + \frac{1}{2}(\lambda^{\$}_c)^2\right)\\
B^{\$}_{\sigma_\pi,n}(i) &= \sum_{j=1}^{2} p_{i,j}\left(B^{\$}_{\sigma_\pi,n-1}(j)\nu_\pi + m^{\$}_{\sigma_\pi}(i,j) + \frac{1}{2}(\lambda^{\$}_\pi)\right)\\
B^{\$}_{\sigma_{xc},n}(i) &= \sum_{j=1}^{2} p_{i,j}\left(B^{\$}_{\sigma_{xc},n-1}(j)\nu_{xc} + m^{\$}_{\sigma_{xc}}(i,j) + \frac{1}{2}\left[\lambda^{\$}_{xc} - B^{\$}_{c,n-1}(j)\right]^2\right)\\
B^{\$}_{\sigma_{x\pi},n}(i) &= \sum_{j=1}^{2} p_{i,j}\left(B^{\$}_{\sigma_{x\pi},n-1}(j)\nu_{x\pi} + m^{\$}_{\sigma_{x\pi}}(i,j) + \frac{1}{2}\left[\lambda^{\$}_{x\pi} - B^{\$}_{\pi,n-1}(j)\right]^2\right)\\
B^{\$}_{0,n}(i) &= \sum_{j=1}^{2} p_{i,j}(B^{\$}_{0,n-1}(j) + m^{\$}_{0}(i,j) + + \frac{1}{2}(\lambda^{\$}_\lambda - B^{\$}_{\lambda,n-1})^2\sigma^2_\lambda\\
&\quad + \sum_{i\in\{\sigma_c,\sigma_\pi,\sigma_{xc},\sigma_{x\pi}\}}\left[(B^{\$}_{i,n-1})(j)\sigma^2_{i,0}(1-\nu_i)\frac{1}{2}(\lambda_i + B^{\$}_{i,n-1}))^2\sigma^2_{\omega_i}\right])
\end{aligned} \tag{D.12}$$

Given the price of a zero-coupon bond, bond yields are defined $y^{\$}_{t,n} = -\frac{1}{n}lnP^{\$}_{t,n}$.

D.4 Evolution of expectations and uncertainty

In this section, we derive the laws of motion for first and second moments of the model. These moments consider all sources of uncertainty in the economy. Specifically, when agents form expectations they face uncertainty about the regime that will prevail in the next period, uncertainty about the current regime, and uncertainty about the Gaussian shocks to the state variables. To compute these moments is useful to express the variables in the model as a Markov-switching VAR:

$$X_{t+1} = \Phi_0 + \Phi_1(S_t)X_t + \Sigma_t\epsilon_{t+1}, \quad \epsilon_{t+1} \sim N(0, I_7)$$

with $X_{t+1} = \left[x_{c,t},\ x_{\pi,t},\ x_{\lambda,t},\ \sigma^2_{xc,t},\ \sigma^2_{x\pi,t},\ \sigma^2_{c,t},\ \sigma^2_{\pi,t}\right]'$ and

$$\Phi_0 = \begin{bmatrix} 0 \\ 0 \\ 0 \\ \sigma^2_{xc,0}(1-\nu_{xc}) \\ \sigma^2_{x\pi,0}(1-\nu_{x\pi}) \\ \sigma^2_{c,0}(1-\nu_c) \\ \sigma^2_{\pi,0}(1-\nu_\pi) \end{bmatrix}_{7\times 1}, \qquad \Sigma_t = \begin{bmatrix} \sigma_{xc,t} & 0 & 0 & 0 & 0 & 0 & 0 \\ 0 & \sigma_{x\pi,t} & 0 & 0 & 0 & 0 & 0 \\ 0 & 0 & \sigma_\lambda & 0 & 0 & 0 & 0 \\ 0 & 0 & 0 & \sigma_{\omega_{xc}} & 0 & 0 & 0 \\ 0 & 0 & 0 & 0 & \sigma_{\omega_{x\pi}} & 0 & 0 \\ 0 & 0 & 0 & 0 & 0 & \sigma_{\omega_c} & 0 \\ 0 & 0 & 0 & 0 & 0 & 0 & \sigma_{\omega_\pi} \end{bmatrix}_{7\times 7}.$$

$$\Phi_1(S_t) = \begin{bmatrix} \rho_{c,c}(S_t) & \rho_{c,\pi}(S_t) & 0 & 0 & 0 & 0 & 0 \\ 0 & \rho_{\pi,\pi}(S_t) & 0 & 0 & 0 & 0 & 0 \\ 0 & 0 & \rho_\lambda & 0 & 0 & 0 & 0 \\ 0 & 0 & 0 & \nu_{xc} & 0 & 0 & 0 \\ 0 & 0 & 0 & 0 & \nu_{x\pi} & 0 & 0 \\ 0 & 0 & 0 & 0 & 0 & \nu_c & 0 \\ 0 & 0 & 0 & 0 & 0 & 0 & \nu_\pi \end{bmatrix}_{7\times 7}$$

and ϵ_{t+1} is the vector of structural shocks. Once the model is the MS-VAR representation, we follow Bianchi (2016) and compute the evolution of the conditional expectations. Once we have these expressions we compute the risk premia moments as we did for the fix-regime economy.

D.5 State-space representation and Posterior Inference

State-space representation and Posterior Inference In this section I describe the state-space representation of the risk-based model, which consist of a measurement equation:

$$Y^o_{t+1} = A_{t+1}(D(S_t) + Z(S_t)s_{t+1} + Z^v s^v_{t+1}(h_{t+1}) + \Sigma^u u_{t+1}), \quad \text{with} \quad u_{t+1} \sim N(0, I) \tag{D.13}$$

and a state-transition equation:

$$\begin{aligned} s_{t+1} &= \Phi(S_t)s_t + v_{t+1}(h_t) \\ h_{t+1} &= \Psi h_t + \Sigma_h \omega_{t+1}, \quad h_{t+1} = [h_{xc,t+1},\ h_{x\pi,t+1},\ h_{c,t+1},\ h_{\pi,t+1}]' \quad \text{with} \quad \omega_{t+1} \sim N(0, I). \end{aligned} \tag{D.14}$$

where the matrices are very similar to the fix-regime case.

Posterior Inference. The estimation procedure is also very similar to the estimation of the fix-regime economy. We just need to add an extra step in the algorithm described in Section B.3. Specifically, conditional on a draw i of the states and parameters, we draw the states $S^{i+1}_{1:T}$ via the multi-move Gibbs-sampling described in Kim, Nelson et al. (1999).

References

Abrahams, M., T. Adrian, R. K. Crump, and E. Moench. 2013. Pricing TIPS and treasuries with linear regressions. *FRB of New York Staff Report* .

Adrian, T., R. K. Crump, and E. Moench. 2013. Pricing the term structure with linear regressions. *Journal of Financial Economics* 110:110–138.

Albuquerque, R., M. Eichenbaum, V. Luo, and S. Rebelo. 2016. Valuation Risk and Asset Pricing. *The Journal of Finance* 71:2861–2904.

An, S., and F. Schorfheide. 2007. Bayesian analysis of DSGE models. *Econometric reviews* 26:113–172.

Andrieu, C., A. Doucet, and R. Holenstein. 2010. Particle markov chain monte carlo methods. *Journal of the Royal Statistical Society: Series B (Statistical Methodology)* 72:269–342.

Bansal, R., and I. Shaliastovich. 2013. A long-run risks explanation of predictability puzzles in bond and currency markets. *Review of Financial Studies* 26:1–33.

Bansal, R., and A. Yaron. 2004. Risks for the long run: A potential resolution of asset pricing puzzles. *The Journal of Finance* 59:1481–1509.

Beeler, J., and J. Y. Campbell. 2009. The long-run risks model and aggregate asset prices: An empirical assessment. Tech. rep., National Bureau of Economic Research.

Bekaert, G., R. J. Hodrick, and D. A. Marshall. 1997. On biases in tests of the expectations hypothesis of the term structure of interest rates. *Journal of Financial Economics* 44:309–348.

Bianchi, F. 2016. Methods for measuring expectations and uncertainty in Markov-switching models. *Journal of Econometrics* 190:79–99.

Campbell, J. Y., C. Pflueger, and L. M. Viceira. 2014. Monetary policy drivers of bond and equity risks. Tech. rep., National Bureau of Economic Research.

Campbell, J. Y., and R. J. Shiller. 1988. The dividend-price ratio and expectations of future dividends and discount factors. *Review of financial studies* 1:195–228.

Campbell, J. Y., and R. J. Shiller. 1991. Yield spreads and interest rate movements: A bird's eye view. *The Review of Economic Studies* 58:495–514.

Campbell, J. Y., A. Sunderam, and L. M. Viceira. 2017. Inflation bets or deflation hedges? The changing risks of nominal bonds. *Critical Finance Review* .

Cieslak, A. 2016. Short-rate expectations and unexpected returns in Treasury bonds. *unpublished paper, Duke University* .

Cieslak, A., and P. Povala. 2015. Expected returns in Treasury bonds. *The Review of Financial Studies* 28:2859–2901.

Cochrane, J. H., and M. Piazzesi. 2005. Bond risk premia. *The American economic review* 95:138–160.

Creal, D. D., and J. C. Wu. 2016. Bond risk premia in consumption-based models. Tech. rep., National Bureau of Economic Research.

Doh, T. 2013. Long-Run Risks In The Term Structure Of Interest Rates: Estimation. *Journal of Applied Econometrics* 28:478–497.

Duffee, G., et al. 2010. Sharpe ratios in term structure models. *manuscript, Johns Hopkins* .

Duffee, G. R. 2002. Term premia and interest rate forecasts in affine models. *The Journal of Finance* 57:405–443.

Duffee, G. R. 2013. Bond pricing and the macroeconomy. In *Handbook of the Economics of Finance*, vol. 2, pp. 907–967. Elsevier.

Duffee, G. R. 2016. Expected inflation and other determinants of Treasury yields. *Johns Hopkins University, Department of Economics Working Paper* .

Duffee, G. R. 2018. Expected inflation and other determinants of Treasury yields. *The Journal of Finance* 73:2139–2180.

d'Amico, S., D. H. Kim, and M. Wei. 2018. Tips from TIPS: the informational content of Treasury Inflation-Protected Security prices. *Journal of Financial and Quantitative Analysis* 53:395–436.

Epstein, L. G., and S. E. Zin. 1989. Substitution, risk aversion, and the temporal behavior of consumption and asset returns: A theoretical framework. *Econometrica: Journal of the Econometric Society* pp. 937–969.

Eraker, B. 2008. Affine general equilibrium models. *Management Science* 54:2068–2080.

Fernández-Villaverde, J., and J. F. Rubio-Ramírez. 2007. Estimating macroeconomic models: A likelihood approach. *The Review of Economic Studies* 74:1059–1087.

Fleming, M. J., and N. Krishnan. 2012. The microstructure of the TIPS market. *Economic Policy Review* .

Fontaine, J.-S., and R. Garcia. 2012. Bond liquidity premia. *The Review of Financial Studies* 25:1207–1254.

Gallmeyer, M., B. Hollifield, F. Palomino, and S. Zin. 2017. Term Premium Dynamics and the Taylor Rule. *Quarterly Journal of Finance* 7:1750011.

Gürkaynak, R. S., B. Sack, and J. H. Wright. 2007. The US Treasury yield curve: 1961 to the present. *Journal of monetary Economics* 54:2291–2304.

Hanson, S. G., and J. C. Stein. 2015. Monetary policy and long-term real rates. *Journal of Financial Economics* 115:429–448.

Haubrich, J., G. Pennacchi, and P. Ritchken. 2012. Inflation expectations, real rates, and risk premia: Evidence from inflation swaps. *The Review of Financial Studies* 25:1588–1629.

Herbst, E. P., and F. Schorfheide. 2015. *Bayesian Estimation of DSGE Models*. Princeton University Press.

Hu, G. X., J. Pan, and J. Wang. 2013. Noise as information for illiquidity. *The Journal of Finance* 68:2341–2382.

Judd, K. L. 1992. Projection methods for solving aggregate growth models. *Journal of Economic Theory* 58:410–452.

Kim, C.-J., C. R. Nelson, et al. 1999. State-space models with regime switching: classical and Gibbs-sampling approaches with applications. *MIT Press Books* 1.

Kim, D. H., and J. H. Wright. 2005. An arbitrage-free three-factor term structure model and the recent behavior of long-term yields and distant-horizon forward rates .

Kung, H. 2015. Macroeconomic linkages between monetary policy and the term structure of interest rates. *Journal of Financial Economics* 115:42–57.

Le, A., and K. J. Singleton. 2010. An equilibrium term structure model with recursive preferences. *American Economic Review* 100:557–61.

Nakamura, E., and J. Steinsson. 2018. High-frequency identification of monetary non-neutrality: the information effect. *The Quarterly Journal of Economics* 133:1283–1330.

Pflueger, C. E., and L. M. Viceira. 2011. *An empirical decomposition of risk and liquidity in nominal and inflation-indexed government bonds*. National Bureau of Economic Research.

Piazzesi, M., and M. Schneider. 2007. Equilibrium yield curves. In *NBER Macroeconomics Annual 2006, Volume 21*, pp. 389–472. MIT Press.

Pohl, W., K. Schmedders, and O. Wilms. 2018. Higher Order Effects in Asset Pricing Models with Long-Run Risks. *The Journal of Finance* 73:1061–1111.

Primiceri, G. E. 2005. Time varying structural vector autoregressions and monetary policy. *The Review of Economic Studies* 72:821–852.

Rudebusch, G. D., and E. T. Swanson. 2012. The bond premium in a dsge model with long-run real and nominal. *American Economic Journal: Macroeconomics* 4:105–143.

Schorfheide, F., D. Song, and A. Yaron. 2017. Identifying long-run risks: A bayesian mixed-frequency approach. *forthcoming, Econometrica* .

Shephard, N. 1996. Statistical aspects of ARCH and stochastic volatility. *Monographs on Statistics and Applied Probability* 65:1–68.

Sims, C. A., and T. Zha. 2006. Were there regime switches in US monetary policy? *American Economic Review* 96:54–81.

Song, D. 2017. Bond market exposures to macroeconomic and monetary policy risks. *The Review of Financial Studies* 30:2761–2817.

Van Binsbergen, J. H., J. Fernández-Villaverde, R. S. Koijen, and J. Rubio-Ramírez. 2012. The term structure of interest rates in a DSGE model with recursive preferences. *Journal of Monetary Economics* 59:634–648.

Verdelhan, A. 2010. A habit-based explanation of the exchange rate risk premium. *The Journal of Finance* 65:123–146.

Wachter, J. A. 2006. A consumption-based model of the term structure of interest rates. *Journal of Financial Economics* 79:365–399.

Wilcox, D. W. 1992. The construction of US consumption data: some facts and their implications for empirical work. *The American economic review* pp. 922–941.